Amphiphilic electrospun fibres of poly(methacrylic acid)-graft-poly(dimethylsiloxane) copolymers as a means to controlling electrospun fibre morphology and obtaining nanofibre hydrogels

by
Freda-Jean Meltz

Thesis presented in partial fulfilment of the requirements for the degree of Master of Science in Polymer Science in the Faculty of Chemistry and Polymer Science at Stellenbosch University

Supervisor: Prof. Peter Mallon
Co-supervisor: Prof. Bert Klumperman

April 2014

Stellenbosch University http://scholar.sun.ac.za

By submitting this thesis, I declare that the entirety of the work contained therein is my own, original work, that I am the sole author thereof (save to the extent explicitly otherwise stated), the reproduction and publication thereof by Stellenbosch University will not infringe any third party rights and that I have not previously in its entirety or in part submitted it for obtaining any qualification.

Signature: Date:

Copyright É 2014 Stellenbosch University
All rights reserved

Stellenbosch University http://scholar.sun.ac.za

Abstract

Novel poly(methacrylic acid)-graft-poly(dimethylsiloxane) copolymers were synthesised by conventional free radical reactions using a poly(dimethylsiloxane) macromonomer. The polymers were electrospun to investigate how the fibre morphology can be modified by manipulating the electrospinning solution parameters, and to determine the possibility of using the polymers as new materials for the production of polymer nanofibre hydrogels. The electrospinning solution parameters were varied by electrospinning the highly amphiphilic copolymers in solvents with variable solvent qualities. Scanning Electron Microscopy (SEM) and Field Emission Scanning Electron Microscopy (FE–SEM) was used to investigate the fibre morphology. Internal morphology was studied using a freeze fracture technique prior to FE-SEM imaging. It is revealed that the polymers in this study does not form any fine structure or pores even when self-assembled structures are present in the solution. Attempts were made to visualise any self-assembled structures of films produced from dilute solutions using TEM. Further studies included investigating the fibres properties, primarily with regards to their rate and extent of moisture and water uptake. The fibres showed hydrogel behaviour and the PDMS content were found to have an impact on the hydrogel stability. Post electrospinning crosslinking of the nanofibres was also explored.

Stellenbosch University http://scholar.sun.ac.za

Opsomming

Unieke ent-kopolimere wat bestaan uit poli(metielakrielsuur) (PMAS) en poli(dimetielsiloksaan) (PDMS) is gesintetiseer deur middel van ‘n “ent-deur” vryeradikaalkopolimerisasie. ‘n PDMS makromonomeer is vir hierdie doel gebruik. Die polimere is geëlektrospin om vesels te vorm. Die doel was om die invloed van verkillende strukture in oplossing op die veselmorfologie te bepaal. Die moontlikheid om hierdie nanovesels as gels te gebruik is ook ondersoek. Die amfifiliese kopolimere is geëlektrospin uit die oplossing waarin dit wisselende oplosbaarheid toon. Skandeer elektron mikroskopie (SEM) is gebruik om die morfologie te ondersoek. Die interne morfologie van die vesels is ondersoek deur die vesels te vries en in die gevriesde toestand te breek. Die studie het getoon dat geen strukture op, of binne, die vesels vorm nie, selfs al moes daar assosiasie tussen segmente van die polimere gewees het. Hierdie tipe assosiasies sou strukture in die oplossing tot gevolg gehad het. ‘n Poging is aangewend om die strukture in oplossing te visualiseer deur transmissie elektron mikroskopie (TEM) van dun films te ondersoek. Films is vanaf verdunde oplossings gevorm. Ander studies het ingesluit om die eienskappe van die vesels te ondersoek, met die fokus op hoeveel en hoe vinnig die vesels waterdamp en water kon absorbeer. Die vesels het soos ‘n gel reageer. Hierdie gedrag is beïnvloed deur die hoeveelheid PDMS wat ‘n definitiewe invloed op die stabiliteit van die gel gehad het. Kruisverbindings van die vesels, nadat dit geëlektrospin is, is ook ondersoek.

Stellenbosch University http://scholar.sun.ac.za

Table of content

CHAPTER 1 - INTRODUCTION

1.1. General introduction 1

1.2. Objectives 4

1.3. References 5

CHAPTER 2 – LITERATURE REVIEW

2.1 Graft copolymers 7

2.1.1 Grafting from 8

2.1.2 Grafting onto 8

2.1.3 Grafting through 9

2.2 Electrospinning 11

2.3 Electrospinning parameters 14

2.3.1 Molecular weight, solution viscosity and surface tension 16

2.3.2 Solution conductivity and solvent dielectric properties 17

2.3.3 Temperature 19

2.3.4 Polymer solution properties 22

2.3.5 Other techniques 29

2.4 Solution behaviour of graft copolymers 31

2.5 Crosslinked fibres/hydrogels 37

2.6 References 39

Stellenbosch University http://scholar.sun.ac.za

CHAPTER 3 - EXPERIMENTAL

3.1. Materials 45

3.2. Synthesis 45

3.2.1. Synthesis of poly(methacrylic acid) graft PDMS 45

3.2.2. Synthesis of poly(methyl methacrylate) from poly(methacrylic acid) 47

3.3. Characterization 48

3.3.1. Gradient elution chromatography 48

3.3.2. Nuclear magnetic resonance (NMR) 48

3.3.3. Scanning electron microscopy (SEM) and FE-SEM 48

3.3.4. Attenuated total reflectance (ATR) fourier transform infra-red (FT-IR) 49

3.3.5. Size exclusion chromatography 49

3.3.6. Static contact angle measurements 49

3.3.7. Rheology 50

3.3.8. TEM 50

3.4. Moisture absorption tests 51

3.4.1. Moisture absorption 51

3.4.2. TGA 52

3.5. Water stability tests 52

3.6. References 52

Stellenbosch University http://scholar.sun.ac.za

CHAPTER 4 – RESULTS AND DISCUSSION

4.1. Synthesis and characterization 53

4.1.1. Synthesis of Poly(methacrylic acid)-g-poly(dimethylsiloxane) copolymers 53

4.1.2. Synthesis of poly(methyl methacrylate)-g-PDMS 54

4.1.3. Characterization 54

4.1.4. Gradient elution high performance liquid chromatography (GPEC) 61

4.2. Electrospinning of amphiphilic molecules 67

4.2.1. Influence of PDMS content 69

4.2.2. Electrospinning parameters 76

4.2.3. Internal morphology of fibres 81

4.3. Properties of the fibres 86

4.3.1. Water contact angle studies 86

4.3.2. Fibres in moisture 90

4.3.3. Water stability 95

4.3.4. Chemical crosslinking 97

4.3.5. Investigating the possibility of crosslinking with nanomaterials 109

4.4. References 117

CHAPTER 5 – CONCLUSIONS AND RECOMMENDATIONS

5.1 Conclusions 120

5.2 Recommendations 124

5.3 References 126

Stellenbosch University http://scholar.sun.ac.za

APPENDIX A

A.1. ^{1}H-NMR spectra for PMAA-graft-PDMS copolymers A1

A.2. ^{1}H-NMR spectra for PMMA-graft-PDMS copolymers A3

A.3. Moisture absorption fitting parameter tables A5

Stellenbosch University http://scholar.sun.ac.za

Abbreviations

AAc	acrylic acid
ABS	acrylonitrile-butadiene-styrene
AIBN	azobisisobutyronitrile
AN	acrylonitrile
ATR-FTIR	attenuated total reflectance fourier transform infra-red
ATRP	atom transfer radical polymerization
tBMA	tert-butyl methacrylate
$CHCl_3$	chloroform
CMC	critical micelle concentration
DMAc	dimethyl acetimide
DMF	N,N dimethylformamide
DMSO	dimethylsulfoxide
DSC	differential scanning calorimetry
FE-SEM	field emission scanning electron microscopy
FTIR	fourier transform infrared
GPEC	gradient elution high performance liquid chromatography
HPLC	high performance liquid chromotography
LCST	lower critical solution temperature
LMA	lauryl methacrylate
LMA-MMA-MPOEMA	poly-(methyl methacrylate-co-lauryl methacrylate)-g-methyl-hydroxypoly(oxyethylene) methacrylates

Stellenbosch University http://scholar.sun.ac.za

MAA	methacrylic acid
MMA	methyl methacrylate
MeOH	methanol
MMP-PDMS	mono-methacryloxypropyl terminal poly(dimethylsiloxane)
MPEG	methoxypoly(ethylene glycol)
MPOEMA	α-methyl-ϖ-hydroxypoly(oxyethylene) methacrylates
NaCl	sodium chloride
NCC	nanocrystalline cellulose
NIPS	non-solvent induced phase separation
NMR	nuclear magetic resonance
P4VP	poly(4-vinylpyridine)
PAN	poly(acrylonitrile)
PANI	Polyaniline
PC	polycarbonate
PDMS	poly(dimethylsiloxane)
PDP	3-n-pentadecylphenol
PE	polyethylene
PEG	poly(ethylene glycol)
PEO	poly(ethylene oxide)
PHEA	poly (N-hydroxyethylacrylamide)
PI	polyisoprene
PLA	poly(lactic acid)
PLGA	poly(lactide-co-glycolide)
PMAA	poly(methacrylic acid)
PMMA	poly(methyl methacrylate)

Stellenbosch University http://scholar.sun.ac.za

POM	polyoxymethylene
PS	polystyrene
PTU	polythiourea
PU	polyurethane
PVDF	polyvinylidene fluoride
PVME	poly(vinylidenefluoride)
PVOH	poly(vinyl alchohol)
PVP	poly(vinyl pyrrolidone)
RAFT	reversible addition fragmentation chain transfer
SAXS	small-angle X-ray scattering
SBR	styrene-butadiene rubber
SCA	static contact angle
SDS	sodium dodecyl sulphate
SEC	size exclusion chromatography
SEM	scanning electron microscopy
SiO_2	silica
SMA	styrene maleic anhydride
TEM	transmission electron microscopy
TGA	thermogravimetric analysis
THF	tetrahydrofuran
TIPS	Temperature induced phase separation
TiO_2	titanium dioxide
UCST	upper critical solution temperature
UV	ultra violet
WCA	water contact angle

Stellenbosch University http://scholar.sun.ac.za

List of symbols

A_1 – constant

A_2 – constant

β – equilibrium moisture content

τ – rate constant

Stellenbosch University http://scholar.sun.ac.za

List of figures

CHAPTER 2

Figure 2-1: Simple illustration of the three routes that can be followed to obtain graft copolymers (A) grafting from (B) grafting onto (C) grafting through 7

Figure 2-2: Illustration of the different graft distributions which can be obtained via different reaction routes. Polymer F – normal free radical, Polymer A – ATRP, Polymer R - RAFT 9

Figure 2-3: Illustration of the electrospinning setup used in this study 12

Figure 2-4: Schematic illustration of the processes that occur during electrospinning 14

Figure 2-5:-Diagram showing the factors that influence the electrospinning process 15

Figure 2-6: Influence of polymer concentration on the porous structures of polystyrene 18

Figure 2-7: Illustration of wrinkle formation that can occur during electrospinning 20

Figure 2-8: Surface morphology of polystyrene fibres formed by electrospinning in solvent mixtures of (A) THF/DMF (4:0) (B)THF/DMF (3:1) (C) THF/DMF (2:2) (D) THF/DMF (1:3) (E) THF/DMF (0:4) 21

Figure 2-9: Internal morphology of polystyrene fibres formed by electrospinning in solvant mixtures of (A) THF/DMF (4:0) (B)THF/DMF (3:1) (C) THF/DMF (2:2) (D) THF/DMF (1:3) (E) THF/DMF (0:4) 21

Figure 2-10: Concentric lamellar circles formed from PI-PS block copolymers under confinement 26

Figure 2-11: Illustration of how the structure in the bulk compares to structures obtained in electrospun fibres from self-assembled solutions 27

Figure 2-12: Fully porous polymer fibres formed from PAN-g-PDMS copolymers that was electrospun from DMF 28

Figure 2-13: Hollow PAN fibre with porous exterior formed by non-solvent induced phase separation 30

Stellenbosch University http://scholar.sun.ac.za

Figure 2-14: Illustration of solution structures possible for low graft density amphiphilic copolymers in solvent combinations ranging from either good for the backbone or good for the branches 33

Figure 2-15: Illustration of structures that can be formed from concentrated amphiphilic graft copolymers in solution 34

Figure 2-16-TEM images of hydrophobic polystyrene chains forming multiple cores surrounded by a PAA shell 34

Figure 2-17: TEM images of micelles of PAA-g-PMMA (A) in water (B) in 1 wt% NaCl solution 35

CHAPTER 3

Figure 3-1: Illustration of instrument used for moisture studies 52

CHAPTER 4

Figure 4-1: ^{1}H-NMR spectra of (A) PMAA homopolymer and (B) copolymer with 12.2 mol % PDMS 55

Figure 4-2: ^{1}H-NMR showing the appearance of the methyl protons at 3.7 ppm for copolymer with 12.2 mol % PDMS 56

Figure 4-3: Infrared spectra for the 1000 g/mol series (A) full spectra shown and (B) zoomed in to show the presence of PDMS 58

Figure 4-4: Infrared spectra showing the disappearance of the acid groups upon esterification of PMAA homopolymer to PMMA homopolymer 59

Figure 4-5: SEC chromatograms of the converted (PMMA) copolymers (PDMS =1000 g/mol) 60

Figure 4-6: Gradient profile of the MeOH/THF mobile phase vs elution time for the gradient chromatographic separation of PMAA-g-PDMS samples (Symmetry300 C18 column, 5 µm, 1 mL/min, 30°C) 63

Figure 4-7: Gradient HPLC chromatograms for polymers containing PMAA backbones with different PDMS graft contents. 64

Stellenbosch University http://scholar.sun.ac.za

Figure 4-8: Gradient profile of the DMF/THF mobile phase vs elution time for the gradient chromatographic separation of PMMA-g-PDMS samples (Symmetry300 C18 column, 5µm, 1 ml/min, 30°C) 65

Figure 4 9: Gradient HPLC chromatograms for polymers containing PMMA backbones with different graft contents. 65

Figure 4-10: Infrared spectra showing the presence of PDMS in fraction 2 (copolymer), but not in fraction 1 (PMAA homopolymer) 67

Figure 4-11: Graph showing the influence of increasing PDMS content on the average fibre diameters and the width of the distribution. 70

Figure 4-12: Bar graphs showing fibre diameter distributions in polymers. (A) PMAA homopolymer (B) 8.6 mol % pdms, (C) 12.2 mol % pdms, (D) 21.4 mol % pdms, (E) 30.6 mol % pdms, (F) 31.5 mol % PDMS 71

Figure 4-13: Rheology curves for polymers containing different PDMS contents (PDMS = 1000 g/mol) (10 wt %) 72

Figure 4-14: Typical images obtained by casting dilute solutions of polymers in DMF on copper grids. (A) PMAA homopolymer (B) 8.6 mol % PDMS (C) 12.2 mol % PDMS (D) 21.4 mol % PDMS (E) 30.6 mol % PDMS (F) 31.5 mol % PDMS 75

Figure 4-15: Example of the beading/spraying observed when fibres are electrospun at high voltages (8.6 mol % PDMS sample shown as example) 76

Figure 4-16: Graphs of fibre diameter and distribution as a function of voltage for samples with different PDMS contents (A) PMAA homopolymer (B) 8.6 mol % PDMS (C) 12.2 mol % PDMS (D) 21.4 mol % PDMS (E) 30.6 mol % PDMS (F) 31.5 mol % PDMS 78

Figure 4-17: Graphs illustrating the influence of solvent on the fibre diameters for samples with different PDMS contents. (A) PMAA homopolymer (B) 8.6 mol % PDMS (C) 12.2 mol % PDMS (D) 21.4 mol % PDMS (E) 30.6 mol % PDMS (F) 31.5 mol % PDMS 80

Figure 4-18: FE-SEM images for the sample containing 21.4 mol % PDMS (A) surface (B) embedded in resin 82

Figure 4-19: Typical FE-SEM images of the surface and internal morphology for copolymer containing 21.4 mol % PDMS as function of solvent composition: A+D) DMF B+E), DMF/CHCl3 (8:2), C+F) DMF/CHCl3 (7:2) 83

Figure 4-20: Surface morphology for fibres with different PDMS content: (A) PMAA homopolymer, (B) 12.2 mol % PDMS, (C) 21.4 mol % PDMS 83

Stellenbosch University http://scholar.sun.ac.za

Figure 4-21: Images showing the change in SCA with increasing PDMS content from A to E 87
Figure 4-22: SCA as a function of PDMS content 88
Figure 4-23: Change in SCA over time for polymers with different PDMS contents. 89
Figure 4-24: Series of images showing how the contact angle changed with time for a sample containing 8.6 mol % PDMS 90
Figure 4-25: Fibre weight as a funtion of time until equilibrium is reached 91
Figure 4-26:τ_1 and τ_2 values as a function of PDMS content 92
Figure 4-27: Equilibrium moisture values (β) as a function of the PDMS content 93
Figure 4-28: SEM images after equilibrium moisture content was reached for samples (A) PMAA homopolymer (B) 8.6 mol % PDMS (C) 12.2 mol % PDMS (D) 21.4 mol % PDMS (E) 30.6 mol % PDMS 95
Figure 4-29: SEM images for samples (A+D) 21.4 mol % PDMS (B+E) 30.6 mol % PDMS (C+F) 31.5 mol % PDMS. The top row was taken after 5min of water exposure and compared to the bottom row which was after 3 hours. Other samples formed films when immersed for 3 hours so no images are included 97
Figure 4-30: Influence of cyclodextrin concentration on the fibre diameters for PMAA homopolymer and a high PDMS content copolymer 101
Figure 4-31: Images showing the swell differences with crosslinking time for a representative sample (containing 21.4 mol % PDMS with 10 % cyclodextrin) (A) 20 min (B) 30 min (C)60 min (D) 120 min 103
Figure 4-32: Influence of crosslinker concentration on fibre swelling. PMAA homopolymer containing (A) 0.8 wt % (B) 2 wt % (C) 4 wt % (D) 5 wt % nanocellulose crosslinked for 60 min and submerges for 5 min 104
Figure 4-33: Weight percent increase with time in a high humidity atmosphere for polymers containing 4% cyclodextrin and crosslinked for 60 min 105
Figure 4-34: TGA curves show the water loss between 20 and 160°C for samples containing cyclodextrin before moisture absorption measurements 107
Figure 4-35: SEM images showing the morphology of fibres after 5 min (left) and 3 hours (right) for samples containing 4% cyclodextrin and crosslinking time of 60 min (A) 8.6 mol % PDMS (B) 12.2 mol % PDMS (C) 21.4 mol % PDMS (D) 30.5 mol % PDMS (E) 31.6 mol % PDMS 108
Figure 4-36: Influence of nanocellulose on the fibre diameters 111

Stellenbosch University http://scholar.sun.ac.za

Figure 4-37: Influence of concentration on fibre swelling for PMAA homopolymer containing (A) 0.8 wt % (B) 2 wt % (C) 4 wt % (D) 5 wt % nanocellulose crosslinked for 60 min and submerges for 5 min 112
Figure 4-38: Moisture absorption graphs for polymers containing 4 wt % NCC 114
Figure 4-39: Comparison of τ_1 and τ_2 values as a function of PDMS content for fibres with and without NCC 115
Figure 4-40: Comparison of β values for samples with and without any NCC 116

List of schemes

CHAPTER 3

Scheme 1: Synthesis of PMAA-g-PDMS copolymers via free radical copolymerization 46
Scheme 2: Synthesis of PMMA-g-PDMS from PMAA-g-PDMS precursors 47

List of tables

CHAPTER 4

Table 4-1: Table comparing the target PDMS molar ratios to the ratios measured from ^{1}H-NMR of PMMA-g-PDMS copolymer 57
Table 4-2: Summary of the feed composition, molar mass and PDMS content of the copolymer as determined from ^{1}H-NMR 60
Table 4-3**:** Summary of the electrospun fibre diameters with and without crosslinker, as well as after crosslinking and moisture exposure 99
Table 4-4: Parameters for polymer moisture absorption curves as fitted to Equation 4.1 for polymers crosslinked with cyclodextrin 105

Stellenbosch University http://scholar.sun.ac.za

Table 4-5: Table relating the initial moisture content to the moisture absorption 107

Table 4-6: Fibre diameters for some copolymers containing 4 wt % NCC 113

Stellenbosch University http://scholar.sun.ac.za

Chapter 1 Introduction

1.1. GENERAL INTRODUCTION

Hydrogels are macromolecular networks that swell, but do not dissolve, in water. The ability of hydrogels to absorb water arises from hydrophilic functional groups attached to the polymeric backbone, while their resistance to dissolution arises from crosslinks between network chains. These crosslinks may be chemical or physical in nature[1]. Substances are typically termed as hydrogels when the amount of water retained in them is between 20 and 100% of the total weight. When the water content exceeds 100% these hydrogels are called superabsorbent hydrogels. A hydrogel can be considered as a "container" of water made of a three dimensional mesh. Many materials, both naturally occurring and synthetic, fit the definition of hydrogels. Crosslinked dextrans and collagens are examples of natural polymers that are modified to produce hydrogels. Classes of synthetic hydrogels include poly(hydroxyalkyl methacrylates), poly(acrylamide), poly(N-vinyl pyrrolidone), poly(acrylic acid), and poly(vinyl alcohol).

Hydrogels are used in applications where the absorption of fluids is required, for example in diapers. It is also used to absorb and retain water in soil. This is important for agricultural use in dry areas where water will be stored in the ground for longer periods of time, preventing dehydration of the ground[2]. Amphiphilic crosslinked networks consisting of poly(dimethylsiloxane) (PDMS) and poly(methacrylic acid) (PMAA) were investigated for this purpose[3]. The inclusion of hydrophobic segments allows for variable release properties to be obtained. Other applications of hydrogels include construction[2], packaging[2], wastewater treatment, sealing materials, and drug delivery systems[4].

There are many potential advantages of producing nanofibrous hydrogels. For example nanofibre texture can enhance mass transport of ions and chemicals from solutions to enzymes and cells that may be embedded in the hydrogel. However, production of hydrogels in a nanofibre form has been a difficult challenge. Since they are composed of cross-linked networks

Stellenbosch University http://scholar.sun.ac.za

of hydrophilic polymers, hydrogels can swell in aqueous solution but not dissolve or melt. Because of this, the typically hydrogels cannot be processed directly with the electrospinning method, which is one of the most widely used techniques to produce polymeric nanofibres from polymer solutions or melts. The only option for using the electrospinning technique is to process the materials into nanofibres and then subject the fibres to some form of post spinning crosslinking or have some form of reactive crosslinking during the electrospinning process.

In the current study, novel poly(methacrylic acid)-graft-poly(dimethylsiloxane) copolymers (PMAA-g-PDMS) were synthesised and investigated as possible new materials for the production of polymer nanofibre hydrogels. The purpose of the study was to study the effect of the PDMS inclusion would have on the morphology and properties of the nanofibre hydrogels primarily with regards to their ability to control the rate and extent of the water uptake (PDMS is very hydrophobic), as well as the surface and internal fibre morphology. The material have also been investigated in terms of the hydrogel stability with regards to ”physical crosslinks” due to the phase separated hydrophobic domains of the PDMS in the nanofibres. Post electrospinning crosslinking of the nanofibres has also been explored.

The challenge to spin fibres in nano dimension with significantly increased surface area is no more. Various polymers have been shown to be electrospun into nano dimensions already[5-9]The challenge nowadays is more directed towards the optimization and control of surface area and fiber morphology in order to be able to design properties and tailor make fibres for specific applications[10-12]. Complex architectures can be obtained such as core-shell, hollow, internal microphase separated, and porous[13-17]. A number of ways exist by which the fiber morphology can be altered, such as controlling and understanding the influence of the electrospinning conditions, controlling/changing the spinning solution, or changing the electrospinning setup. A lot of information is available on the control of electrospun fibres by varying electrospinning conditions, but much less information is available on the interesting fibre morphologies that can be realised when the behaviour of polymers in solution is manipulated. In this study, highly amphiphilic graft copolymers of PMAA-g-PDMS have been electrospun. The electrospinning of these amphiphillic materials offer the possibility for the investigation of how the fibre morphology may be manipulated by varying the electrospinning solution parameters. Due to the amphiphillic

Stellenbosch University http://scholar.sun.ac.za

nature, it would be expected that the self-assembled solution structure would be influenced by changing the solution parameters.

Amphiphilic graft material solution behaviour is not as well studied as that of block copolymers and blends. Complex solution behaviour and multiple types of associations that are possible[18] contribute to the fact that graft copolymer behaviour is less represented in literature. This same observation is made i.t.o. electrospinning. Although less studied than other electrospinning parameters, various authors have shown that fine structure and porosity of fibers can be obtained by electrospinning self-assembled polymer solutions of blends[13;19] and block copolymers[20;21]. These studies showed that structures in and on the fibres was related to the self-assembly behaviour of the polymers. The transfer of structure was actualized by the rapid evaporation of solvent during the electrospinning process. The time scale of evaporation, stretching, and solidification of the polymers, is much smaller than the relaxation times of the polymers to obtain equilibrium structures. A thermodynamically unstable system where polymer rich phases dry before polymer poor phases is thus created, essentially leading to porous fibers with polymer domains resembling that of the solution[22]. It was only recently that Bayley and Mallon were the first to reveal how graft copolymers of PAN-g-PDMS could be electrospun to produce fully porous fibres[23]. The fibre structures related well to structures observed for films prepared from dilute solution, indicating that the different phase separated structures had an influence on the fine structure that was observed. This study aimed to follow up on this finding using PMAA-g-PDMS. PMAA-g-PDMS is highly amphiphilic, but differs from the PAN-g-PDMS in the sense that no crystallisation occurs during electrospinning, which should have a big influence on the fiber morphology.

The graft copolymers were synthesized using a grafting through approach where methacryloxy terminated PDMS was used as macromonomer. This technique was already used to successfully synthesise PAN-g-PDMS[23] and PMMA-g-PDMS[24] using the methacryloxy terminated PDMS as macromonomer. The two polymers chosen have very different properties, the biggest difference being the hydrophobicity. PDMS is very hydrophobic and is usually used to induce superhydrobhobicity to materials. PMAA on the other hand is very hydrophilic and water soluble. Characterization of the materials was performed using techniques such as ^{1}H-NMR, ATR-FTIR, SEC, and HPLC.

Stellenbosch University http://scholar.sun.ac.za

PMAA has been investigated in applications such as soil release, removal of copper from water, and superabsorbent materials. The difficulty with fibres formed from water soluble polymers is the fact that they will dissolve in water, even in moisture, which is usually undesired. In addition, when nanofibres are used, the loss of fibres, or in some cases excessive swelling, will eliminate the advantages gained by using nanomaterials. To overcome this crosslinking is usually employed. Crosslinking can include the interactions such as hydrogen bonding, ionic bonding, non-polar interactions, chain entanglements, or the formation of crystals which connect the chains[1;25]. Other studies have shown how hydrophobic interactions can be used to obtain swellable materials and improve the mechanical properties of polymer hydrogels[26]. In the present study the influence of PDMS on the stability and swelling of PMAA was investigated.

1.2. OBJECTIVES

The objectives of this study were as follows:

- The direct synthesis of PMAA-g-PDMS via grafting through approach
- Characterization of the copolymers using ^{1}H-NMR, FTIR, SEC, HPLC
- Optimisation of spinning conditions for PMAA-g-PDMS polymers
- To investigate the influence of the PDMS content on the morphology of the fibres
- To investigate how the structures formed from the amphiphilic molecules in solutions with different solvent qualities will affect the fibre morphology
- To investigate how PDMS affects the hydrophobic properties of the fibre mats
- Determine the ability to control the rate and extent of the water uptake by PDMS content
- To determine the effect of chemical crosslinking on PMAA-g-PDMS copolymer behaviour

Stellenbosch University http://scholar.sun.ac.za

1.3. REFERENCES

1. Hoffman, A. S. *Advanced Drug Delivery Reviews,* **2002,** 54, (1), 3-12

2. Philippova, O. E., *Polymer Science, Series C,* **2000,** 42, 208

3. Rusu, T., Loan, S. & Corneliu Buraga, S. *European Polymer Journal,* **2001,** 37, (10), 2005-2009

4. Wang, W. & Wang, A. *Carbohydrate Polymers,* **2010,** 80, (4), 1028-1036

5. Huang, G., Dong, F., Wang, J. & Jia, Y. *Polymer Degradation and Stability,* **2012,** 97, (6), 1067-1073

6. Sun, J., Bubel, K., Chen, F., Kissel, T., Agarwal, S. & Greiner, A. *Macromolecular Rapid Communications,* **2010,** 31, (23), 2077-2083

7. Fong, H. & Reneker, D.H. *Journal of Polymer Science Part B: Polymer Physics,* 37, (24). 3488-3493

8. Qin, X., Yang, E., Li, N. & Wang, S. *Journal of Applied Polymer Science,* **2007,** 103, (6), 3865-3870

9. Greiner, A. & Wendorff, J. *Angewandte Chemie International Edition,* **2007,** 46, (30), 5670-5703

10. Ma, M., Hill, R. M., Lowery, J. L., Fridrikh, S. V. & Rutledge, G. C. *Langmuir,* **2005,** 21, (12), 5549-5554

11. Ruotsalainen, T. *Advanced Materials,* **2005,** 17, (8), 1048-1052

12. Ruotsalainen, T. *Soft Matter,* **2007**, 8, (3),978

13. Zhang, J. & Nie, J. *Polymer International,* **2012,** 61, (1), 135-140

14. Pakravan, M., Heuzey, M., Ajji, A. & Pakravan, M. *Biomacromolecules,* **2012,** (2), 412

15. Wei, M., Lee, J., Kang, B. & Mead, J. *Macromolecular Rapid Communications,* **2005,** 26, (14), 1127-1132

16. Nayani, K., Katepalli, H., Sharma, C. S., Sharma, A., Patil, S. & Venkataraghavan, R. *Industrial & Engineering Chemistry Research,* **2012,** 51, (4), 1761-1766

17. Dayal, P., Liu, J., Kumar, S. & Kyu, T. *Macromolecules,* **2007,** 40, (21), 7689-7694

18. Kikuchi, A. & Nose, T. *Society,* **1997,** 9297, (96), 896-902

Stellenbosch University http://scholar.sun.ac.za

19. Valiquette, D. & Pellerin, C. *Macromolecules,* **2011,** 44, (8), 2838-2843

20. Ma, M., Krikorian, V., Yu, J. H., Thomas, E. L. & Rutledge, G. C. *Nano Letters,* **2006,** 6, (12), 2969-2972

21. Kalra, V., Kakad, P. A., Mendez, S., Ivannikov, T., Kamperman, M. & Joo, Y. L. *Macromolecules,* **2006,** 39, (16), 5453-5457

22. Lin, J., Ding, B., Yu, J. & Hsieh, Y. *ACS Applied Materials & Interfaces,* **2010,** 2, (2), 521-528

23. Bayley, G. M. & Mallon, P. E. *Polymer,* **2012,** 53, (24), 5523–5539

24. Swart, M., Olsson, R. T., Hedenqvist, M. S. & Mallon, P. E. *Polymer Engineering & Science,* **2010,** 50, (11), 2143-2152

25. Lee, S. J., Lee, S. G., Kim, H. & Lyoo, W. S. *Journal of Applied Polymer Science,* **2007,** 106, (5), 3430-3434

26. Cui, J. *Biomacromolecules,* **2012,** 13, (3), 584-588

Stellenbosch University http://scholar.sun.ac.za

Chapter 2 Literature Review

2.1 Graft copolymers

Polymers used in this study consist of a poly(methacrylic acid) backbone with poly(dimethylsiloxane) grafts. Graft copolymers are types of branched polymers which consists of long, linear sequences of one monomer (known as the backbone), with long sequences of a second monomer (branches) attached to it, forming a “brush-like” structure. In most cases the grafts/branches consist of different monomers to that of the backbone, although grafts of homopolymers have been synthesised. Three different routes exist for the synthesis of these types of polymers (illustrated in Figure 2-1). A short discussion on each will follow.

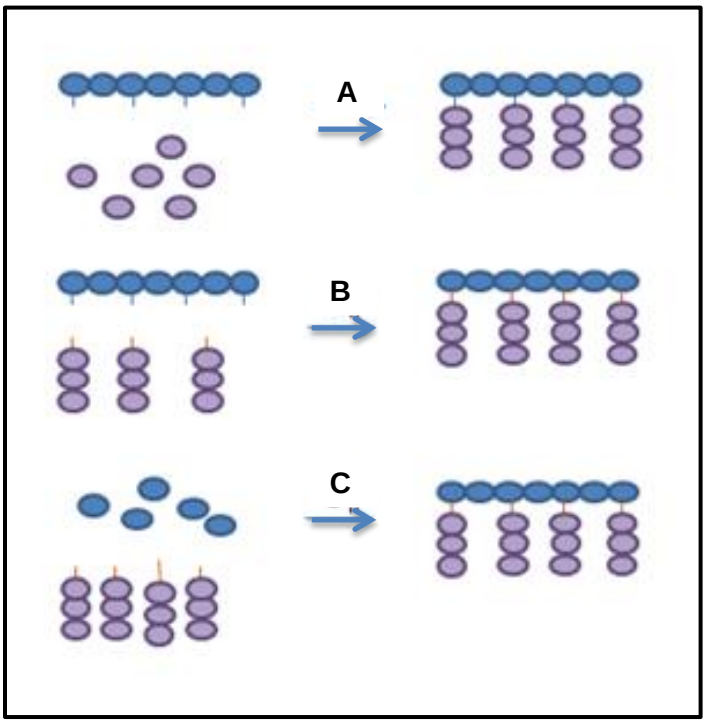

Figure 2-1: Simple illustration of the three routes that can be followed to obtain graft copolymers: (A) grafting from, (B) grafting onto, (C) grafting through

Stellenbosch University http://scholar.sun.ac.za

2.1.1 Grafting from

Grafting from, as the name suggests, involves the growing of polymer chains from the backbone. As a first step, a backbone is synthesised which should have reactive groups able to initiate the polymerization of branches in a second reaction. Reactive groups are either present in the monomer itself, or comonomers containing reactive groups are added[1;2]. Post-modification of reactive groups is also a possibility to obtain the desired functionality. For example, olefins can be transformed into ATRP initiators via hydrosilation[3].

This technique has the advantage of allowing one to control the number and density of branches by controlling the number of active sites introduced into the polymer backbone. In addition, the functional groups can be chosen to suit various controlled polymerization techniques such as ATRP, RAFT and ionic polymerisation[4]. The use of these reactions allows control over molecular weight and molecular weight distribution of the side chains.

The grafting from technique is also often used for the post electrospinning modification of fibres. Reactive groups are present on the polymer being electrospun, followed usually by ATRP or other living radical reactions. Fibres with different functionalities, properties and morphologies such as core-sheath fibres can be obtained in this way[5]. A good example for this is styrene maleic anhydride (SMA) copolymers. The anhydride functionality allows easy modification using reactions with a variety of functional groups such as alcohols, amines, and thiols. Anti-microbial molecules can, for example, be attached to fibres electrospun form SMA copolymers[6].

2.1.2 Grafting onto

The polymer backbone and branches are synthesised during two separate polymerization reactions. The reactions are carried out using living or controlled polymerization techniques in order to control the molecular weights and dispersity index of both the branches and backbone.

Stellenbosch University http://scholar.sun.ac.za

As with grafting from, functional groups are distributed through the backbone. These groups will be able to react with end-groups of the branch polymers directly or after changing the functionality of the monomer units after polymerization[7;8].

A coupling reaction is used to attach the functional groups present on the backbone with end groups from the graft polymer chains[9]. This route can also be used to functionalize fibres, which opens up a route to get nanofibres for otherwise unspinnable polymers or molecules. One example is the introduction of azide groups which are not compatible with the electrospinning process[9].

2.1.3 Grafting through

This is the only technique that does not require the pre-synthesis of a functionalized backbone. Instead, a copolymerization reaction between backbone monomers and macromonomers of the branches are used. This of course means that the amount and distribution of the branches will be controlled in a different way as with the other reactions, since in this technique there is not the possibility of controlling the number and concentration of reactive groups prior to brush formation. Other factors play a role in this case, such as the ratio of macromonomer to monomers and their reactivity ratios[4].

The initial ratio of monomers added will, to some extent, determine the ratio of monomers in the final product. The reactivity ratios will influence how the grafts are distributed as well as their inclusion in the final polymer. Reactivity ratio refers to ratio of the reactivity of one monomer vs the other. Similar reactivity ratios indicate that a more or less alternating polymer can be obtained, as monomers have similar reactivates.

Techniques such as ATRP and RAFT can also be used to produce backbones with controlled molar mass and dispersity indexes. Shinoda *et al.*[10] compared PMMA-g-PDMS polymers

Stellenbosch University http://scholar.sun.ac.za

synthesised using three different techniques: normal free radical, ATRP and RAFT. Different distributions of grafts were found. They gave a good representation of how grafts can be distributed using the different reactions. This is shown in Figure 2-2. Polymer F represents a polymer prepared from conventional free radical reactions. The distributions as illustrated depend on the reactivity ratios and concentrations of the monomers.

In the case where big differences exist between the reactivity ratios, a gradient distribution will be found. During the early stages of polymerization the monomer with higher reactivity ratio will tend to homopolymerize, with little inclusion of the comonomer. As the concentration of this monomer is reduced, incorporation of the second monomer will increase. In Figure 2-2 this can be observed from top to bottom – representing the start and end of the reaction. The first part of the chains will thus consist mostly of homopolymer of higher reactivity ratio (top row of polymer F). The polymers towards the end will consist of a large number of branches/lower reactivity monomer (bottom row of polymer F).

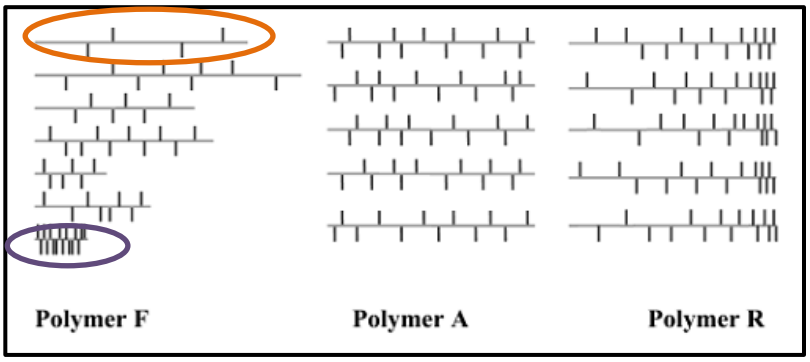

Figure 2-2: Illustration of the different graft distributions which can be obtained via different reaction routes. Polymer F – normal free radical, Polymer A – ATRP, Polymer R - RAFT[10]

Various polymers have been synthesised using this technique and employing different macromonomers such as: PDMS macromonomers[11;12] PEO-alkyl macromonomer, polystyrenes[13] and polyolefin macromonomers. Macromonomers are synthesised by anionic polymerizations, ring-opening metathesis or radical polymerizations[14]. Based on the discussion above regarding the polymerization, it is clear that in this study we can expect complex polymers with a wide range of branch distributions. The incompatibility, as well as the big

Stellenbosch University http://scholar.sun.ac.za

difference in reactivity ratios, between PDMS macromonomer and MAA monomers used in this study, will contribute to this. In addition, the highly amphiphilic nature of the copolymers should affect the solution properties and final fibre morphology due to phase separation.

2.2 ELECTROSPINNING

Electrospinning has become an increasingly important and well-studied research field since the 1990s. This was after the publications from Reneker's group[15;16] sparked renewed interest into a field that dates as far back as 1900. It all started with J.F. Cooley who patented the technique[17]. This was followed by Anton Formals who, between 1934 and 1944, were the first to use and publish a series of patents on the application of the technique to produce textile yarns[18-24]. As knowledge about the potential application of nanofibres in fields such as high efficiency filter media, protective clothing, catalyst substrates, and adsorbent materials grew, so also did research in this area. Nowadays, it is well known to be one of the most successful and simplest techniques to produce sub-micron fibres[25].

The technique owes its popularity to the relative simplicity, easy to understand, easy to use, and straightforward setup. A few other techniques to produce nanofibres exist such as self-assembly, phase separation, chemical vapour deposition, and nanolithography, but these techniques are usually more expensive and labour intensive. The electrospinning setup is simple; Figure 2-3 shows a simple diagram of the setup. It consists of a spinneret, voltage supply, syringe pump, and collector.

The process consists of a complex interplay between a number of forces which include surface tension, electrostatic, viscoelastic, and gravitational forces[26;27]. A liquid droplet held at the tip of the spinneret (in most case a blunt steel needle) by surface tension, is charged by connecting it to one of the electrodes from the voltage supply. A collector, usually a piece of foil, is either neutral or charged with opposite charge to that of the spinneret. This creates an electric field which is responsible for the electrostatic force that opposes that of the surface tension. The

Stellenbosch University http://scholar.sun.ac.za

balance between these two forces causes the formation of a cone shaped structure known as the Taylor cone[25]. When the electrostatic force becomes high enough, liquid jets are ejected from the Taylor cone. As a result of mutual charge repulsion, the jet undergoes a whipping motion and follows a spiral path during which solidification occurs. The speed by which the fluid is ejected from the spinneret is controlled with a syringe pump. A detailed report on the stages of the electrospinning process is available from a paper by Garg and Bowlin[26].

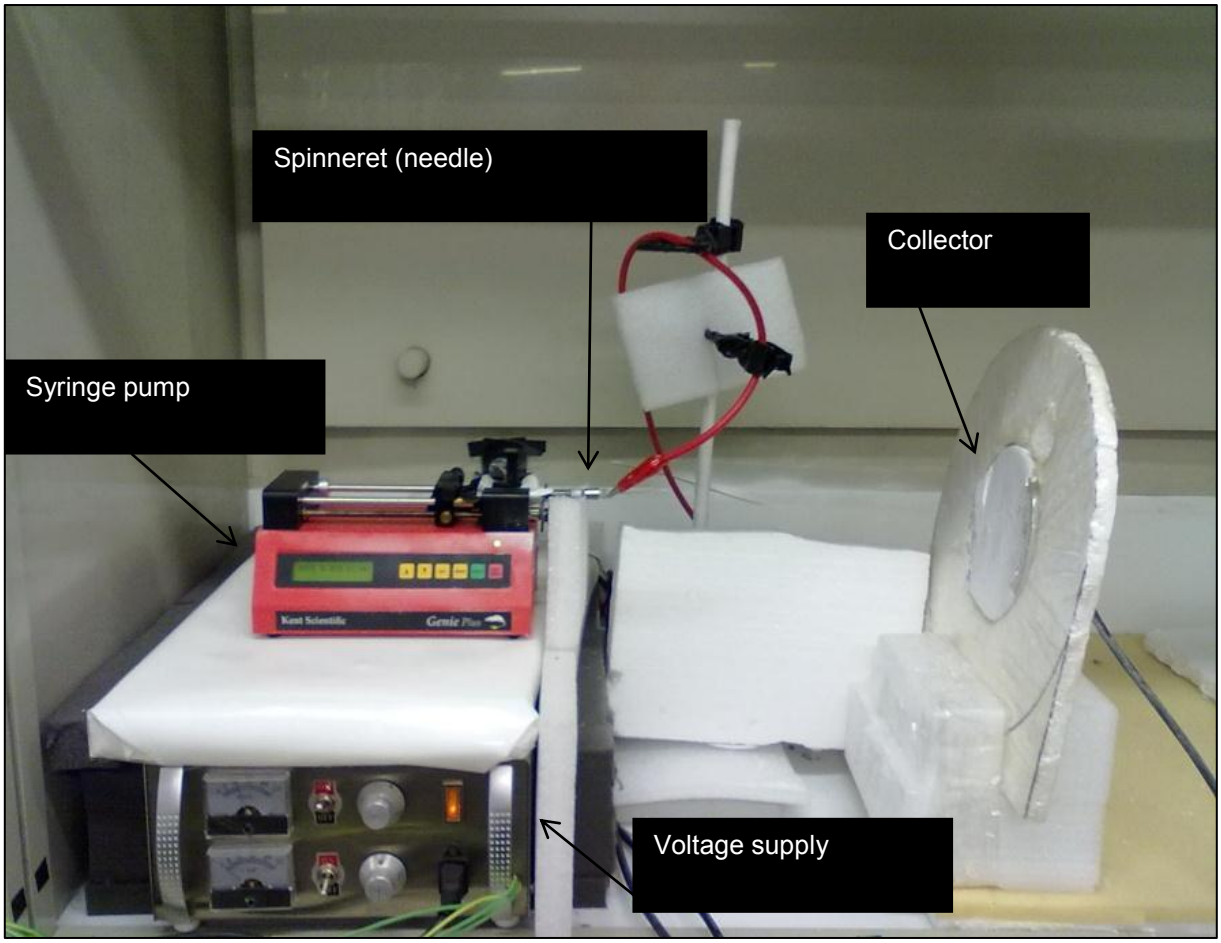

Figure 2-3: Illustration of the electrospinning setup used in this study

Stellenbosch University http://scholar.sun.ac.za

2.2.1 Fibre morphology

Although the setup for electrospinning is simple, the process itself is a complex interplay between factors such as the electrical charges, surface tension, solvent evaporation, solidification, stretching, and rheology[28]. The structure of polymer fibres is controlled simultaneously by the combined effects of solvent evaporation and the stretching of the jet. The process is very rapid, with fibres reaching the collector in about 0.1s. Such fast fibre formation can lead to non-equilibrium morphologies in the fibres, and in the case of crystallisable polymers, the crystal structures are imperfect and small.

Figure 2.4 shows a schematic illustration of the processes that occur when fibres are electrospun. The initial liquid jet consisting of polymer and solvent molecules undergo flash vaporization once ejected from the Taylor cone[25]. At this time, there is a simultaneous movement of solvent molecules outward and air molecules inward at the jet-skin interface. The flash vaporization reduces the temperature due to the heat of vaporization taken up from the surroundings. This cooling effect is responsible for thermally induced phase separation which results in polymer rich and polymer poor domains. Both amorphous and semi-crystalline polymers will undergo liquid-liquid separation. Phase separation occurs by spinodal or bimodal decomposition. In addition to this, semi-crystalline polymers have simultaneous crystallization occurring[29].

Stellenbosch University http://scholar.sun.ac.za

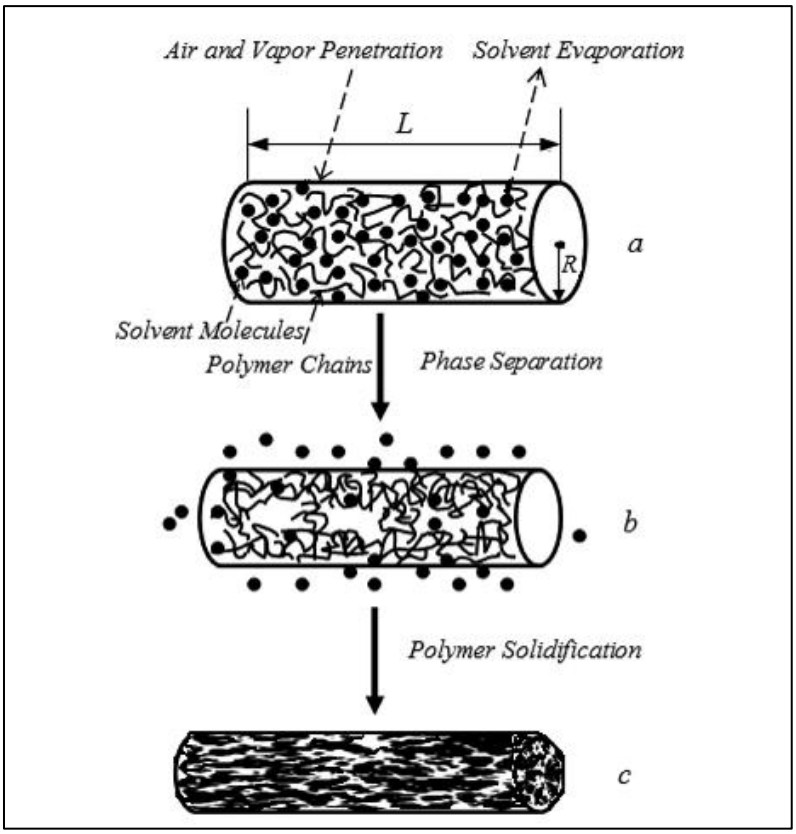

Figure 2-4: Schematic illustration of the processes that occur during electrospinning[29]

It is possible to control the morphology of the fibres by manipulating the various factors that has an influence on the process. Three main variables exist which can be used to manipulate fibre morphology namely, electrospinning conditions, polymer solution properties, and variation of the electrospinning setup.

2.3 Electrospinning parameters

Most research in electrospinning initially focused on how the electrospinning parameters influenced the mat properties and fibre morphology such as fibre size, and shape. Less research was focused on the internal fibre morphology and how this can be manipulated[30]. The factors that influence spinning are divided into three main categories with their sub categories

Stellenbosch University http://scholar.sun.ac.za

as indicated in Figure 2-5[25]. This organisation, however, makes no mention of another important solution parameter - the self-assembly behaviour of polymers in the electrospinning solution. The self-assembly of polymer molecules may have a remarkable influence on how the polymers behave under electrospinning conditions[31;32]. For this reason it was deemed necessary in this review to report this as a separate and important solution parameter (indicated as the shaded block). The current study initially focused on this parameter.

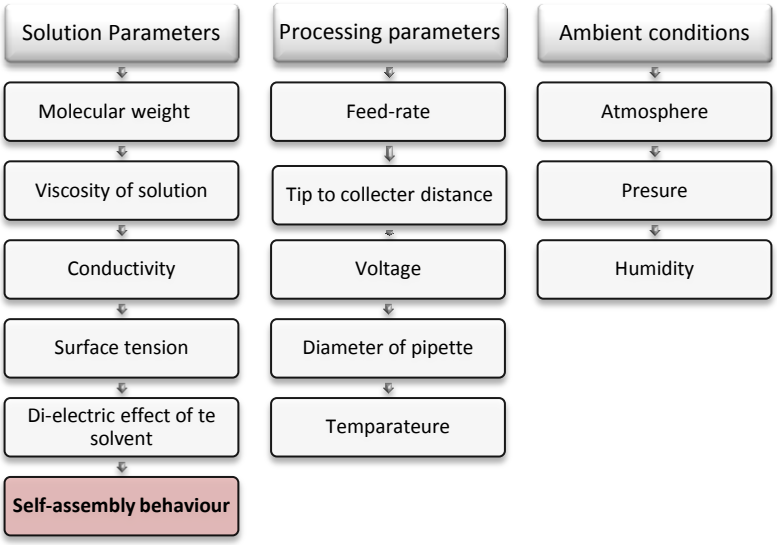

Figure 2-5: Diagram showing the factors that influence the electrospinning process

Excellent reviews are available with detailed discussions on how these parameters affect the fibre properties[26;33;34]. Here, the discussion will focus on the parameters which have a significant influence not only on the mat properties, but also on the internal phase morphology of the fibres.

Stellenbosch University http://scholar.sun.ac.za

2.3.1 Molecular weight, solution viscosity and surface tension

As mentioned during the discussion on the process of electrospinning, the polymer solution is subjected to strong pulling forces. This places an important requirement on the solution to be able to resist the forces without the jet breaking apart. The ability to do this depends very much on the entanglement density. With sufficient entanglements present, the polymer molecules will be able to form a continuous, stable electrospinning jet instead of a spray. The entanglement density is a function of the molar mass as well as the concentration of the solution. Higher molar mass molecules will obviously entangle more than small molecules, so a certain minimum molar mass is required for electrospinning to occur. As the molar mass and the entanglement density increase, so also does the viscosity. This has consequences in terms of the ability of the fibre to be pumped, the fibre diameter and fibre breakage. Since viscosity is the resistance of the polymer solution to flow, the higher viscosity solution will be stretched less in an electric field, when compared to a solution of lower viscosity (less resistance to the stretching due to the force)[35;36]. This reduced stretching will generally lead to fibres with larger diameters. Too high viscosities will prevent pumping of the solution and premature drying[37]. The latter of course will lead to large fibre diameters, or in severe cases, to fibre breakage before the collector is reached.

Another consequence of changing the molar mass is the change in surface tension. The surface tension is related to the tendency of solvent molecules to be attracted to each other. When the polymer concentration is low, the solvent molecules will tend to cluster together, which will be observed as beads. In some cases the addition of surfactant or the use of a solvent with a lower surface tension is required in order to prevent beading of the fibres[25].

Wei *et al.*[38] demonstrated how the texture and internal morphology of fibres of polymer blends show a dependence on molar mass. PANI/PMMA blends showed beaded structures when low molar mass PMMA was used, whereas elongated, dispersed PANI domains were observed with higher molar mass PMMA. The variation of surface tension is responsible for the phenomenon. In the case of lower molar mass PMMA, the PANI molecules will tend to aggregate and form

Stellenbosch University http://scholar.sun.ac.za

spherical domains. The reduced surface tension that results when using higher molar mass molecules reduced the tendency of PANI to form aggregates.

The mobility of different molar masses before solidification occurs can also play an important role. Fibres with core-sheath morphology could be produced using low molar mass PANI in blends with PS and PC. This could not be achieved with higher molar mass PANI, as it requires the PANI to migrate to the surface during phase separation in a very short time frame. Higher molar mass molecules will not be able to do this[38]. The formation of other ordered structures with higher molar mass chains are hindered because of the increased relaxation time for these chains[39].

The surface porous morphology of the fibres is also affected by varying the molar mass of the polymer. Polystyrene of high molar mass electrospun in humid atmosphere showed larger pores with a larger distribution when compared to lower molar mass polymers[40]. Pore formation occurs on some fibres when electrospun in humid atmosphere due to condensation of water droplets on the fibre surface. Fast evaporation leads to cooling at the surface, this in turn will cause condensation of water droplets. The droplets will grow, until it also eventually evaporates. So essentially what happens is that the water will evaporate later, after solidification of the polymer surface. It is this complete evaporation of solvent and water droplets that leads to the phenomena of what is known as breath figures (pores on the surface). The size and shape of pores is influenced by the moisture content, but also, as mentioned, the molar mass[41].

2.3.2 Solution conductivity and solvent dielectric properties

The ability of the spinning solution to carry charges is of the utmost importance during electrospinning. The technique relies on a charged solution to be pulled by an electrostatic force. Electrical conductivity is achieved either by the inherent conductivity of the polymer and/or solvent combination, or by the addition of additives. The dielectric constant of the solvent is one of the determinants of conductivity. Solvents such as DMF have high dielectric constants which

Stellenbosch University http://scholar.sun.ac.za

mean they will be charged to a greater extent than a solvent such as THF. When the same sample is electrospun in DMF and THF, the fibre diameter is much lower for the DM solvent[37;40]. Higher conductivity leads to greater forces acting on the fibre jet as well as more charge repulsion due to a higher number of charged groups. This will increase the bending instability which again increases the path length. An increased path length will result in more time for the fibre to be stretched; resulting in thinner fibres. In addition, the formation and preservation of phase-separated structures seems to be influenced in an important way by the stretching forces. When the same force is applied to samples of different viscosities (different concentration), the lower viscosity sample will be stretched more[25].

Conductivity is not only a determinant of spinability, but also influences the fibre morphology. The impact of conductivity on the surface porous structure of polystyrene was reported by Lin *et al.*[29] Samples with different concentrations (and thus different conductivities and electrostatic forces) showed different porous structures when electrospun under the same conditions. The lower concentration sample, with lower viscosity and higher conductivity, had deformed pores that were elongated along the fibre axis. This was as a result of the greater force acting on the fibres in this case. The comparison of pore structures of two different concentrations is shown in Figure 2-6.

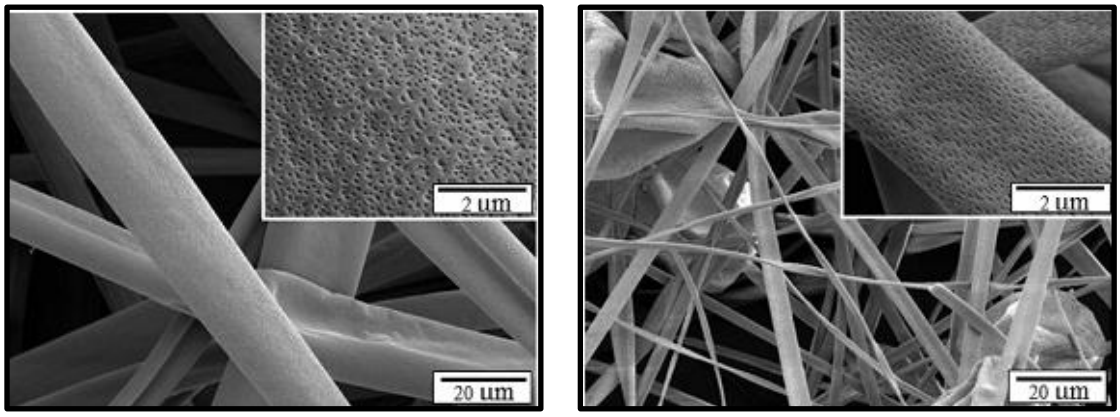

Figure 2-6: Influence of polymer concentration on the porous structures of polystyrene[29]

Stellenbosch University http://scholar.sun.ac.za

If the polymer and solvent combination does not have a high enough conductivity, additives such as salt need to be added. Adding salt increases the ion content of the solution, which increases the charge carrying capacity[42]. This is also the reason why charged polymers, or polyelectrolytes, have a high intrinsic conductivity, since it contains a larger number of charged groups[43]. The behaviour of polyelectrolytes when charged can be used to obtain more complex morphologies. In the case of chitosan/PEO blends, for example, the polyelectrolyte nature of the chitosan molecules contributed to the formation of core shell structured fibres. The electrostatic tension and Coulombic repulsion lead to the migration of chitosan to the outer layer due to the charging of the chitosan molecules[44].

2.3.3 Temperature

The temperature during electrospinning can influence the fibre morphology in a number of ways by affecting factors such as:

2.3.3.1 Viscosity

The influence of viscosity on the electrospun fibres has already been discussed in Section 2.3.1 and will not be discussed again. Note that in most cases, higher temperatures will lead to a reduced viscosity which could lead to more uniform fibres[25].

2.3.3.2 Evaporation rate of the solvent

The evaporation rate will determine the amount of elongation that the fibres undergo, as dried fibres will not be elongated as much as that still in solution, leading to increased fibre diameters. If the evaporation rate is too fast, premature drying will occur which will cause fibres to break under the influence of the electric field. In the opposite case, if evaporation is too slow, it will cause the fibres to be deposited in a wet state, which will lead to film formation. Using solvents with different vapour pressures thus provides a way to obtain fibres with different sizes[27].

Stellenbosch University http://scholar.sun.ac.za

In addition, the internal and surface morphology will be affected by the evaporation rate. Polycarbonate electrospun from DMF/THF and chloroform showed wrinkles on the surface which the authors described as a "raisin like" structure[36]. The formation of such structures is shown in Figure 2-7. The wrinkles occur when fast evaporation of the solvent from the surface takes place, forming a dried polymer layer surrounding a core which still consists of polymer and solvent molecules. The formation of such a skin layer could be clearly seen in work by Lin *et al.*[29] (See images B and C in Figure 2-8). Diffusion of solvent molecules occurs from this core to the atmosphere, resulting in warping of the fibre.

Similar wrinkled structures were reported more recently for polystyrene electrospun in a DMF/THF solvent mixture. As the vapour pressure of the mixtures were varied, by varying the ratios of the solvent in the mixtures, the surface as well as internal morphologies could be varied (see Figure 2-8 and Figure 2-9). As predicted by theory, high vapour pressure solvents are required to form porous structures on the surface[45]. When high vapour pressure liquids such as DMF are used, the evaporation rate of the solvent is much slower, less cooling occurs, and as a result less condensation of moisture to form pores will occur. Furthermore, the slower evaporation keeps the jets in liquid form for a longer period of time. The polymer rich and solvent rich phases are thus allowed more time to undergo further phase separation under the influence of stretching, and thus the initial polymer rich and solvent rich phases are not preserved as when lower vapour pressure solvents are used[29].

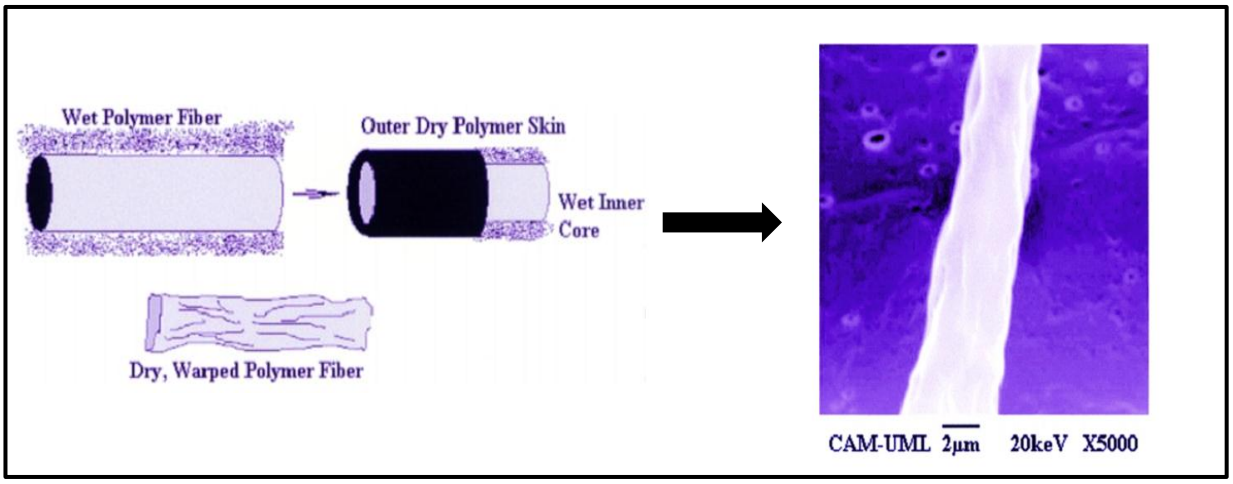

Figure 2-7: Illustration of wrinkle formation that can occur during electrospinning[36]

Stellenbosch University http://scholar.sun.ac.za

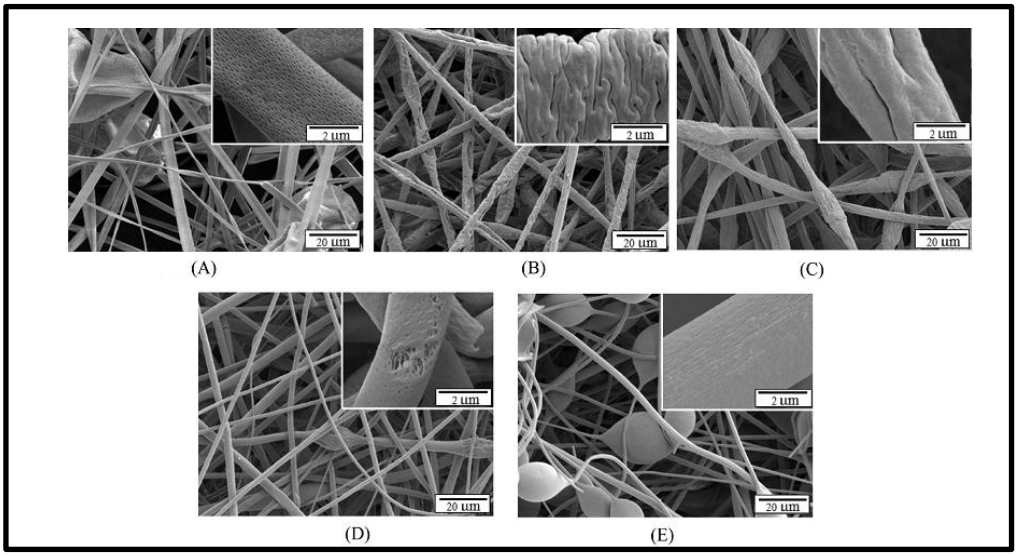

Figure 2-8: Surface morphology of polystyrene fibres formed by electrospinning in solvent mixtures of (A) THF/DMF (4:0) (B)THF/DMF (3:1) (C) THF/DMF (2:2) (D) THF/DMF (1:3) (E) THF/DMF (0:4)[29]

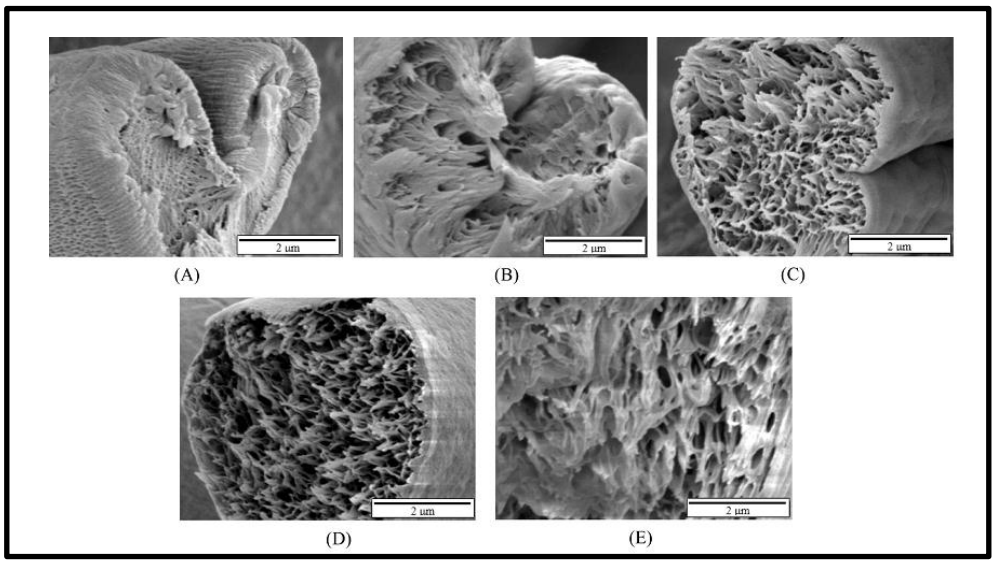

Figure 2-9: Internal morphology of polystyrene fibres formed by electrospinning in solvent mixtures of (A) THF/DMF (4:0) (B)THF/DMF (3:1) (C) THF/DMF (2:2) (D) THF/DMF (1:3) (E) THF/DMF (0:4)[29]

Stellenbosch University http://scholar.sun.ac.za

2.3.4 Polymer solution properties

Mention was made earlier about another parameter which has received less attention when control of fibre morphology and properties is discussed, namely the solution properties. In Section 2.3.4.1 to 2.3.4.3 the complicated structures that may arise when phase separated polymers solutions are electrospun will be discussed. The discussion will include fibre structures obtained from the electrospinning of blends, amphiphilic blocks, and graft copolymers.

2.3.4.1 Blends

Blends of two immiscible polymers are well known to form ordered structures in the bulk. Studies which include the combination of this structural ordering induced by phase separation and the electrospinning process have been investigated as a means to obtain highly structured fibres. Structures such as lamellar, concentric lamellar, core-shell, fibres with elongated spheres and grooves, and porous fibres are examples of what can be obtained[44]. The phase separation of blends is influenced by factors such as the blend ratios, the solubility parameter differences between the blend (solvent selection), molar masses and surface energy[46]. The same factors will also have an impact on the morphology of the fibres electrospun from the blend solutions. During electrospinning, the phase separation of blends is influenced by both the fast evaporation of solvent from the jet, as well as the kinetics of phase separation. In cases where the solvent evaporation is much faster than the kinetics of phase separation, it is possible to obtain miscible fibres from immiscible blends. Films of PLA/polyaniline, an immiscible blend, formed phase separated structures when slow solution casted from a homogeneous solution. When the same solutions were electrospun no phase separation was detected. This observation was attributed to “freezing” of the miscible nature in solution as a result of very fast evaporation of the solvent during electrospinning[47]. With other blends this is not observed. PS/PVME fibres were influenced both by kinetics and evaporation of the solvent[47]. When slow solution casted from a solvent which had a more favourable interaction with the PVME segments, the films showed PVME domains dispersed in the PS matrix. The fibres, electrospun from the same solution, showed core-sheath morphology. This was observed over a range of compositions, with the PVME shell thickness increasing with an increase in the PVME content. When a non-

Stellenbosch University http://scholar.sun.ac.za

selective solvent was used, miscible films and fibres were produced. This indicated that the electrospinning process did not influence the phase separation behaviour of miscible blends.

Blends of PEO and chitosan also formed core-sheath fibres with a chitosan shell. It was possible to control the size of the shell by varying the PEO/chitosan blend ratio[44]. Core shell structures were also observed for binary blends of polyfluorene derivative/poly(methyl methacrylate) (PMMA), but only when high concentration of polyfluorene was used.

The mechanism of core shell and other structure formation was studied by investigating the structure of fibres electrospun from blends of PANI with PC, PS, PMMA and PEO respectively[38]. It was found that solubility parameter differences play a crucial role, as polymers with similar parameters will not undergo enough phase separation. In addition, it was also shown that when PANI is less soluble in the solvent of choice, core shell formation is enhanced, due to the fact that it will demix first. This was also suggested as a driving force for core-sheath formation from PS/PVME blends form $CHCl_3$, where polystyrene will solidify first[47].

Another study highlights the importance of the decomposition mechanism on the fibre morphology. That is, whether it occurs via a nucleation and growth or spinodal decomposition. This was investigated for PEO and PC blends[44]. It was found that in the case where decomposition follows a nucleation and growth mechanism, core-sheath fibres were obtained, with PEO as the core. In the case of spinodal decomposition occurring, microphase-separated morphology was observed. The simultaneous occurrence of both mechanisms were shown to be possible, with the resulting fibres having both phase separated and core sheath structures. It was demonstrated that the blend ratios, in this case the fraction of PEO in a PEO/PC blend, was the determinant factor of which mechanism is followed. This was correlated to the quenching path that the solution follows on the phase diagram for the blend.

Other morphologies such as porous fibres are produced from blends. Commonly this is done by selective removal of one of the components after electrospinning. Examples include blends of

Stellenbosch University http://scholar.sun.ac.za

gelatine and polycaprolactone which produced porous PCL fibres after removal of the gelatine[48]. The same idea was used on fibres spun from PVP/PLA blends[49;50], where specific surface topologies or fine pores were formed. Post-electrospinning removal of one component was also used to produce porous carbon fibres. PAN was electrospun with PMMA and PEO separately. Removal of either PMMA or PEO resulted in porous PAN fibres which, after carbonization, formed porous carbon fibres[48].

Blends of POM/PTU could produce porous fibres without the need for post spinning removal of one of the components[51]. Fibres containing only POM were porous whereas that of homo PTU was not. This was explained by the difference in crystallinity and hydrogen bond capability of the polymers. POM is a semi-crystalline material, during evaporation it will solidify and dry more quickly than PTU. Also, PTU has higher hydrogen bonding capabilities, which will bind the solvent molecules more strongly, thus creating smooth fibres even in humid atmospheres. This shows that it is possible for semi crystalline polymers to produce pores without post spinning modifications.

2.3.4.2 Block copolymers

The electrospinning of block copolymers is of interest due to the possibility of applying these in applications where drug delivery and multifunctional textiles are of interest[52], and where properties such as the surface chemistry needs to be modified. Block copolymers, similar to blends adopt a number of self-assembled structures depending on the composition, molar masses, solvent, and the time frame in which self-assembly occurs. Transformation of these self-assembled structures into fibres has been investigated as a means to tune the fibre properties.

In an effort to obtain superhydrophobic fibres, Ma *et al.*[32] electrospun PS-PDMS block copolymers. Electrospinning of block copolymers of PDMS with styrene made it possible to benefit from the superhydrophobic properties of PDMS, which is not possible for homopolymers

Stellenbosch University http://scholar.sun.ac.za

due to it being a fluid at room temperature. Microporous structures were observed for fibres spun in THF/DMF (3:1). TEM images indicated the formation of elongated PDMS domains in the PS matrix[52].

Another study, involving PS-b-PDMS, investigated the effect of different solvent compositions on the surface morphology, and the resulting static water contact angle (SCA)[53]. Fibres were electrospun in THF, DMF, and mixtures of the two. All solvent compositions showed the appearance of self-assembled structures, except those electospun from pure DMF. Different porous structures were obtained as the solvent composition was varied, also resulting in different SCA. This was a very nice illustration of how self-assembly behaviour of polymers can be used to tailor make fibres with specific properties.

One of the first examples where self-assembled structures were observed in fibres was the electrospinning of a triblock copolymer of polystyrene-butadiene-styrene (SBS). Small, elongated phase separated domains were observed with TEM. These were irregular and without any long range order. More ordered structures were introduced by annealing of the fibres, this leading to larger domains. The shape of the domains were affected by the concentration of the solution. A few other papers also mention the requirement of annealing in order to obtain long range order within the fibres[54].

Symmetric PS-PI block copolymers that form lamellar as well as cylindrical morphology were first reported by Kalra *et al.*[31] Self-assembled structures in films were compared to that of the fibres and a resemblance was found, although the cylinders in the fibres were small and lacked the order that was found in films. The lack of order in the fibres was due to the fast evaporation in combination with strong stretching forces that is part of the electrospinning process. Rupture of the PI domains occurs under the influence of the strong forces, with the fast evaporation of solvent essentially leading to freezing of the deformed shape in the fibres[31]. In order to get more ordered structures, annealing was required. Annealing, however, often leads to the loss of fibre integrity because of the fact that it is performed at temparetures above the glass transition temperature of the polymers. To overcome this problem, researchers electrospin fibres with an outer layer that has a higher T_g. In this way the fibre structures are preserved even at high

Stellenbosch University http://scholar.sun.ac.za

temperatures for prolonged periods of time. This was shown by Kalra *et al.* in a follow up paper where they introduced a silica outer layer onto the PI-b-PS fibres[55]. Other authors used a copolymer of poly(methyl methacrylate-co-methacrylic acid), P(MMA-co-MAA)[32].

Another interesting consequence of confinement of PI-b-PS during the self-assembly is the formation of concentric lamellar structures (Figure 2-10). Blocks of PI-PS are known to form lamellar structures in the bulk and concentric lamellar structures when placed in confinement. Long range concentric lamellar structures could be formed by the combined effects of confinement and annealing. The fibre cores and lamellar thickness could be controlled by varying the copolymer ratios. Without the annealing step, the long range concentric lamellar order could not be achieved, because of rapid solidification of the fibres[32].

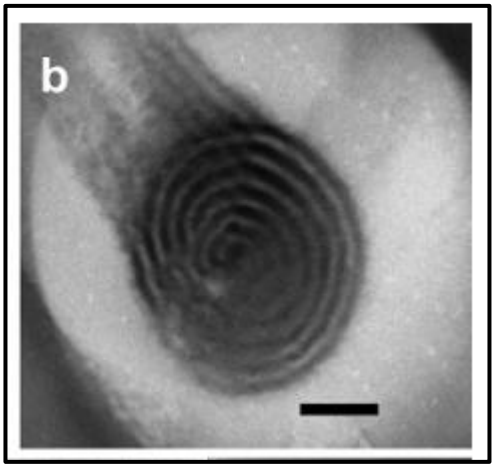

Figure 2-10: Concentric lamellar circles formed from PI-PS block copolymers under confinement[32]

In another study, the influence of polymer structure on the electrospinning of block copolymers was investigated by comparing PS-b-PI with that of PS-PI-PS triblock copolymers. With the molar masses and viscosity the same, the fibres still differed in appearance. The PS-PI blocks had larger diameters over all the concentration ranges investigated, possibly due to differences in entanglements[54]. Small pores were reported for PS-PI fibres, but no mention is made regarding the presence of pores in the case of triblocks.

Stellenbosch University http://scholar.sun.ac.za

PS-b-P4VP (polystyrene-block-poly(4-vinylpyridine) block copolymers were electrospun to compare the morphologies of the well annealed bulk state with those of the as-spun fibres. See Figure 2-11 that compares structures of the annealed bulk state to what can be expected in the fibers. PDP (3-n-pentadecylphenol) was hydrogen bonded to the pyridine units as plasticizer. The composition of the blocks was found to be a useful way in which the hierarchical structure within the fibres could be tuned. Although no long range order could be obtained as in the annealed bulk state, the shape, length and distribution of the elongated worm-like domains of PS and P4VP(PDP) could be adjusted[39]. Porous fibres were also obtained by the removal of PDP from the fibres[56].

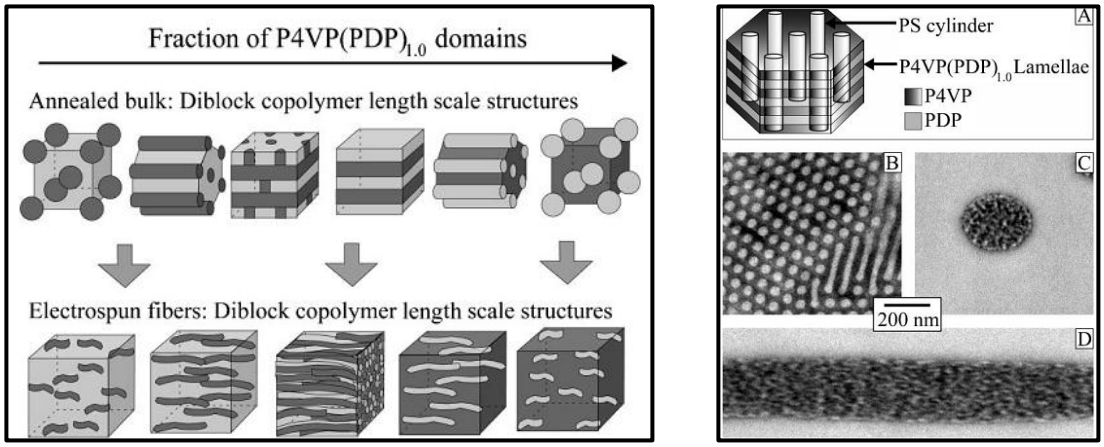

Figure 2-11: Illustration of how the structure in the bulk compares to structures obtained in electrospun fibres from self-assembled solutions[39]

As a last example, the emulsion electrospinning of a block copolymer of poly(ethylene glycol)-poly(L-lactic acid) is mentioned. The polymers were electrospun as water in oil emulsion. Fluorescence labelling and TEM was used to visualize the fibre morphology and indicated the formation of core-sheath structures. These structures are a result of the electrospinning process, where the combination of stretching, evaporation and the formation of a viscosity gradient leads to merging of the emulsion particles, to form the core. The authors refer to this as "evaporation and stretching induced de-emulsification"[57].

Stellenbosch University http://scholar.sun.ac.za

2.3.4.3 Graft copolymers

The electrospinning of graft copolymers is much less reported than that of block copolymers. This is surprising since graft polymers show interesting solution behaviour. Graft copolymers are known to have much more complex solution behaviour than that of block copolymers (see section 2.4). The complexity of graft copolymer solution behaviour is probably also the contributing factor to the lack of research in this regard. None the less, some examples for graft copolymers do exist, showing promising results.

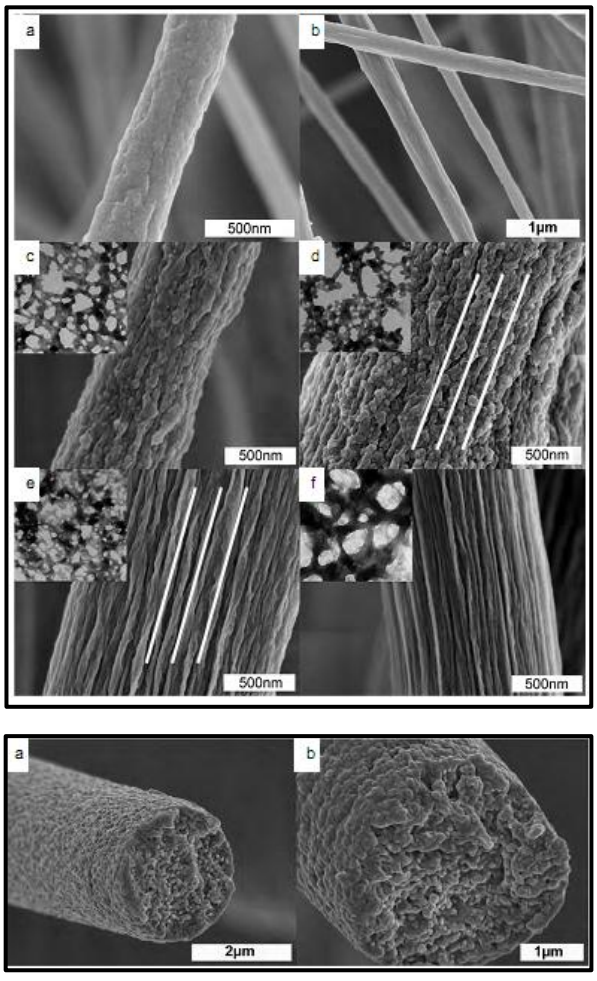

Figure 2-12: Fully porous polymer fibres formed from PAN-g-PDMS copolymers that was electrospun from DMF[58]

Stellenbosch University http://scholar.sun.ac.za

PAN-g-PDMS fibres with rough surfaces as well as internal porous structures were formed by spinning the polymers in a solvent selective for the PAN backbone (DMF)[58]. By varying the amount of PDMS in the copolymers the structures could be modified. The structures obtained in the fibres were linked to the complex self-assembled structures that occurred in solution. See Figure 2-12. The advantage of using this method is that no post spinning modifications are required in order to obtain fully porous fibres.

Other examples of electrospun graft copolymers exist, but no studies of the self-assembly behaviour of these were done. Examples include chitosan-g-PLGA[59], α,β-Poly(N-2-hydroxyethyl)-DL-aspartamide grafted with polylactic acid (PHEA-g-PLA)[60], poly(lactide-co-glycolide) (PLGA) and poly(ethylene glycol)-g-chitosan (PEG-g-CHN)[61], PMMA-g-PS[12;62].

2.3.5 Other techniques

2.3.5.1 Surface functionalization

Fibre mats with initiating groups on the surface provides another interesting way of obtaining fibres with core-shell structures and additional and unique functionalities[5]. The drawback to this method is the fact that it is a multi-step process, and care has to be taken to not lose the fibre integrity after functionalization.

2.3.5.2 Temperature induced phase separation (TIPS) and non-solvent induced phase separation (NIPS)

Both temperature induced phase separation (TIPS) and non-solvent induced phase separation (NIPS) are used to create porous membranes. The use has been extended to the creation of

Stellenbosch University http://scholar.sun.ac.za

porous electrospun fibres. Thermally induced phase separation that occurs as a result of solvent evaporation was discussed in Section 2.3.3. Here, reference is made to the phase separation that can be induced by changing the collector properties.

During TIPS, the collector (eg. foil) is placed in a bath of liquid nitrogen. Fibres are frozen before complete solidification, essentially freezing both the polymer and the remaining solvent. Rapid cooling causes separation into polymer rich and polymer poor phases. If kept frozen in this state until being subjected to drying in vacuo, a porous fibre structure will be obtained. This technique offers some advantages over techniques such as the solvent extraction methods, since with the latter, structures can be lost or interconnections can be formed. Porous fibres of PS, PAN, PVDF, and poly(-caprolactone) were all successfully obtained via TIPS[63].

Non-solvent induced phase separation take place when exchange of a good solvent with a non-solvent occurs. The exchange with a non-solvent produces phase separation. This was demonstrated for PAN, PS, and PMMA which could all be spun with surface as well as interior pores when electrospun into water as a non-solvent. Even more interesting fibres were obtained when a core-sheath fibre with PAN shell and PMMA core was electrospun into a solvent which consisted of both a solvent for the core and a non-solvent for the shell. This resulted in hollow PAN fibres with a porous exterior (Figure 2-13)[64].

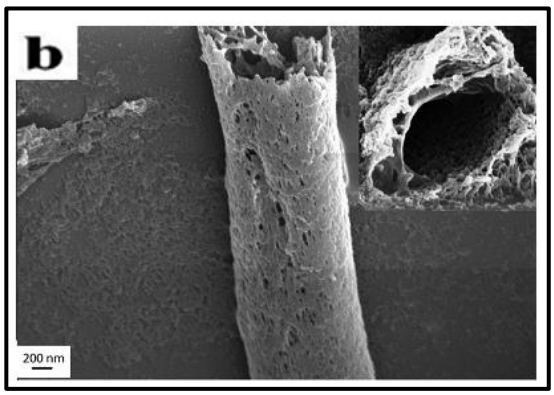

Figure 2-13: Hollow PAN fibre with porous exterior formed by non-solvent induced phase separation[67]

Stellenbosch University http://scholar.sun.ac.za

2.4 Solution behaviour of graft copolymers

It was discussed in the previous section how the self-assembly behaviour of amphiphilic molecules can affect the fibre morphology, so of course some understanding of the solution behaviour of these kinds of molecules are required. As mentioned before, the solution behaviour of graft copolymers is remarkably more complex than their block copolymer counterparts. The reason for this is the many variables which affects the self-assembly behaviour. Unlike block copolymers in which variables such as molar mass, dispersity index, and type of polymers affect the solution behaviour, graft copolymers are also dependant on the number and distribution of the branches[65]. In addition, the distribution that exists within the branches (eg. the molar mass distribution of the grafts) will also have an influence. This added complexity is probably why the behaviour is much less reported than that of linear block copolymers, even though associated structures of graft copolymers were observed as early as the 1950s[66].

Polymers with two or more components which are chemically different from each other are known to form ordered self-assembled structures in solution. The self-assembly is directed by placing the molecules in an environment which has a favourable interaction with only one of the components, which in the case of amphiphilic molecules is achieved by selective solvation[67]. The soluble components will tend to form a corona around the aggregated and collapsed insoluble components. This leads to a variety of micellar structures such as spherical, rod like, lamellae, vesicles, and even more complex morhpologies[68;69]. Although mostly observed for linear block copolymers, similar behaviour has been reported for amphiphilic grafts, where either the backbone of grafts can be selectively solvated. Theoretical[69-71] and experimental[1;13;66;72;73] work have been done to try and understand and control the behaviour of these molecules.

The most detailed description of the structures that graft copolymers can adopt in different environments is probably the work done by Kikuchi and Nose[68;74]. They investigated grafts of PMMA-g-PS having short polystyrene branches with low branch density. They focused on both situations where the backbone or the branches are selectively solvated.

Stellenbosch University http://scholar.sun.ac.za

Kikuchi and Nose described the behaviour of these polymers by constructing a type of graph where they used excluded volume parameters to indicate degrees of solubility of the backbone (bb) and the branches (br). Four general situations can exist as indicated in Figure 2-14. Either the solvent can be good for the both, bad for both, or just selective towards one of the segments as represented by region 1 and 2.

In region 1 the solvent is good for the branches. If the solvent quality for the backbone is progressively worsened (indicated by line A), the backbone will collapse and the branches extend into the solvent, forming rod-like structures. In the extreme case the backbone will form a normal micelle structure resembling that obtained from linear block copolymers.

In region 2, good for the backbone, the opposite trend is indicated by line B, with the solvent quality progressively reduced for the branches. Completely different types of structures are obtained in this case. The branches will tend to associate in multiple aggregates with the backbone forming loops to cover the aggregated assemblies of non-soluble components. The result is the formation of flower-like micelles. The flowers can be connected to form a rigid-rod-like structure.

In another paper by the same authors it was shown how much more complicated the situation gets when the higher concentration solutions are investigated[65]. In this case the focus was on the study on the connected flower-like micelles indicated in line B. Various types of associated structures start to form as indicated in Figure 2-15. Unimolecular micelles can aggregate either by middle to middle (M-M), end to end (E-E), end to middle (E-M), or via multipoint associations.

Stellenbosch University http://scholar.sun.ac.za

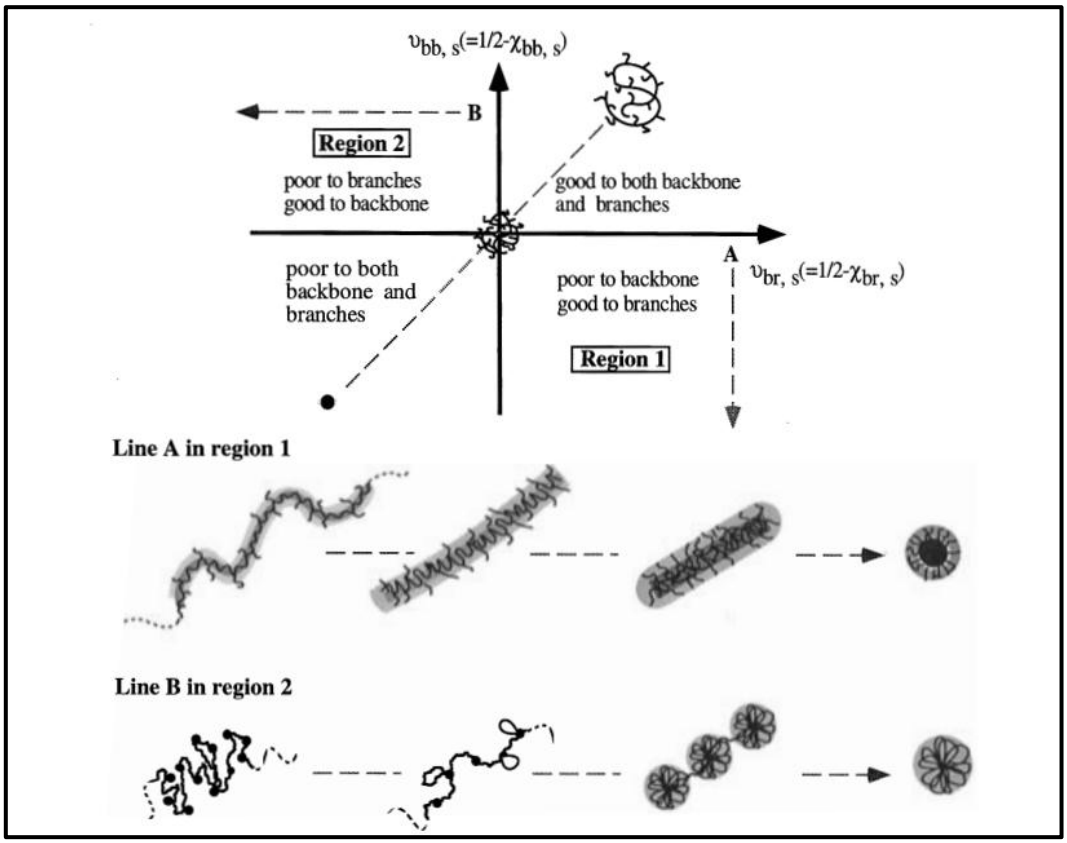

Figure 2-14: Illustration of solution structures possible for low graft density amphiphilic copolymers in solvent combinations ranging from either good for the backbone or good for the branches[68; 68; 69; 70; 71]

Visual presentations of the complicated structures obtained for graft copolymers are scarce, although some have been reported. Most research regarding the micellar structures are based on light scattering methods[65;68;72;73;75;76], fluorescence, NMR[77], SAXS[78], and DSC[1]. Peng *et al.* reported types of multi core structures that were observed for PAA-g-PS[79], which resembles the structures as proposed by Kikushi and Nose[68;74]. The micelles were formed from dioxane solutions which were added to water containing NaCl. The hydrophobic polystyrene chains formed multiple cores surrounded by a PAA shell[79]. The TEM images are shown in Figure 2-16.

Stellenbosch University http://scholar.sun.ac.za

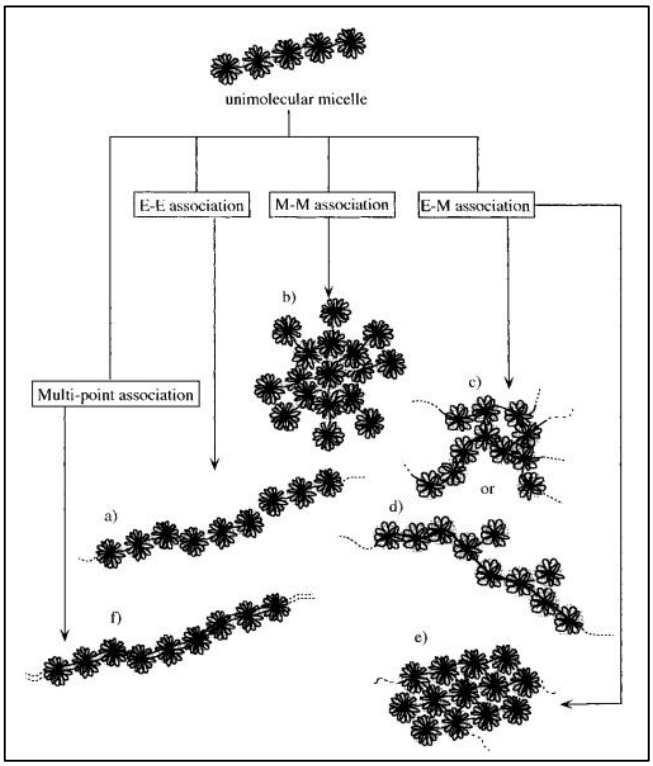

Figure 2-15: Illustration of structures that can be formed from concentrated amphiphilic graft copolymers in solution[68]

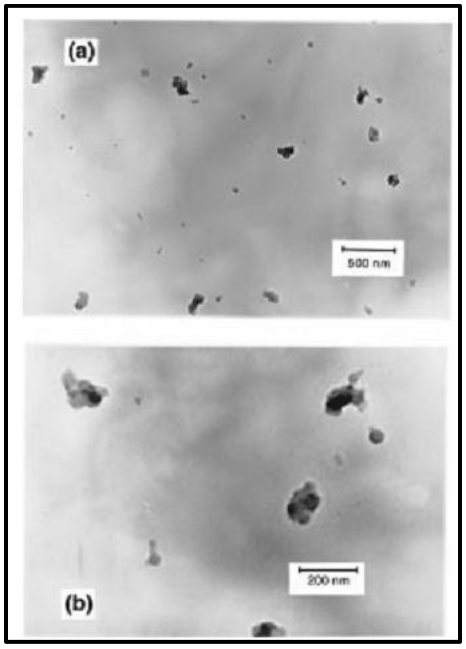

Figure 2-16: TEM images of hydrophobic polystyrene chains forming multiple cores surrounded by a PAA shell[79]

Stellenbosch University http://scholar.sun.ac.za

Both vesicles and spheres were observed for PAA-g-PMMA copolymers, depending on the strength or the polarity of the solvent[80]. In water, vesicles were formed for a variety of molar masses. The ability of PMMA to interact with water through ester bonds helped with the formation of vesicles. With the addition of NaCl, and the resultant increased polarity, spheres were observed. See Figure 2-17.

.

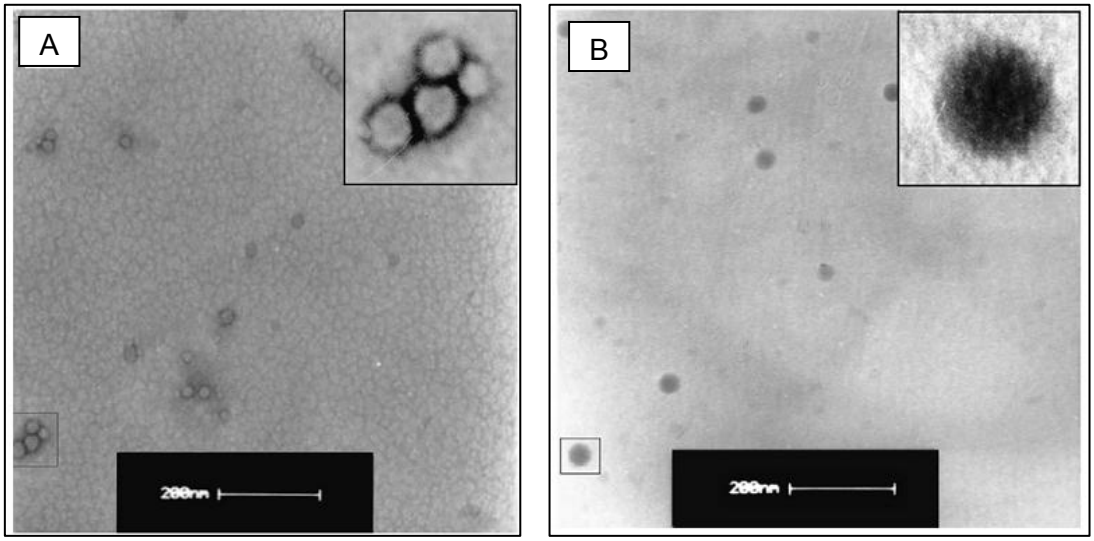

Figure 2-17: TEM images of micelles of PAA-g-PMMA (A) in water (B) in 1 wt% NaCl solution[81]

Even though no visual pictures of the micelles are reported, other studies employing the techniques mentioned earlier give some important insight into the factors affecting the graft copolymer solution behaviour and the micelles obtained.

N-vinylcaprolactam, below the LCST values, showed the occurrence of both monomolecular and polymolecular associated structures for low graft densities, but with higher graft densities only interpolymer associated structures were formed[81]. The dependence of micellar structures on graft density was also shown by studies involving (PS-SMA)-g-MPEG polymers[1]. The general observation of an inverse relationship between graft density and micelle size was observed for these polymers and also resulted in lower CMC values. PAA-g-PS showed decreased CMC values when the number of PS grafts increased on the polymer[80]. Spherical micelles were observed for this system with the size of the spheres influenced by the time over which the self-assembly occurred. Faster formation by direct injection into water yielded bigger

Stellenbosch University http://scholar.sun.ac.za

spheres. Domain sizes of PAA-g-PS in the solid state were also dependent on the graft number, with a lower number[80] of grafts leading to larger domain sizes[78].

Another study also involving PAA-g-PS investigated the effect of molar mass of the branches and ionic strength of the solution on the micellar structures[82]. The molar mass of the chains in this case seemed to have an insignificant influence. The ionic strength, however, changed the morphology of the micelles. Shielding of charge occurred in higher ionic strength liquids which lowers repulsion between micelles.

Another important factor affecting the micellar structure is how amphiphilic the polymers are, that is, how big the difference between the solubilities of the different segments in a specific solvent is. It was found that for LMA-MMA-MPOEMA polymers (poly-((methyl methacrylate)-co-(lauryl methacrylate))-g-methyl-ϖ-hydroxypoly(oxyethylene) methacrylates), micelles only form in a solvent that strongly favours dissolution of one of the segments[66]. The polymers in water-ethanol mixtures formed random associations, which are basically just hydrophobic chains which interact to form interpolymeric multiplets. These types of unordered structures were also mentioned in other papers[66]. The addition of water (greater than 30%) to the solvent mixture was required to induce micelle formation. Due to the complexity of these types of structures, as also noted earlier, only qualitative verification of these structures were possible.

Other interesting information regarding the micellar structures were obtained from a study where the behaviour of PS-g-tBMA and PS-g-PMAA were compared[83]. In a non-selective solvent such as THF the PS-g-tBMA showed no aggregation. In a solvent selective for tBMA branches, however, compact structures were formed. The tBMA acted as a solubilizing agent for the PS units, which prevented the formation of larger micelles. When PS-g-PMAA was investigated in THF, the situation was quite different. THF was now selective towards the backbone only, and in this case micelles were observed. Very compact structures were obtained as a result of the PS preventing any PMAA segment-segment interactions. They further looked at the effect of degree of solubility differences of the polymer segments in solution. PS and PMAA segment have smaller solubility differences than that of PS and PtBMA in tert-amyl alcohol. The result of

Stellenbosch University http://scholar.sun.ac.za

this is that a higher number of PMAA branches are required in order to obtain the same degree of micellation.

2.5 Crosslinked fibres/hydrogels

The materials synthesised in the current project are not only of interest due to their complex solution behaviour and possible interesting fibre morphologies, but also for the possible application in areas such as obtaining fibres with varying moisture absorption and release properties, and the formation of nanofibres hydrogels.

Both polymers have interesting, and in some cases opposite, applications. PMAA is used as water absorbing polymers or hydrogels, whereas PDMS is often used to create superhydrophobic surfaces. This can be an advantage where solvent stability is required for the PMAA for example. Nanofibres, due to the numerous advantageous they possess, are ideal candidates for the use in applications such as filtration, wound dressing materials, tissue engineering scaffolds, catalytic films, sensors, controlled drug delivery. Often, the applications can require stability in solvents or aqueous environments. In these instances, fibre structures are usually kept intact by introducing crosslinks to produce network polymers. The networks will prevent dissolution, but will allow swelling when the solvent molecules are absorbed by the polymer. Network polymers which swell in water are applied in areas such as contact lenses, protein separation, cell-encapsulation matrices and controlled drug delivery[84].

Crosslinking can be introduced via chemical or physical means. Chemical crosslinking refers the formation of covalent bonds between polymer chains. Physical crosslinks are introduced by interactions such as hydrogen bonding, ionic bonding, non-polar interactions, chain entanglements, or crystals which connect the chains and can preserve the fibre integrities[85; 86]. It is possible that the PDMS present in the graft copolymers can act as such physical crosslinks. When the crosslinked polymers absorb and swell in water, anything from 10 to 20%, they can be referred to as hydrogels[85].

Stellenbosch University http://scholar.sun.ac.za

In addition to rendering fibres water/solvent stable, they also affect the thermal and mechanical properties, such as stiffness and toughness, of the fibres. These effects are not always advantageous, water swollen gels are known to have low strain to break and toughness and high stress−strain hysteresis[87]. It is believed that higher crosslink densities, non-uniformity of crosslinks, and secondary structure formation are responsible for the weakness in this regard. Attempts to achieve better mechanical performance include the use of nanocomposites[88] and amphiphilic polymers[89;90] amongst others[88;89;91-93]. In the latter case the hydrophobic segments are used to tune the amount of water absorbed and to influence the mechanical properties[89].

Cui *et al.*[87] crosslinked PEG in the presence of PDMS with the aim of obtaining hydrogels with good mechanical properties and high resilience, resembling that of elastin. Inclusion of PDMS was shown to provide a means of controlling the amount of water in the gels although it did not lead to changes in the resilience values. Other properties such as Young's Modulus in tension, maximum tensile strain, and critical strain energy release rate were affected by the inclusion of PDMS.

Fibrous hydrogels have been synthesised for a number of polymers such as PVA[86;94], chitosan[95], PEG, PAA[96;97]. A crosslinking agent is usually electrospun with the polymer solution, which can be either multifunctional small molecules or other polymers. Poly(acrylic acid) has, for example, been crosslinked with cyclodextrin[98-99], cellulose nanocrystals (cnc)[100], and PVA[96]. All of these rely on the formation of ester bonds between the hydroxyl group of PAA and the alcohol groups on the molecules. This is achieved simply by heating of the polymer fibres[96]. Swelling capacity and kinetics of swelling[101], morphological stability[99], thermal and mechanical properties[99], and inter fibre pore volume[94] are examples of properties of the fibrous mats that were determined to characterize the fibres.

Stellenbosch University http://scholar.sun.ac.za

2.6 References

1. Hou, S. S. & Kuo, P. L. *Polymer,* **2001,** 42, (6), 2387-2394

2. Fang, W., LingShu, W. & ZhiKang, X. *Science China Chemistry,* **2012,** 55, (6), 1125-1133

3. Cheng, G., Böker, A., Zhang, M., Krausch, G. & MÜller, A.H.E. *Macromolecules,* **2001,** 34, (20), 6883-6888

4. Odian, G. *Principles of polymerization.* John Wiley & Sons, **2004**

5. Fu, G.D. *Macromolecules,* **2008,** 41, (18), 6854-6858

6. Gule, N.P., Bshena, O., de Kwaadsteniet, M., Cloete, T.E. & Klumperman, B. *Biomacromolecules,* **2012,** 13, (10), 3138-3150

7. Gao, H. & Matyjaszewski, K. *Journal of the American Chemical Society,* **2007,** 129, (20), 6633-6639

8. Zhang, H. & Ruckenstein, E. *Macromolecules,* **2000,** 33, (3), 814-819

9. Yang, H., Zhang, Q., Lin, B., Fu, G., Zhang, X. & Guo, L. *Journal of Polymer Science Part A: Polymer Chemistry,* **2012,** n/a-n/a

10. Shinoda, H., Matyjaszewski, K., Okrasa, L., Mierzwa, M. & Pakula, T. *Macromolecules,* **2003,** 36, (13), 4772-4778

11. Wu, N., Huang, L. & Zheng, A. *Frontiers of Chemistry in China,* 1, (3). 350-356

12. Swart, M., Olsson, R. T., Hedenqvist, M. S. & Mallon, P. E. *Polymer Engineering & Science,* **2010,** 50, (11), 2143-2152

13. Carrot, G., Hilborn, J. & Knauss, D. M. *Polymer,* **1997,** 38, (26), 6401-6407

14. Sheiko, S. S., Sumerlin, B. S. & Matyjaszewski, K. *Progress in Polymer Science,* **2008,** 33, (7), 759-785

15. Reneker, D. H. & Chun, I. *Nanotechnology,* **1996,** 7, 216

16. Doshi, J. & Reneker, D. H. *J.Electrostat.,* **1995,** 35, 151

17. J. F. Cooley. *Improved methods of and apparatus for electrically separating the relatively volatile liquid component from the component of relatively fixed substances of composite fluids*, US Patent 06385, **1900**

18. Formhals, A. Process and apparatus for preparing artificial threads. US Patent 1975504, **1934**

Stellenbosch University http://scholar.sun.ac.za

19. Formhals, A. Production of artificial fibers, US Patent 2077373, **1937**

20. Formhals, A. Artificial fiber construction, US Patent 2109333, **1938**

21. Formhals, A. Method and apparatus for the production of artificial fibers. US Patent 2158416, **1939**

22. Formhals, A. Artificial thread and method of producing same. US Patent 2187306. **1940**

23. Formhals, A. Production of artificial fibers from fiber forming liquids, US Patent 2323025, **1943**

24. Formhals, A. Method and apparatus for the production of fibers, US Patent 2116942, **1938**

25. Ramakrishna, S., Fujihara, K., Teo, W. E., Lim, T. C., Ma, Z. *An introduction to electrospinning and nanofibers.* Singapore: World Scientific, **2005**.

26. Garg, K. & Bowlin, G. L *Biomicrofluidics,* **2011,** 5, (1), 13403

27. Wannatong, L., Sirivat, A. & Supaphol, P. *Polymer International,* **2004,** 53, (11), 1851-1859

28. Robb, B. & Lennox, B. *Electrospinning for tissue regeneration.* Woodhead Publishing, **2011**

29. Lin, J., Ding, B., Yu, J. & Hsieh, Y. *ACS Applied Materials & Interfaces,* **2010,** 2, (2), 521-528

30. Wei, M. *Phase morphology control in electrospun nanofibers from the electrospinning of polymer blends. Unpublished thesis.* United States, Massachusetts: University of Massachusetts Lowell.D.Eng. **2005**.

31. Kalra, V., Kakad, P. A., Mendez, S., Ivannikov, T., Kamperman, M. & Joo, Y. L. *Macromolecules,* **2006,** 39, (16), 5453-5457

32. Ma, M., Krikorian, V., Yu, J. H., Thomas, E. L. & Rutledge, G. C. *Nano Letters,* **2006,** 6, (12), 2969-2972

33. Huang, Z. M., Zhang, Y. Z, Kotaki, M. & Ramakrishna, S. *Composites Science and Technology,* **2003,** 63, (15), 2223-2253

34. Bhardwaj, N. & Kundu, S. C. *Biotechnology Advances,* **2010,** 28, (3), 325-347

35. Deitze, J. M., Kleinmeyer, J. D., Hirvonen, J. K. & Beck, T. *Polymer,* **2001,** 42, (19), 8163-8170

36. Krishnappa, R. V. N., Desai, K. & Sung, C. *J.Mater.Sci.,* **2003,** 38, (11), 2357

37. Chuangchote, S., Sirivat, A. & Supaphol, P. *Polymer Journal,* **2006,** 38, (9), 961-969

Stellenbosch University http://scholar.sun.ac.za

38. Wei, M., Lee, J., Kang, B. & Mead, J. *Macromolecular Rapid Communications,* **2005,** 26, (14), 1127-1132

39. Ruotsalainen, T. *Soft Matter,* **2007,** 8, (3), 978

40. Casper, C. L., Stephens, J. S., Tassi, N. G., Chase, D. B. & Rabolt, J.F. *Macromolecules,* **2004,** 37, (2), 573-578

41. Madej, W., Budkowski, A., Raczkowska, J. & Rysz, J. *Langmuir,* **2008,** 24, (7), 3517-3524

42. Qin, X., Yang, E., Li, N. & Wang, S. *Journal of Applied Polymer Science,* **2007,** 103, (6), 3865-3870

43. McKee, M. G., Hunley, M. T., Layman, J. M. & Long, T. E. *Macromolecules,* **2006,** 39, (2), 575-583

44. Zhang, J. & Nie, J. *Polymer International,* **2012,** 61, (1), 135-140

45. Megelski, S., Stephens, J.S., Chase, D.B. & Rabolt, J.F. *Macromolecules,* **2002,** 35, (22), 8456-8466

46. Xue, L., Zhang, J. & Han, Y. *Progress in Polymer Science,* **2012,** 37, (4), 564-594

47. Valiquette, D. & Pellerin, C. *Macromolecules,* **2011,** 44, (8), 2838-2843

48. Zhang, Y., Feng, Y., Huang, Z., Ramakrishna, S. & Lim, C. *Nanotechnology,* **2006,** (17), 901

49. Zhang, Y. & Hsieh, Y. *Nanotechnology,* **2006,** (17), 4416

50. Bognitzki, M. *Polymer Engineering & Science,* **2001,** 41, (6), 982-989

51. Peng, P., Chen, Y., Gao, Y., Yu, J. & Guo, Z. *Journal of Polymer Science Part B: Polymer Physics,* **2009,** 47, (19), 1853-1859

52. Ma, M., Hill, R. M., Lowery, J. L., Fridrikh, S. V. & Rutledge, G. C. *Langmuir,* **2005,** 21, (12), 5549-5554

53. Miyauchi, Y., Ding, B. & Shiratori, S. *Nanotechnology,* **2006,** 17, (20), 5151

54. Fong, H. & Reneker, D. H. *Journal of Polymer Science Part B: Polymer Physics,* 37, (24). 3488-3493

55. Kalra, V., Mendez, S., Lee, J., Nguyen, H., Marquez, M. & Joo, Y. *Advanced Materials,* **2006,** 18, (24), 3299-3303

56. Ruotsalainen, T. *Advanced Materials,* **2005,** 17, (8), 1048-1052

57. Xu, X., Zhuang, X., Chen, X., Wang, X., Yang, L. & Jing, X. *Macromolecular Rapid Communications,* **2006,** 27, (19), 1637-1642

Stellenbosch University http://scholar.sun.ac.za

58. Bayley, G. M. & Mallon, P. E. *Polymer,* **2012,** 53, (24), 5523–5539

59. Xie, D., Huang, H., Blackwood. K. & MacNeil, S. *Biomedical Materials,* **2010,** 5, (6), 065016

60. Pitarresi, G., Palumbo, F.S., Fiorica, C., Calascibetta, F. & Giammona, G. *European Polymer Journal,* **2010,** 46, (2), 181-184

61. Jiang, H., Fang, D., Hsiao, B., Chu, B. & Chen, W. *Journal of Biomaterials Science, Polymer Edition,* **2004,** 15, (3), 279-296

62. Swart, M. & Mallon, P. E. *Pure Applied Chemistry,* **2009,** (81), 495-511

63. McCann, J. T., Marquez, M. & Xia, Y. *Journal of the American Chemical Society,* **2006,** 128, (5), 1436-1437

64. Nayani, K., Katepalli, H., Sharma, C. S., Sharma, A., Patil, S. & Venkataraghavan, R. *Industrial & Engineering Chemistry Research,* **2012,** 51, (4), 1761-1766

65. Kikuchi, A. & Nose, T. *Society,* **1997,** 9297, (96), 896-902

66. Konak, C., Helmstedt, M., Kopeckova, P., & Kopecek, J. *Journal of colloid and interface science,* **1998,** 208, (1), 252-258

67. Alexandridis, P. & Lindman, B. *Amphiphilic block copolymers.* Elsevier Science, **2000**.

68. Kikuchi, A. & Nose, T. *Polymer,* **1996,** 37, (26), 5889-5896

69. Zhang, L., Lin, J. & Lin, S. *The Journal of Physical Chemistry B,* **2007,** 111, (31), 9209-9217

70. Borisov, O. V. & Zhulina, E. B. *Macromolecules,* **2005,** 38, 2506

71. Semenov, A. N., Joanny, J. & Khokhlov, A. R. *Macromolecules,* **1995,** 28, (4), 1066-1075

72. Horgan, A., Saunders, B., Vincent, B. & Heenan, R.K. *Journal of colloid and interface science,* **2003,** 262, (2), 548-559

73. Papanagopoulos, D. & Dondos, A. *European Polymer Journal,* **1995,** 31, (10), 977-980

74. Kikuchi, A. & Nose, T. *Macromolecules,* **1996,** 9297, (96), 6770-6777

75. Watanabe, A. & Matsuda, M. *Macromolecules,* **1985,** 18, (2), 273-277

76. Jeong, J. H. & Park, T. G. *Journal of Controlled Release,* **2002,** 82, (1), 159-166

77. Zushun, X., Linxian, F., Jian, J., Shiyuan, C., Yongchun, C. & Changfeng, Y. *European Polymer Journal,* **1998,** 34, (10), 1499-1504

78. De la Fuente, J. L., Wilhelm, M., Spiess, H. W., Madruga, E. L., Fernández-Garcia, M. & Cerrada, M. L. *Polymer,* **2005,** 46, (13), 4544-4553

Stellenbosch University http://scholar.sun.ac.za

79. Peng, D., Zhang, X. & Huang, X. *Polymer,* **2006,** 47, (17), 6072-6080

80. Peng, D., Zhang, X., Feng, C., Lu, G., Zhang, S. & Huang, X. *Polymer,* **2007,** 48, (18), 5250-5258

81. Laukkanen, A., Valtola, L., Winnik, F. M. & Tenhu, H. *Polymer,* **2005,** 46, (18), 7055-7065

82. Xie, H. & Liu, Y. *European Polymer Journal,* **1991,** 27, (12), 1339-1343

83. Pitsikalis, M., Woodward, J., Mays, J. W. & Hadjichristidis, N. *Macromolecules,* **1997,** 30, (18), 5384-5389

84. Hennink, W. E. & Van Nostrum, C. F. *Advanced Drug Delivery Reviews,* **2002,** 54, 223-236

85. Hoffman, A. S. *Advanced Drug Delivery Reviews,* **2002,** 54, (1), 3-12

86. Lee, S. J., Lee, S. G., Kim, H. & Lyoo, W. S. *Journal of Applied Polymer Science,* **2007,** 106, (5), 3430-3434

87. Cui, J. *Biomacromolecules,* **2012,** 13, (3), 584-588

88. Zhu, M. F., Liu, Y., Sun, B., Zhang, W., Liu, X. L., Yu, H., Zhang, Y., Kuckling, D. & Adler, H. J. P. *Macromolecular Rapid Communication,* **2006,** 27, 1023

89. Xiao, L., Liu, C., Zhu, J., Pochan, D. J. & Jia, X. *Soft Matter,* **2010,** 6, 5293

90. Gao, D., Ma, J. and Guo, H. *New Journal of Chemistry,* **2010**, 34, (9), 2034-2039

91. Johnson, J. A., Turro, N. J., Koberstein, J. T. & Mark, J. E. *Progress Polymer Science.,* **2010,** 35, 332

92. Webber, R. E., Creton, C., Brown, H. R. & Gong, J. P. *Macromolecules,* **2007,** 40, 2919

93. Hou, Y., Schoener, C. A., Regan, K. R., Munoz-Pinto, D., Hahn, M. S. & Grunlan, M. A. *Biomacromolecules,* 11, 648-648-656

94. Wang, Y. & Hsieh, Y. *Journal of Applied Polymer Science,* **2010,** 116, (6), 3249-3255

95. Noble, L., Gray, A. I., Sadiq, L. & Uchegbu, I. F. *International journal of pharmaceutics,* **1999,** 192, (2), 173-182

96. Xiao, S. *Journal of Applied Polymer Science,* **2010,** 116, (4), 2409-2417

97. GarcÍa, D. M., Escobar, J. L., Bada, N., Casquero, J., Hernáez, E. & Katime, I. *European Polymer Journal,* **2004,** 40, (8), 1637-1643

98. Li, L. & Hsieh, Y.L, *Nanotechnology,* **2005,** 16, (12), 2852

Stellenbosch University http://scholar.sun.ac.za

99. Peresin, M. S., Habibi, Y., Zoppe, J. O., Pawlak, J. J. & Rojas, O. J. *Biomacromolecules,* **2010,** 11, (3), 674

100. Ping, L. & Hsieh, Y, *Nanotechnology,* **2009,** (41), 415604

101. Spagnol, C. *European Polymer Journal,* **2012,** 48, (3), 454-463

Stellenbosch University http://scholar.sun.ac.za

Chapter 3 EXPERIMENTAL

3.1. Materials

Methacrylic acid monomer was passed through a monomethyl ether hydroquinone inhibitor removal column (Sigma Aldrich) prior to polymerization. Mono methacryloxy propyl terminated polydimethylsiloxane (MMP-PDMS, Gelest Inc.) was used as received. Azobisisobutyronitrile (AIBN) used as initiator was recrystallized from methanol. Toluene used during polymerizations was distilled over sodium/benzophenone. Chromatography and electrospinning solvents included tetrahydrofuran (THF, Chromasolve plus HPLC grade, Sigma Aldrich); N,N dimethylformamide (DMF, Chromasolve plus HPLC grade, Sigma Aldrich); and chloroform (Chromasolve plus, HPLC grade). (Trimethylsilyl)diazomethane (Sigma Aldrich) used for the methylation of polymethacrylic acid was used as received.

3.2. Synthesis

The synthesis of PMAA-g-PDMS and PMMA-g-PDMS will be described in the following section. Their characterization by nuclear magnetic resonance (NMR), infrared spectroscopy (IR), size exclusion chromatography (SEC), and gradient elution high performance liquid chromatography (HPLC) will be discussed in Chapter 4.

3.2.1. Synthesis of poly(methacrylic acid) graft PDMS

PMAA-g-PDMS copolymers were synthesized by conventional free-radical reactions in toluene. The reaction scheme is shown in Scheme 1. The procedure was as follows: To a 100 mL round-bottomed flask was added monomethacryloxy-terminated PDMS macromonomer, monomer (methacrylic acid), initiator (AIBN), solvent (toluene) and a stirrer bar. The reaction mixture was degassed for 15 min by purging with Argon gas and then placed in an oil bath set at 70 °C.

Stellenbosch University http://scholar.sun.ac.za

The amount of monomer was added according to a weight by weight ratio. Typically, if 5 g of a 10% PDMS copolymer was targeted, 0.5 g PDMS macromonomer was added and 4.5 g MAA. AIBN was added as 0.1% or 0.15% of the mass of MAA added. Reactions for MAA were performed at 10% solids content, as higher content became difficult to stir.

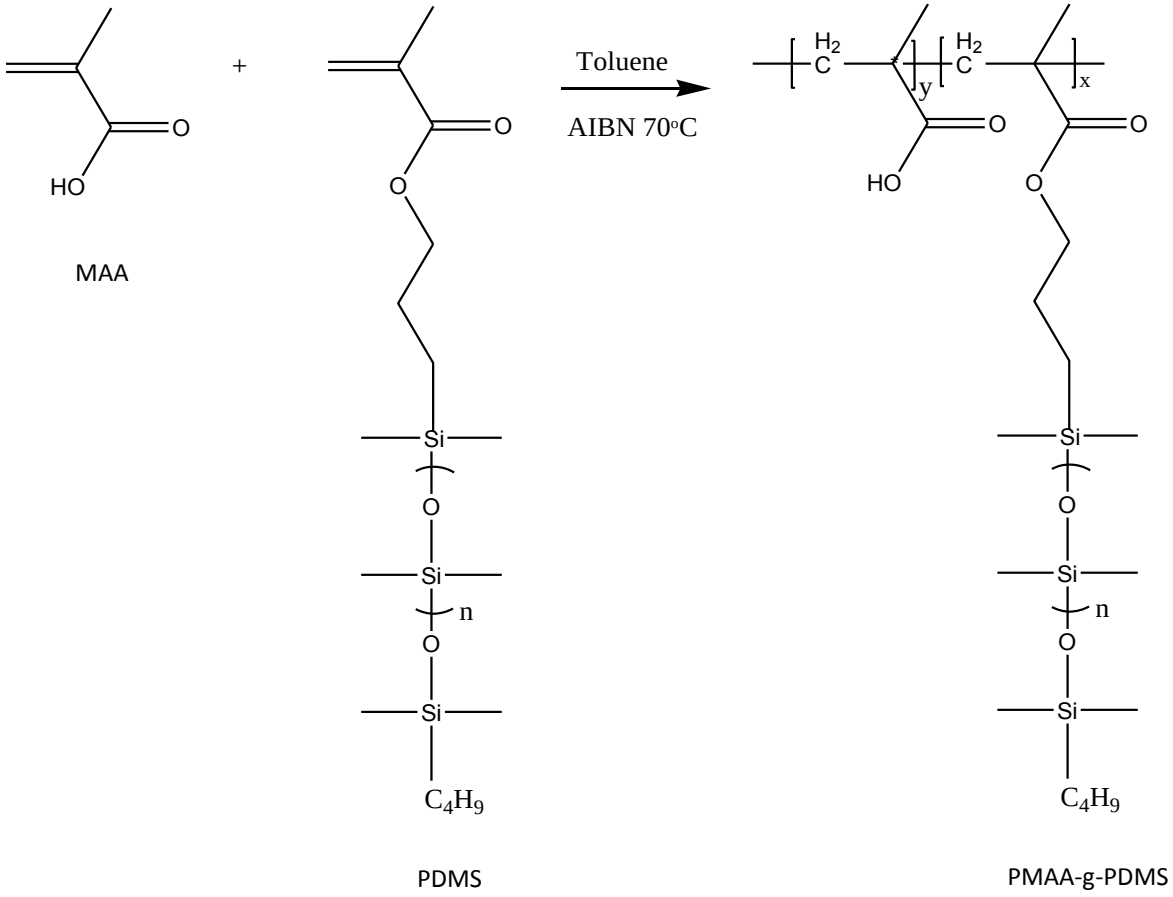

SCHEME 1: Synthesis of PMAA-g-PDMS copolymers via free radical copolymerization

Stellenbosch University http://scholar.sun.ac.za

3.2.2. Synthesis of poly(methyl methacrylate) from poly(methacrylic acid)

The transformation of acids to esters was performed in order to simplify analysis of the copolymers. The reactions were performed using trimethylsilyl diazomethane according to the reaction scheme shown in Scheme 2[1].

The procedure was as follows: About 100 mg of polymer was dissolved in 2 mL of a MeOH/H_2O (19:1) solvent. The solution was left to stir overnight to ensure swelling of the polymer. Trimethylsilyldiazomethane was then added drop-wise via syringe until no more nitrogen bubbles were observed, and the colour of the solution remained yellow. Samples were left to stand 4 hours after which it was dried in a vacuum oven overnight.

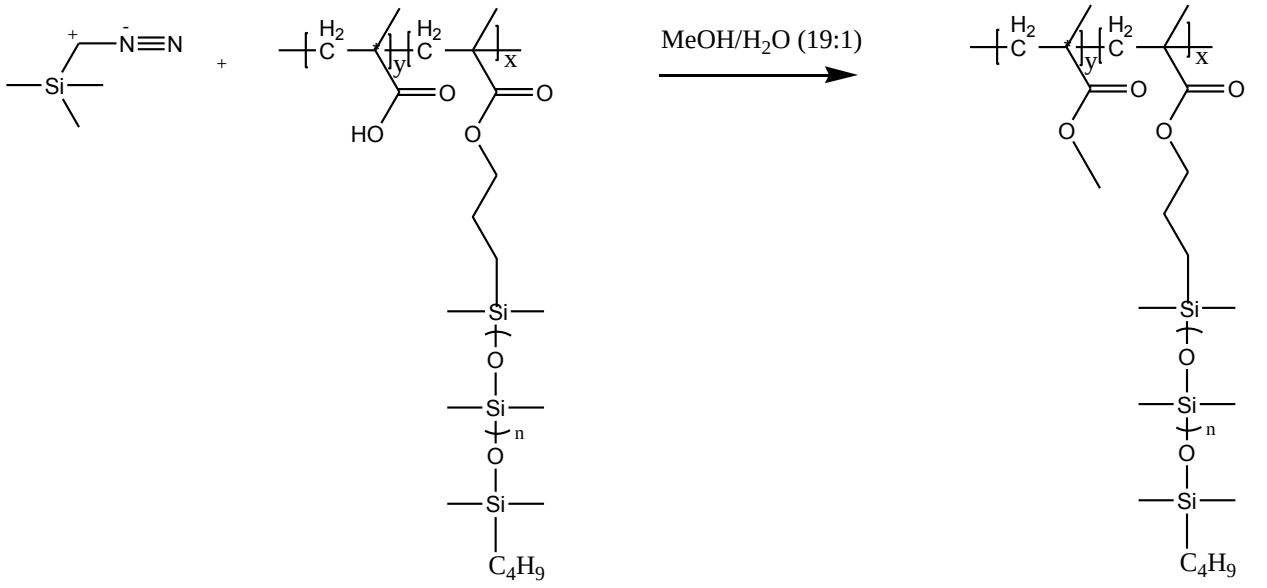

PMAA-g-PDMS PMMA-g-PDMS

SCHEME 2: Synthesis of PMMA-g-PDMS from PMAA-g-PDMS precursors

Stellenbosch University http://scholar.sun.ac.za

3.3. Characterization

3.3.1. Gradient elution chromatography

Gradient elution chromatography was performed on a dual pump HPLC consisting of a Waters 2690 Separations module (Alliance) connected to an Agilent 1100 variable wavelength UV detector and a PL-ELS 1000 evaporative light scattering detector. Data capture was performed using PSS WinGPC unity (Build 2019) software. A Waters C18 column was used at 30 °C. Samples were dissolved and sonicated for 30 minutes before being analysed.

3.3.2. Nuclear magnetic resonance (NMR)

NMR was used for structure determination as well as to calculate incorporation of PDMS within copolymers. Varian VXR 300, Varian^{unity} Inova400, Varian VXR-unity (400) instruments were used with borosilicate NMR tubes. Samples were prepared by dissolving 15-30 mg of sample in 1 mL of solvent. The NMR tube was filled to the 5 cm height mark. Solvents used were DMSO-d_6 and $CDCl_3$ without any TMS internal reference added, as this will overlap with the PDMS peaks.

3.3.3. Scanning electron microscopy (SEM) and field emission scanning electron microscopy (FE-SEM)

SEM was used to characterize the fibre morphology. Analysis to determine fibre diameter was performed on a LEO 1430VP Scanning Electron Microscope fitted with Backscatter, Cathodoluminescence, Variable pressure and Energy Dispersive detectors, as well as a Link EDS system and software for microanalysis. Samples were attached onto SEM pegs with carbon tape and coated with gold sputter for 2-3 minutes.

Stellenbosch University http://scholar.sun.ac.za

FE-SEM was used to characterize fibre surface morphology and to visualize the inside of the fibres. For internal fibre morphology the fibres were freeze fractured. The process consisted of sticking fibres to carbon tape, freezing the sample for 5 min under liquid nitrogen, and then cutting the sample under liquid nitrogen with scissors cooled prior to cutting.

3.3.4. Attenuated total reflectance (ATR) Fourier-transform infra-red (FTIR) spectroscopy

ATR-FTIR provides an easy route to FTIR spectra as no sample preparation is required for this technique. In addition, samples in either solid or liquid form can be analysed. A Thermo-Nicolet iS10 FTIR spectrometer with a ZnSe ATR, Smart Golden Gate accessory with diamond window was used to record the spectra. Data acquisition and processing was performed with Omnic software (version 8.1).

3.3.5. Size exclusion chromatography

SEC is the most common way of determining molar mass and dispersity index of polymer samples based on their hydrodynamic volume in solution. The SEC instrument used during this project comprised of the following: a Waters 1515 isocratic pump, a Waters 717 plus auto-sampler, a refractive index detector, a Waters 2487 dual wavelength UV detector. The column consisted of two PLgel 5 µm mixed-C, 300x7.5 mm with a 5 µm, 50 x7.5 mm guard column . Solution of 1 mg/mL were analysed using THF as mobile phase. Polystyrene was used to calibrate the system.

3.3.6. Static contact angle measurements

This technique provides an easy way to visualise the hydrophobicity differences of the fibre mats. The apparatus used consisted of a KSV instrument CAM 200 with a Basler A602f camera (100 frames per second). Droplets were placed on the sample surface using a 1 µL syringe. At

Stellenbosch University http://scholar.sun.ac.za

least ten photographs of each sample were taken and contact angles were determined using CAM software. The values reported are the average values for the 10 measurements. For the time series data, a droplet was placed on the fibre mat and photos were taken at set intervals. This was continued until the droplet disappeared. The angles after specific times were measured and plotted against time.

3.3.7. Rheology

The instrument used for rheology measurements was a Modular Compact Rheometer, Physica MCR 300 (Paar Physica) from Advanced Laboratory Solutions. A TEK 150 P-C (measuring cell) and Physica VT2 (temperature control). Data capture and processing was performed on Rheoplus/32 V2.66 software.

Sample solutions were prepared by dissolving polymer to form 12 wt % solutions (resembling that of the electrospinning solutions). Sample was placed on the surface directly from polytops before starting the runs.

3.3.8. Transmission electron microscopy (TEM)

TEM analysis was performed to determine the solution structures that exist in for polymers with various PDMS content and different solvent compositions. Dilute solutions of the polymers in various solvent compositions were made and cast on copper grids. The solvent was evaporated to form thin films. Samples were analysed using a LEO 912 EM TEM instrument

Stellenbosch University http://scholar.sun.ac.za

3.4. Determining the ability of PDMS to control the rate and extent of moisture and water absorption

3.4.1. Moisture absorption

Moisture stability test were performed using an in-house built instrument as shown in Figure 3-1. Fibre mats were cut into 1 cm x 1 cm pieces and weighed before being placed in the pan. The instrument was set to zero with the dry chamber attached; the chamber was then removed to add 75 mL of a saturated NaCl solution. Data points were collected every 2 seconds for up to 180 min. The saturated salt solution was used to control the humidity in the chamber. The solution was prepared by heating water to 30 °C and preparing a saturated solution. The solution was added to the chamber at room temperature (around 23 °C).

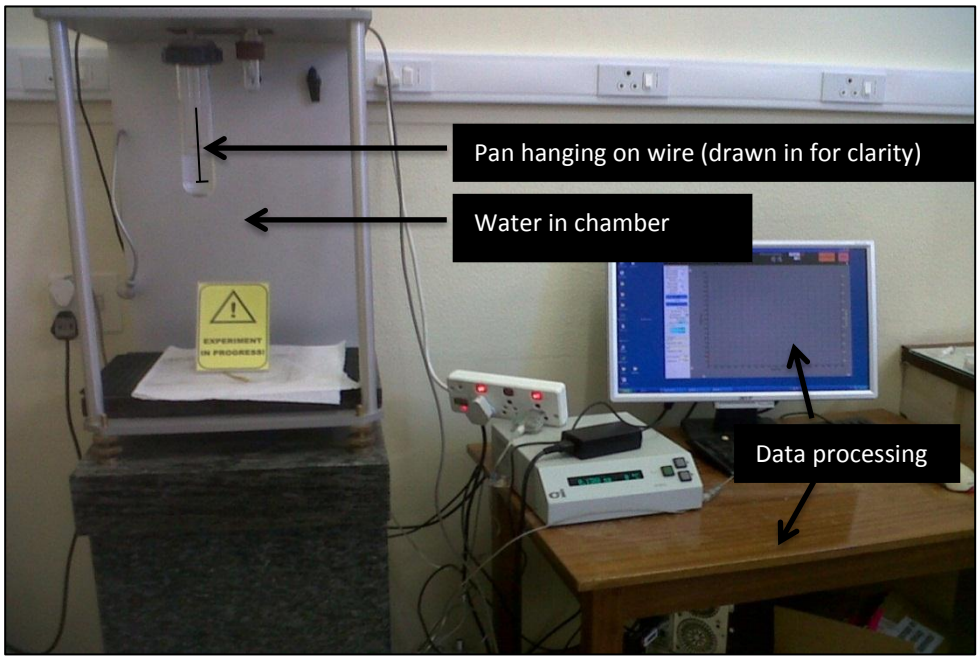

FIGURE 3-1: Illustration of instrument used for moisture studies

Stellenbosch University http://scholar.sun.ac.za

3.4.2. TGA

TGA measurements were performed on some samples to determine the initial water content of fibre mats prior to the moisture absorption test. TGA consist of weighing of a sample as the temperature is increased. As the temperature rises the loss of water molecules will be detected as weight loss and the percentage weight loss determined. Samples were studied using a Perkin Elmer TGA7 instrument. The samples (+/– 3mg) were heated under nitrogen flow (10 mL/min) from room temperature to 160 °C at a rate of 10 °C/min.

3.4.3. Water stability tests

Water stability tests were performed by placing fibre mats in polytops filled with water. Samples were submerged for 5 minutes and 3 hours respectively. The mats were then removed, dried in a fumehood for 1 hour and placed in a desiccator overnight before being analysed with SEM.

3.5. References

1. Kühnel, E., Laffan, D., Lloyd-Jones, G., Martínez del Campo, T., Shepperson, I. & Slaughter, J. L. *Angewandte Chemie International Edition,* **2007,** 46, (37): 7075-7078.

Stellenbosch University http://scholar.sun.ac.za

Chapter 4 Results and Discussion

4.1. SYNTHESIS AND CHARACTERIZATION

4.1.1. Synthesis of poly(methacrylic acid)-g-poly(dimethylsiloxane) copolymers

The polymers investigated in this study are highly amphiphilic. They consist on the one hand of polymers used for water absorption applications, and on the other, polymers used to induce superhydrophobicity to fibres. The highly amphiphilic nature of the polymers was desired in order to induce phase separation and to possibly transfer the solution structures into the fibres. In the section to follow, the characterization of these amphiphilic polymers will be discussed. Only one other example could, to our knowledge, be found on the synthesis of similar polymers, although via a different route. Lin *et al.* recently reported the synthesis of similar polymers via a RAFT mediated polymerization of tert (butyl methacrylate) and subsequent hydrolysis of the ester group[1].

The synthesis in this study was performed in toluene which is a good solvent for both PDMS macromonomers and MAA monomers. The polymer product, PMAA, was however not soluble in the reaction medium and precipitation occurred as the polymerization proceeded. The polymer synthesis was performed at a solids content of 15 wt % as was previously used for PAN-g-PDMS copolymer synthesis[2]. Incorporation of PDMS into the copolymer in such a system was expected to be difficult due to the fact that MAA monomers usually have high reactivity ratios when copolymerized with other monomers. This will favour homo polymerization. One example is the copolymerization of MAA with acetonitrile. In this case the MAA had a reactivity ratio of 2.4 vs the acrylonitrile which was 0.128[3]. This difference in reactivity ratios will be even more exaggerated in the present study due to the size and hydrophobicity of the PDMS macromonomer. PDMS is much larger and more hydrophobic than

Stellenbosch University http://scholar.sun.ac.za

the acetonitrile monomer that was used as example. Also, as the reaction proceeds, precipitation occurs, which can reduce the likelihood that end-groups from the PDMS macromonomer will come in contact with propagating radicals, especially in the case of macromonomers[3]. The range of copolymers synthesized included feed ratios of 10, 20, 30, 40, and 50 wt% PDMS.

4.1.2. Synthesis of poly(methyl methacrylate)-g-PDMS

The PMAA-g-PDMS copolymers were converted to the PMMA-g-PDMS to simplify the analysis of the polymers using liquid chromatographic techniques. Attempts to directly determine the molar mass of these compounds via SEC in DMAc were unsuccessful due to the irreversible retention of the molecules on the column. In addition, analysing the esterified form eliminates the polyelectrolyte effect which is known to cause significant errors and complications in SEC analysis[4]. The PMAA samples were esterified using trimethyl silyl diazomethane to form the PMMA analogue[5]. This route provides an easy, one step method for obtaining almost exclusively the methyl ester of the acid. The characterization and PDMS inclusion will be discussed in the following sections.

4.1.3. Characterization

4.1.3.1. ^{1}H-NMR characterization

All samples were analysed with ^{1}H-NMR. PMAA and copolymers were analysed to determine if PDMS signals were present in the polymers. This gave an indication on the success of the reaction. The ^{1}H-NMR spectra for the PMAA homopolymer (A) and a representative copolymer (B) are shown in Figure 4-1. The spectra for both of the polymers show the characteristic acid proton peak at around 12 ppm. No peak at 0 ppm was observed for the PMAA homopolymer. This peak is characteristic for the CH_3 protons attached to the siloxane group of the PDMS segments[6].

Stellenbosch University http://scholar.sun.ac.za

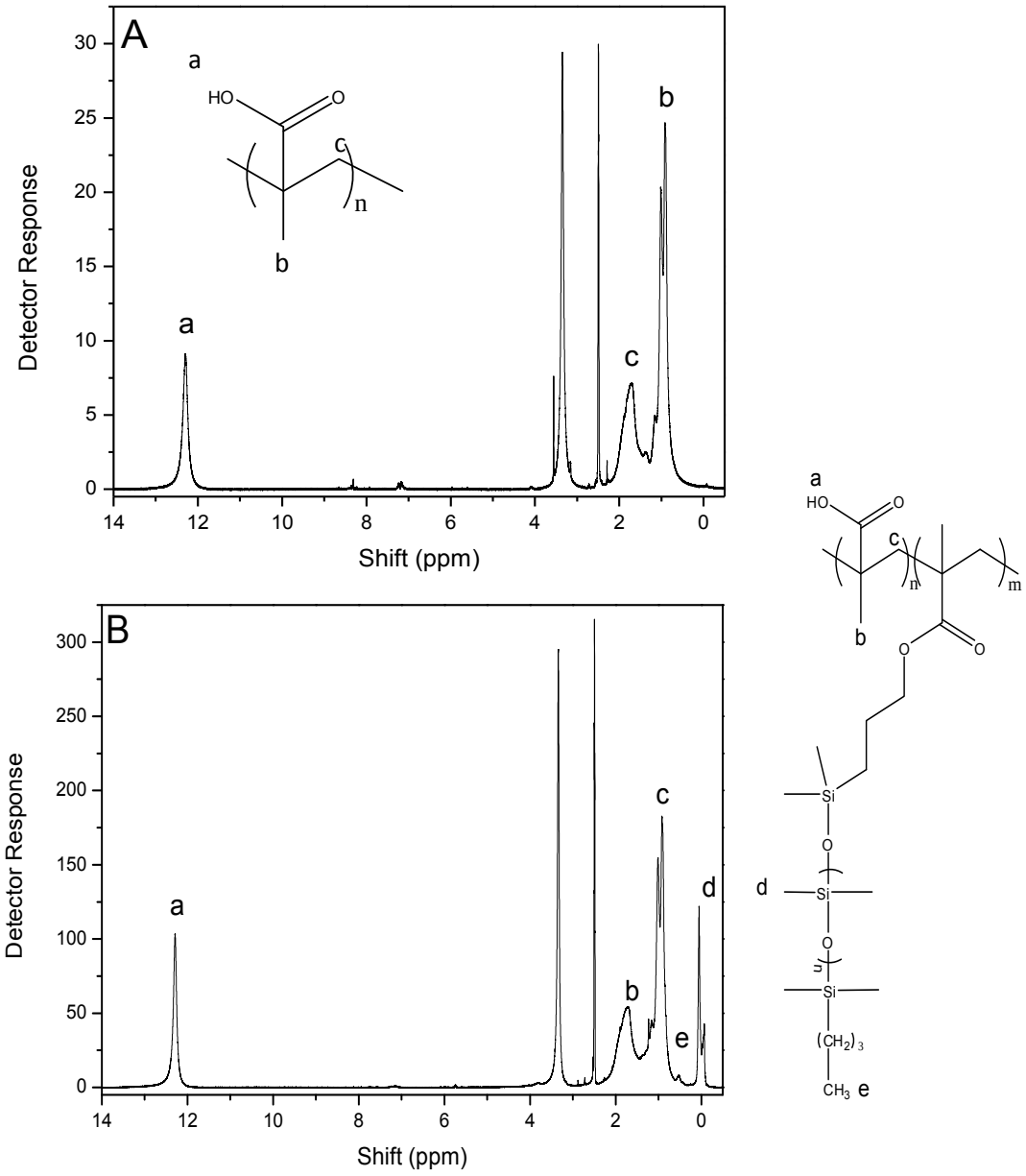

FIGURE 4-1: ^{1}H-NMR spectra of (A) PMAA homopolymer and (B) copolymer with 12.2 mol % PDMS (DMSO-d_6)

The ^{1}H-NMR of the PMMA-g-PDMS samples was used to determine the ratio of PMAA groups to PDMS groups present. The ^{1}H-NMR spectra of the converted PMMA analogue of the

Stellenbosch University http://scholar.sun.ac.za

copolymers is shown in Figure 4.2. The ^{1}H-NMR confirmed the disappearance of the acid protons at 12 ppm. A new peak appears at 3.7 ppm due to the O-CH_3. Integration of the peaks at 0 ppm (Si(CH_3)-O-) and 3.7 ppm (O-CH_3) was compared to establish the amount of PDMS inclusion in the copolymers. The results of this analysis are tabulated in Table 4-1.

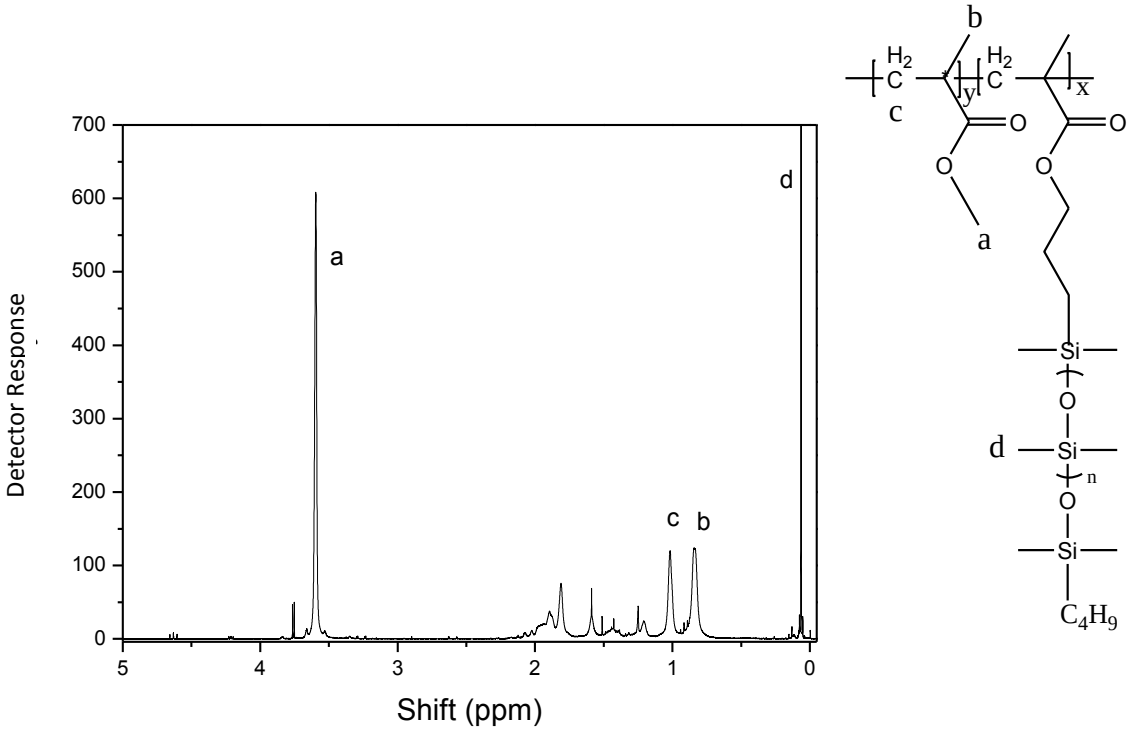

FIGURE 4-2: ^{1}H-NMR showing the appearance of the methyl protons at 3.7 ppm for copolymer with 12.2 mol % PDMS ($CDCl_3$)

Stellenbosch University http://scholar.sun.ac.za

TABLE 4-1: Table comparing the target PDMS molar ratios to the ratios measured from ^{1}H-NMR of PMMA-g-PDMS copolymer

Sample	PDMS Feed ratio (%)	PDMS feed ratio (molar ratio acid/siloxane groups)	PDMS content from ^{1}H-NMR (molar % acid to siloxane groups)[a]
PMAA	0	0	0
110	10	13.6	8.6
120	20	26.3	12.2
130	30	38	21.4
140	40	64.2	30.6
150	50	74.4	31.5
510	10	44.3	15.4
520	20	64.2	17.9
530	30	74.4	19.8

(a) Determined using ^{1}H-NMR integration of the PMMA and PDMS peaks.

From the values in Table 4-1 a good correlation between the incorporation of PDMS as measured with ^{1}H-NMR and the feed ratio is seen. As the feed ratio increased, the PDMS fraction in the copolymer increased. The mole fraction for the 1000 g/mol series was good, with the percent inclusion values generally above 50%.

Results for samples synthesised using PDMS with higher molar mass of 5000 g/mol was compared to the 1000 g/mol series. The use of larger macromonomers (5000 g/mol) resulted in lower incorporation. This is expected due to the viscosity effect[7]. The higher viscosity of the larger molecules limits movement of the chains and also reduces the effective end-group concentration which is available to react[7]. Better PDMS inclusion is obtained when lower molar mass PDMS is used. This will be the focus of the present study.

4.1.3.2. ATR-FTIR

Further evidence for the presence of PDMS in the copolymers was obtained from ATR-FTIR. Peaks at 800 cm^{-1} (Si-CH_3) and 1260 cm^{-1} (Si-CH_3) and 1090 cm^{-1} (Si-O-Si) appeared in the

Stellenbosch University http://scholar.sun.ac.za

copolymer spectra[1;7], which are characteristic for PDMS. The main peaks of the acid at 3500 cm^{-1} (COOH) and 1700 cm^{-1} (C=O) were also present. The peaks corresponding to PDMS increased as the initial feed ratio of the PDMS increased. This is in agreement with the results determined from the PMMA-g-PDMS ^{1}H-NMR spectra (see Table 4-1).

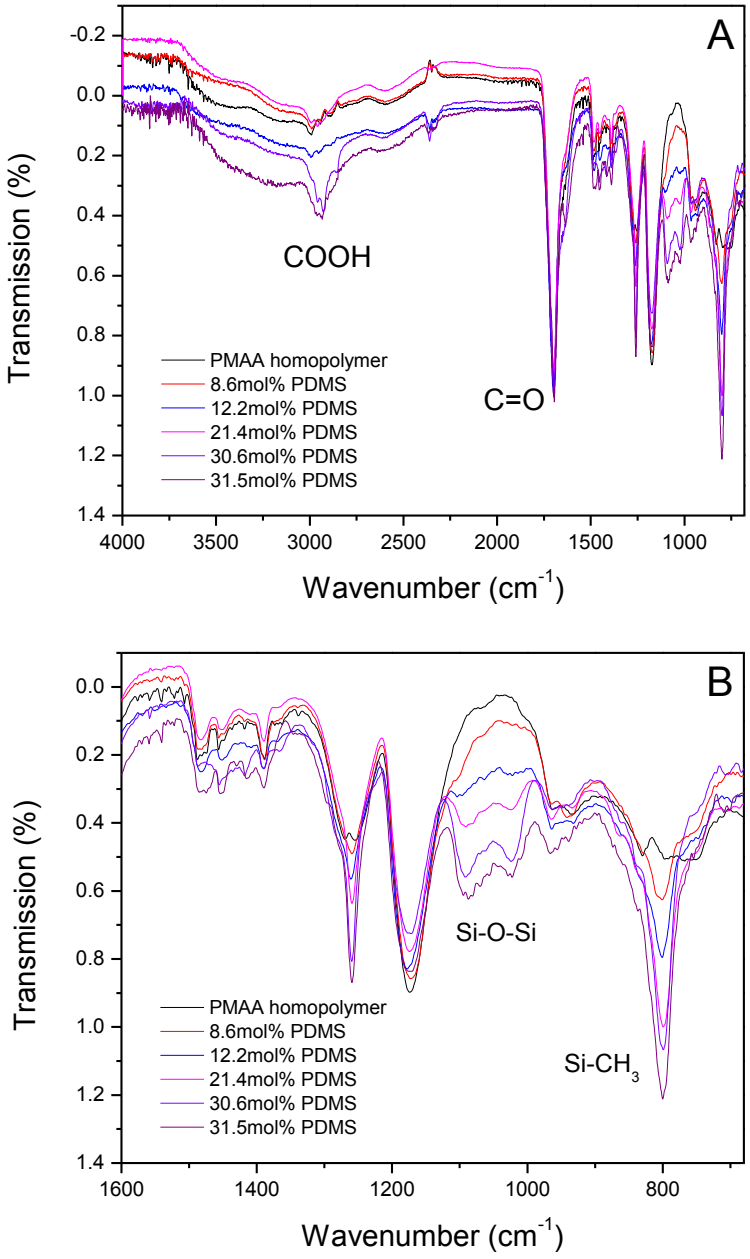

FIGURE 4-3: Infrared spectra for the copolymers series (PDMS = 1000 g/mol) (A) full spectra shown and (B) zoomed in to show the presence of PDMS

Stellenbosch University http://scholar.sun.ac.za

ATR-FTIR was also used to determine if the esterification reaction was successful for the conversion of the PMAA to the PMMA analogue. The IR spectrum shown in Figure 4-4 shows the disappearance of the acid OH absorption at 3500 cm^{-1}, and the appearance of CH_3 twisting peaks[8] at 1143 and 1190 cm^{-1}. This confirmed the esterification of the acid molecules.

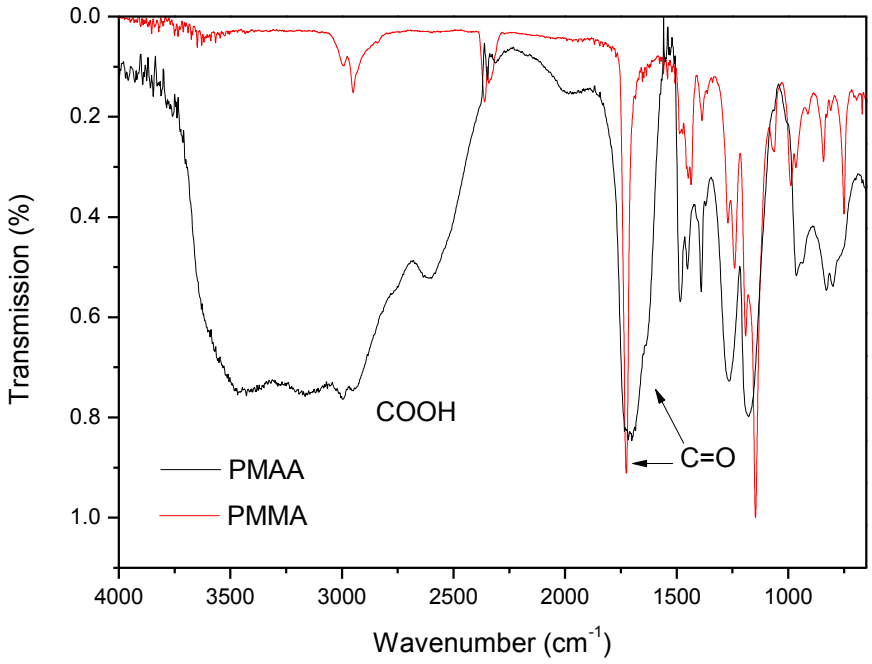

FIGURE 4-4: Infrared spectra showing the disappearance of the acid groups upon esterification of PMAA homopolymer to PMMA homopolymer

4.1.3.3. Size exclusion chromatography (SEC)

SEC is the most common way of determining the molar mass and molar mass distribution of polymers. In this study, the molar masses were determined in THF using the PMMA analogue of the copolymers. Table 4-2 shows a summary of the SEC analysis, and Figure 4-5 shows the SEC chromatograms for the PMMA copolymers.

Stellenbosch University http://scholar.sun.ac.za

TABLE 4-2: Summary of the feed composition, molar mass and PDMS content of the copolymer as determined from ^{1}H-NMR

Sample	PDMS Feed ratio (wt %)	PDMS feed ratio (molar ratio acid/siloxane groups)	$<M_n>$ (10^4 g/mol)[a]	Dispersity Index Đ	PDMS content[b] (molar % acid to siloxane groups)	Percentage PDMS inclusion[c]
PMAA	0	0	9.7	3.2	0	0
110	10	13.6	10.1	3.8	8.6	62.8
120	20	26.3	10.5	3.6	12.2	46.4
130	30	38	9.4	5.1	21.4	56.4
140	40	48.8	8.5	3.1	30.6	62.7
150	50	58.8	9.1	4	31.5	53.4
510	10	44.3	10.1	2.9	15.4	34.7
520	20	64.2	11.2	3.6	17.9	27.8
530	30	74.4	10.1	3.2	19.8	26.2

(a) Determined by the SEC of PMMA-g-PDMS samples on a column with THF as mobile phase

(b) Determined using ^{1}H-NMR integration of the PMMA and PDMS peaks.

(c) Determined as the ratio between PDMS molar feed ratio and the molar ratio calculated using ^{1}H-NMR

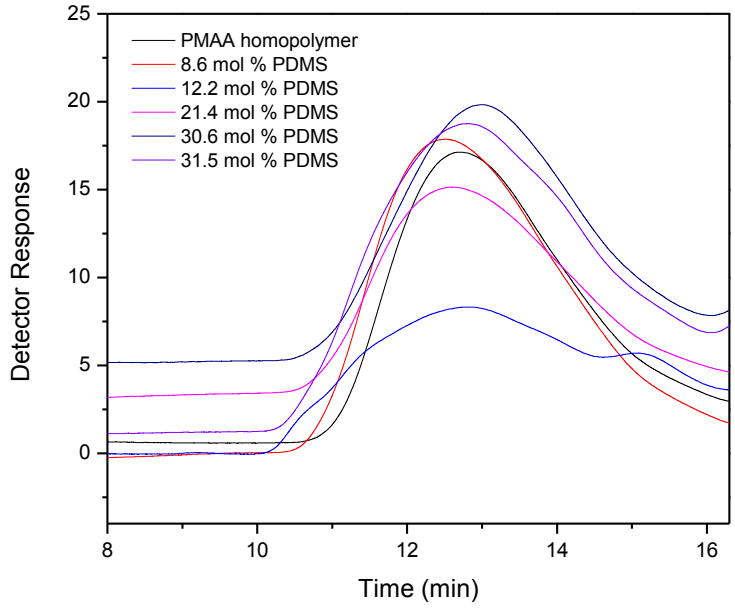

FIGURE 4-5: SEC chromatograms of the converted (PMMA) copolymers (PDMS =1000 g/mol)

Stellenbosch University http://scholar.sun.ac.za

The molar masses for the samples were around 90 000 – 100 000 g/mol. The samples did not show significant differences in molar mass, except for the sample 140 in Table 4.1. This sample had a lower molar mass compared to the rest. There does not, however, seem to be a trend relating the molar mass to the PDMS content of polymers.

The dispersity indexes of the copolymers were relatively high. Large molar mass distributions are expected during free radical reactions[9], although these values were exceptionally high. The high dispersity can in part be explained by the shoulder peaks and tailings observed for some samples. If acid groups were still present after esterification, this tailing could be explained as being due to some interaction with the column. However, no acid groups were detected from ^{1}H-NMR and FT-IR analysis. A further factor leading to broadening of the molar mass distribution could be the fact that the reactions were performed to very high conversions (above 90%). At high conversions, various transfer reactions may occur that can lead to increases in the width of the molar mass distribution of the products[10;11]. Again, as with the molar mass, the distribution does not seem to have a clear correlation to the PDMS content. If the PMAA homopolymer result is compared to the copolymers, we observe that the sample indicated as 130 had a much higher dispersity index. However, sample 140 showed a lower dispersity index, which is probably related to the lower molar mass. This would suggest that the dispersity index is more related to other factors than the PDMS content.

4.1.4. Gradient elution high performance liquid chromatography (GPEC)

The characterization of the polymers as discussed above (using ^{1}H-NMR, IR and SEC) gave information on the average copolymer composition, the molar mass, and dispersity, but lacked information on the exact composition and distribution that exists within the samples. Copolymers produced via free radical reactions are well known to be complex and may contain both homopolymer as well as the copolymer. They may also contain residual macromonomer[12]. One of the techniques commonly used to obtain more detailed information on the composition and the actual graft content of the polymers is gradient elution chromatography (GPEC)[12;13].

Stellenbosch University http://scholar.sun.ac.za

The mechanism by which separation occurs in GPEC is by adsorption/desorption. Separation is based on the solubility differences between different components of the polymers[14;15]. A solvent which favours adsorption of the polymers on the column is referred to as an adsorli and is a weak solvent for the polymers. A desorli is the opposite; the solubility of the polymer in this solvent is higher and favours desorption. In general, a gradient is started with a weak eluent to promote initial adsorption on the column. This is then followed by a gradual increase of the desorli. Molecules with different solubilities should then elute at different mobile phase compositions.

The first attempt was to perform gradient elution on the PMAA copolymer samples using the same gradient as employed for the separation of PAN-g-PDMS samples. Unfortunately, gradient elution chromatography of the PMAA-g-PDMS samples did not provide sufficient separation to characterize the samples. Other solvent combinations were investigated in an attempt to directly examine the PMAA-g-PDMS copolymers, this included MeOH/THF gradient profiles. Although slight differences in the peaks were observed for the copolymers of different compositions, no clear separation of the various components could be confirmed. In the MeOH/THF system the PMAA homopolymer was expected to elute early, followed by the graft material and lastly the PDMS. In the case of PMAA and copolymers, the use of pure adsorli was not possible as the polymers were not soluble in THF at all. Starting with MeOH was also not a successful option due to the fact that MeOH was a too strong solvent, preventing sufficient interaction with the column and selective solvation. To overcome this, samples were dissolved using a mixture of the adsorli (THF) and desorli (MeOH), with the THF added in the highest possible ratio which still allowed dissolution of the polymers. This composition was found to be 20:80 MeOH/THF. The gradient was then started with pure THF as shown in Figure 4.6.

Stellenbosch University http://scholar.sun.ac.za

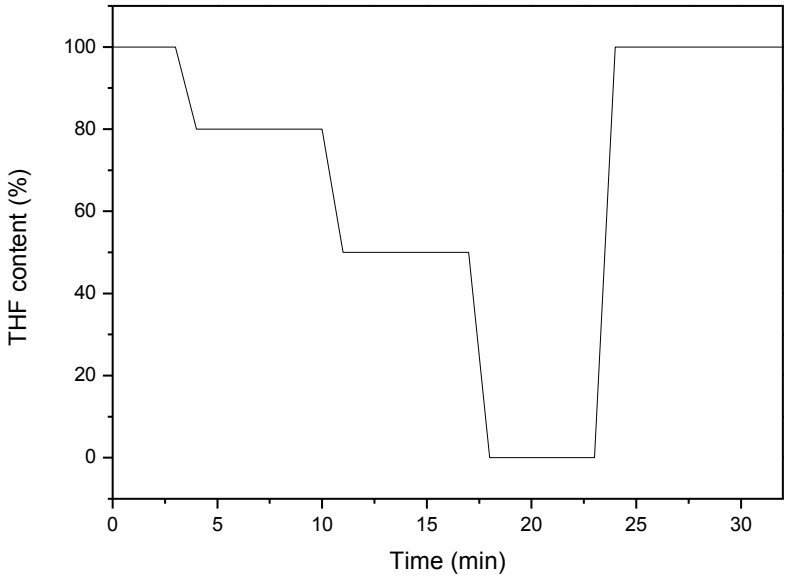

FIGURE 4-6: Gradient profile of the MeOH/THF mobile phase vs elution time for the gradient chromatographic separation of PMAA-g-PDMS samples (Symmetry300 C18 column, 5 µm, 1 mL/min, 30 °C)

Figure 4-7 shows the analysis of the copolymers analysed with this gradient. Three peaks were observed. It became evident using this gradient that differences did exist among the polymers. As the PDMS feed increased, the intensity of the peak between 2 and 3 mL also increased. It was, however, not possible to simply conclude that this peak was due to copolymers, since PMAA homopolymer also showed a peak in the same region. Due to the high THF content of the mobile phase, we expected the PMAA homopolymer to interact with the column more than with the solvent. The peak observed at 7 to 8 mL for PMAA homopolymer agreed with this expectation. The peaks at around 2 mL appeared to be copolymers as it was separated from PDMS homopolymer which eluted at 3 mL. However, the peak at 3 mL that was observed for PMAA homopolymer overlapped with the PDMS homopolymer peak. This made it impossible to tell whether the peaks in the other polymer samples were due to residual PDMS, or was part of the breakthrough peak of PMAA homopolymer. What was clear though is that differences existed between PMAA homopolymers and the copolymer samples. This conclusion was based on the fact that as the PDMS feed ratio changed, the intensities of the peaks at around 2 mL

Stellenbosch University http://scholar.sun.ac.za

and at 7 mL changed. A great reduction in the intensity of the peak at 7 mL was observed for samples with high PDMS contents – the 30.6 and 31.5 mol % PDMS samples.

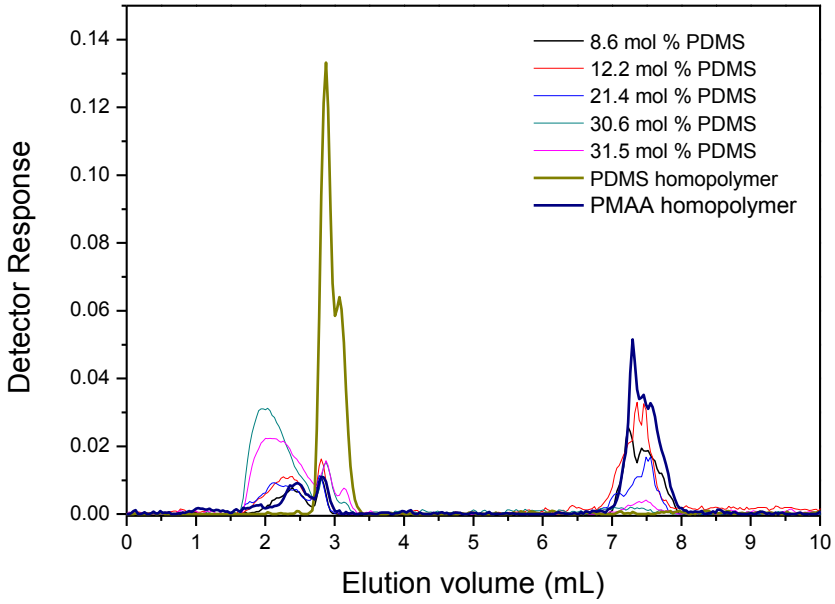

FIGURE 4-7: Gradient HPLC chromatograms for polymers containing PMAA backbones with different PDMS contents.

Instead of directly examining the PMAA-g-PDMS polymers, the analysis was performed on the esterified copolymers. Established methods already exist for the separation of PMMA-g-PDMS[15]. We thus knew that separation would be relatively simple using PMMA. In this study the same gradient that was used to separate PAN-g-PDMS copolymers[2] was used, which consists of a DMF to THF gradient. This gradient was also investigated for the PMAA-g-PDMS samples, but should be more effective when separating PMMA copolymers. PMMA is less polar than PMAA, so DMF will act as adsorli. By increasing the THF content, the PMMA and PDMS became more soluble and desorbed from the column at different composition. The gradient used for separation is shown in Figure 4-8. The chromatograms are shown in Figure 4-9 for the analysis of the PMMA copolymers.

Stellenbosch University http://scholar.sun.ac.za

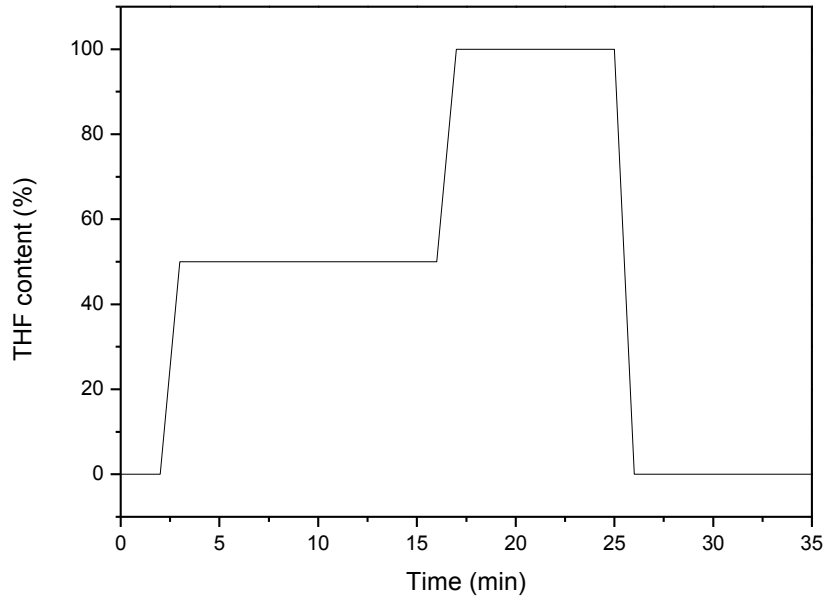

FIGURE 4-8: Gradient profile of the DMF/THF mobile phase vs elution time for the gradient chromatographic separation of PMMA-g-PDMS samples (Symmetry300 C18 column, 5µm, 1 ml/min, 30°C)

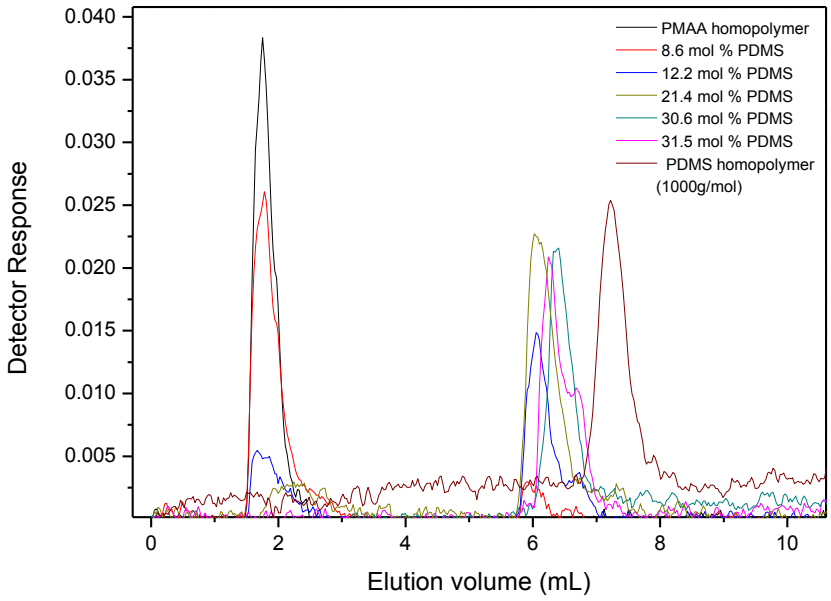

FIGURE 4-9: Gradient HPLC chromatograms for polymers containing PMMA backbones with different graft contents.

Stellenbosch University http://scholar.sun.ac.za

The appearance of a peak at around 6 mL, which was separated from both PDMS and PMAA homopolymer peaks, indicated the presence of graft material. The increase in graft material was clearly evident with and increasing PDMS feed ratio. The amount of graft material relative to that of PMAA homopolymer increased as the PDMS feed was increased. A gradual shift to later elution of this peak was observed as the PDMS content increased. This was expected since an increased PDMS content should increase the adsorption interactions with the column and thus the retention times. A shoulder peak appeared for the samples with more than 12.2 mol % PDMS, which tailed into the PDMS homopolymer region. This peak increased as the loading of the PDMS was increased. It probably represents some chains that contain a high PDMS fraction. The synthesis route to the polymers could explain that. The lower reactivity ratio of the macromonomers together with the severe incompatibility and precipitation of polymers during the reaction could have led to a gradient type polymer. Due to the fast homo polymerization of MAA, the initial polymer formed will probably consist mostly of PMAA homopolymer with little graft material. Chains formed towards the end of the reaction at higher conversions, will contain a larger fraction of PDMS and elute at later retention times[16].

4.1.4.1. FTIR characterization of fractions

The above results suggest that copolymers are present in the samples and that the graft content is related to the fraction of PDMS added to the feed. In order to confirm that separation occurred according to chemical composition, the composition of the peaks needed to be characterized[12]. Characterization was performed on the different fractions by collecting the samples as it eluted from the column. Fractions were collected for a representative copolymer sample. The sample containing 12.2 mol % PDMS was chosen as the representative sample as at it contained clear peaks at around 2 mL as well as 7 mL. Fraction 1 was collected between 1.5 and 1.9 mL. Fraction 2 was collected between 5.8 and 6.4 mL. The spectra for the two components are shown in Figure 4-10. Fraction 1 only had the peaks characteristic of PMMA at 1730.7 cm^{-1} (C=O) and 1150 and 1193 cm^{-1} (CH_3 deformation modes). Fraction 2 however also had peaks at 800 cm^{-1}, (Si-CH_3), 1260 cm^{-1} (Si-CH_3) and 1090 cm^{-1} (Si-O-Si), indicative of the presence of PDMS. Overlap of the pure PDMS peak in the chromatograms did not occur in this fraction. Any PDMS present must be part of the copolymer samples.

Stellenbosch University http://scholar.sun.ac.za

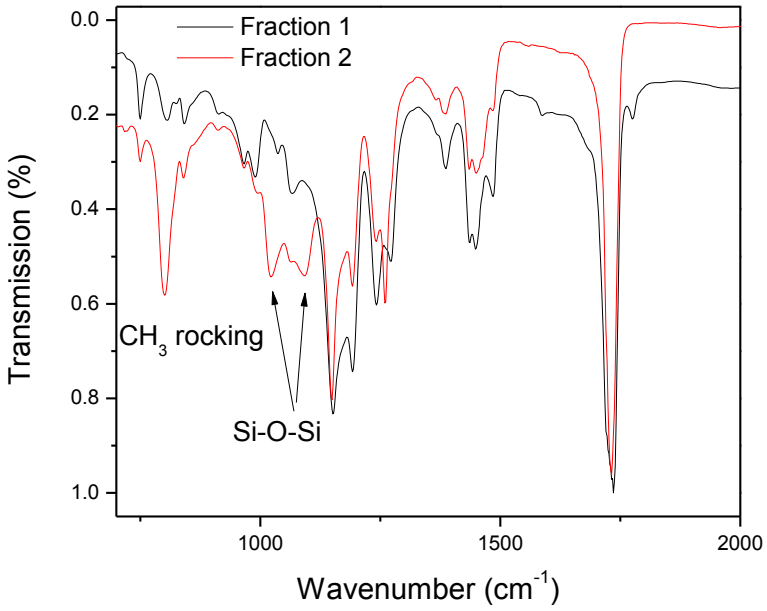

FIGURE 4-10: Infrared spectra showing the presence of PDMS in fraction 2 (copolymer), but not in fraction 1 (PMAA homopolymer)

From the above results it was concluded that synthesis of copolymers was successful. It also supported the ^{1}H-NMR results that suggested that the graft content increased as the feed ratio was increased. The high feed ratio polymers, 40 and 50 wt %, showed almost no PMAA homopolymer. No information on the chemical composition distribution was however obtained. More in depth analysis using 2 D chromatography is needed which could yield valuable results; and could be a very interesting study to pursue in future.

4.2. ELECTROSPINNING OF AMPHIPHILIC MOLECULES

The synthesised copolymers were used to produce fibres using electrospinning. Electrospinning became popular due to the simplicity of the set-up by which nanofibres can be formed. Although simple, a number of factors influence the properties of the fibre product that is obtained. These factors have been discussed in Chapter 2. The multitude of factors that influence the fibre formation can make this a complicated process to control. The large number of variables

Stellenbosch University http://scholar.sun.ac.za

affecting the fibre properties can, however, also be an advantage, as it provides a variety of options with which fibre properties can be altered. One way, which has not received a lot of attention, is the manipulation of the structures that exist in polymer electrospinning solution. Various authors have already shown that the self-assembled structures in solution can be used to alter the surface as well as internal properties of the fibres[17-20]. The polymers in the current study are highly amphiphilic which allows for the possibility to study how the PDMS content will affect the electrospinning of these molecules by manipulation of the electrospinning solution properties. Nanofibres have been obtained by electrospinning of a large variety of polymers including acidic polymers such as PAA. However, very few examples can be found on the electrospinning of polymers containing methacrylic acid monomer[21;22]. In this following section, the electrospinning of PMAA and its copolymers will be discussed, focusing on the effect of PDMS content, voltage, and solvent on the fibres.

All samples were electrospun under the same atmospheric and electrospinning conditions to ensure accurate comparisons were made. The conditions used were as follows:

Feed rate:	0.010 mL/min
Distance:	20 cm
Temperature:	23 °C
Relative humidity:	48-52%
Solvent:	DMF, DMF/$CHCl_3$ (8:2), DMF/$CHCl_3$ (7:3)
Polymer concentration:	12 wt %
Voltage:	18 kV (collector at -13 kV)

The conditions above were determined by a trial and error approach. Initially samples were electrospun by applying a charge to the needle tip, but keeping the collector neutral. The electrospinning setup used for these initial studies did not allow for the collector charge to be adjusted. This setup was, however, found not to be effective. Very few fibres were observed. Instead, circles of wet areas formed on the foil due to droplet spitting. This could've been due to too high viscosity. This will prevent the formation of a smooth fibre jet. Also, if fibres did form

Stellenbosch University http://scholar.sun.ac.za

they would probably break before reaching the collector. Another possibility was that the solution was charged too high, and because PMAA is a polyelectrolyte, the repulsion increased to the extent where no fibres are observed.

The use of a setup which allows the setting of both needle and collector voltage was investigated. Spitting was continuously a problem, but could be minimised by having the collector at a higher voltage than the polymer solution. Placing the minimum charge (of around 5 kV) on the needle tip and thus solution, and a higher, opposite voltage on the collector, resulted in higher fibre yields (based on simple visual observation).

4.2.1. Influence of PDMS content

This section focuses on the influence of PDMS content on the resulting fibre morphology. The samples were labelled according to PDMS content as determined by ^{1}H-NMR. Figure 4-11 shows the influence of the PDMS content on the fibre diameters. It should be noted that the "error bars" in the figure indicate the fibre diameter distribution and not the standard error. In general, the resulting fibre diameters increased as a function of the PDMS content in the polymers. The results are consistent with results obtained for PMMA-g-PDMS[23] and PAN-g-PDMS[2] fibres where a similar increase in fibre diameters was observed with an increasing PDMS content.

Figure 4-12 shows the fibre diameter distributions for each of the electrospun copolymers. The shift to higher molar mass was clearly visible as the PDMS content increased. Copolymer samples showed broader fibre diameter distributions when compared to PMAA homopolymer. This is most probably due to the presence of both PMAA homopolymer and copolymers in the samples although it is extremely unlikely that individual fibres consist of only PMAA homopolymers or copolymer. No significant differences were observed between the fibre diameter distributions for the copolymers and the width of the distribution did not change significantly as a function of PDMS content. This was also observed in the case of PAN-g-PDMS samples, although some broadening was observed when the PDMS content was as high

Stellenbosch University http://scholar.sun.ac.za

as 20 %. In general the distribution in fibre diameters were a lot lower in the case of PAN copolymers[2].

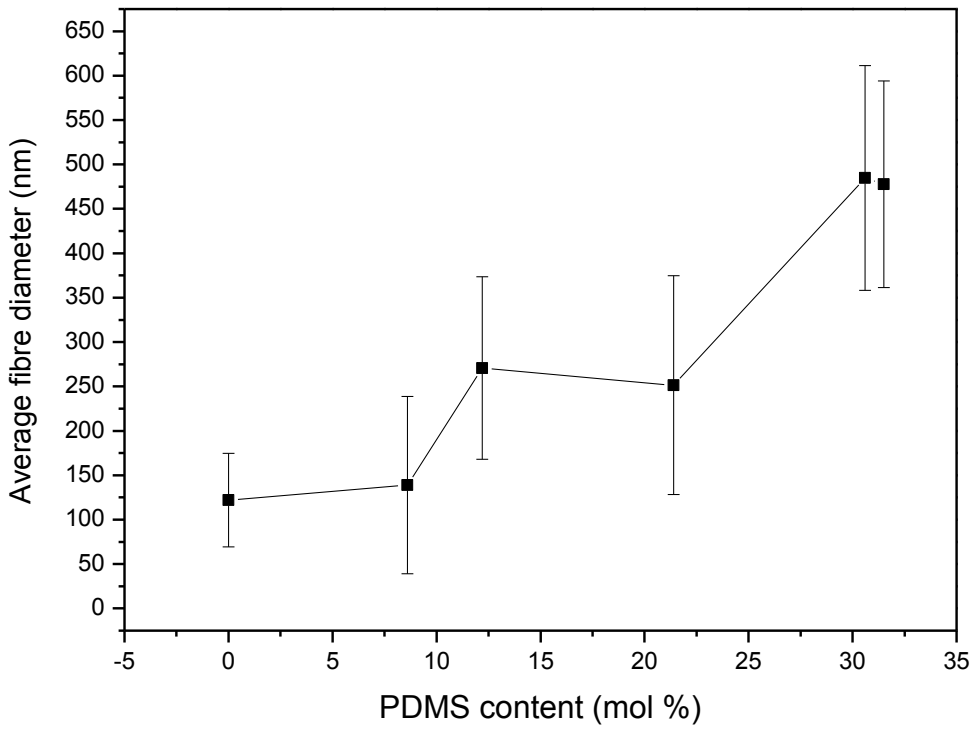

FIGURE 4-11: Graph showing the influence of increasing PDMS content on the average fibre diameter and the width of the distribution.

Stellenbosch University http://scholar.sun.ac.za

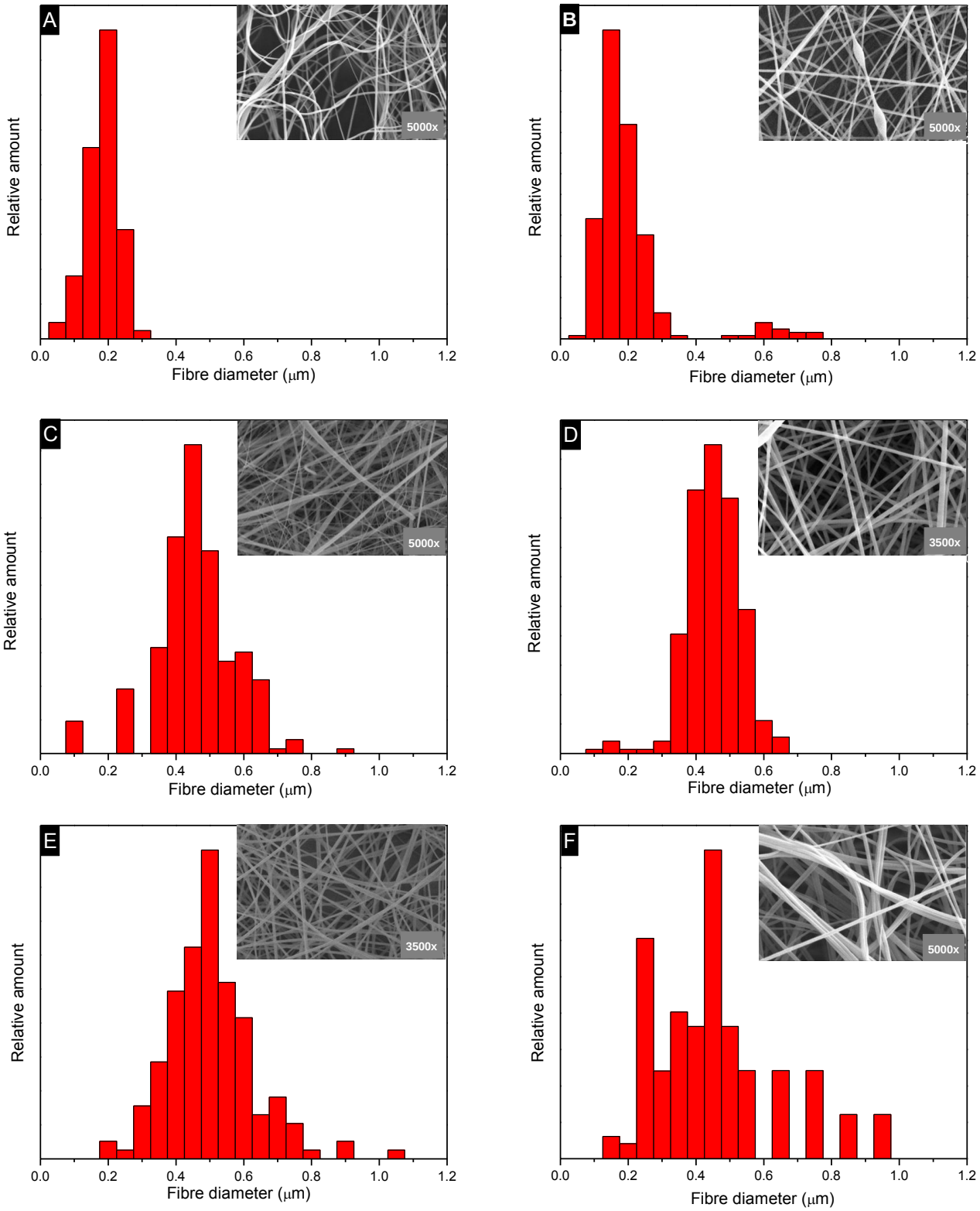

FIGURE 4-12: Fibre diameter distributions in polymers. (A) PMAA homopolymer (B) 8.6 mol % PDMS, (C) 12.2 mol % PDMS, (D) 21.4 mol % PDMS, (E) 30.6 mol % PDMS, (F) 31.5 mol % PDMS

Stellenbosch University http://scholar.sun.ac.za

The increase in fibre diameters can be discussed in terms of viscosity, conductivity, and self-assembly of the molecules in solution. Rheology was performed to determine the variation of the solution viscosity as a function of the PDMS content. The rheology curves of the solutions are shown in Figure 4-13.

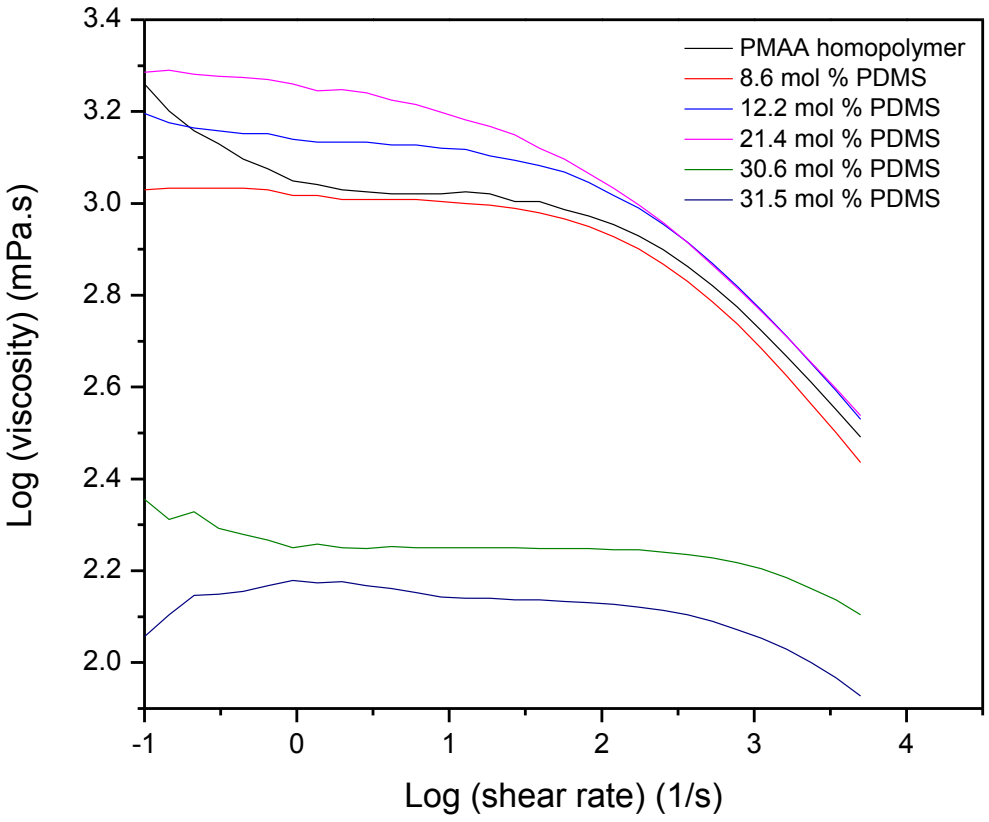

FIGURE 4-13: Rheology curves for polymers containing different PDMS contents (PDMS = 1000 g/mol) (10 wt %)

The viscosities of samples with 21.4 and 12.2 mol % PDMS was higher than that of PMAA homopolymer. This would explain the larger fibre diameters as compared to PMAA homopolymer. Viscosity differences do not, however, explain the larger diameters observed for the higher PDMS content polymers. The samples with above 30 mol % PDMS had lower viscosities. Based on this one would expect smaller fibre diameters. Viscosity refers to the resistance of a solution to flow. In electrospinning, this resistance will also act to resist the

Stellenbosch University http://scholar.sun.ac.za

pulling forces generated by the potential difference between the needle and collector. With all other conditions remaining the same, it has generally been observed that the solutions with higher viscosity will tend to have larger fibre diameters due to the higher resistive forces of the solution resulting in less "stretching" of the solution during the electrospinning[24] . In the case of the PAN-graft-PDMS series, it was found that an increasing in the PDMS graft content led to an increased solution viscosity and this was resulting in the larger fibre diameter[2].

In the case of the current study, it is clear that there is a far more complex relationship than was the case for the PAN series. In the current study, some of the higher PDMS content polymers have lower solution viscosities than the lower content samples, but still have larger average fibre diameters. There are a number of possibilities for the observed lower viscosities of these polymers. One possibility is that these samples have slightly lower molar masses (see Table 4.3), although the differences are not significant enough to lead to the large difference observed. Another possibility is that the difference is due to hydrophobic interactions and complex formation that occur in the molecules[25]. When hydrophobic interactions occur in an effort to reduce contact with water/polar solvents, the formation of compact structures can take place which reduces the viscosity. This would explain the reduction in viscosity as the content of PDMS increased. One would expect the fibre diameters to follow the same trends as observed for the viscosities. This was however not the case, which is very interesting since lower viscosities usually result in lower fibre diameters. This indicated that some other factors contribute to the fibre morphology.

Self-assembled structures will not only affect the solution viscosity, but can have some interesting effects on the morphology of the fibre surface. A study by Bayley and Mallon[2]. showed how the surface structures could be directly related to the solution structures as was observed by TEM. The same study was performed for the PMAA-g-PDMS samples in the present study to see how the morphology was affected. TEM images were obtained for polymer films by dropcasting dilute solutions onto copper grids. The idea was to visualize to some extent the changes that occur in solution as a result of PDMS content. Figure 4-14 shows the TEM images of the self-assembled structures in solution for the different copolymers. Note that in the images the white parts represent the polymer samples. A negative staining technique using

Stellenbosch University http://scholar.sun.ac.za

uranyl acetate was used. Unfortunately, it was not possible to identify the individual PDMS and PMAA segments from each other.

The images in Figure 4-14 appear to show some agglomerated network structures were present in the electrospinning solution. The structures are, however, a lot less evident than those observed by Bayley and Mallon[2]. The complexity of the self-assembled structures that can be obtained in the case of graft copolymers were highlighted in the literature section. It appeared as though some of the structures observed for the copolymers in DMF resembled the system investigated by Kikuchi and Nose[26]. They proposed that flower-like micelles form in dilute solutions where the solvent is good for the backbone. With increased concentration, associations between the micelles will lead to various multimolecular micelles. A range of intermolecular associations are possible which can lead to these complex self-assembled structures.

The network structures increase in size as the PDMS content increased. Furthermore, the size of the agglomerated structures that were observed seemed to correlate with the increase in fibre diameters as observed in Figure 4-11. It should be noted, however, that the method used in the sample preparation for the images shown in Figure 4-14 is not ideal for observing solution structure. Various processes can affect the film formation such as coalescence during drying. In addition, the negative staining agent used, uranyl acetate, possibly could've formed bonds with the carboxylate groups and cause agglomeration as is experienced with sialic acid[27]. Cryo-TEM would be a more suitable technique to directly observe the structure, but unfortunately this was not performed during this study. However, the sample preparation method does to a certain extent simulate the processes that occur during the rapid solvent evaporation that occurs during electrospinning. In previous studies[2], this preparation method proved very useful to study the relationship between solution structure and fibre morphology. Further studies, including the use of cryo-TEM should be considered for similar studies in future. Nevertheless, the results still give an idea that differences exist at least in the size of self-assembled/coalesced structures, which could give a hint at what happens when the polymers dry during electrospinning. If this is the case, then it explains why the higher PDMS content had bigger fibre diameters, since bigger agglomerated structures will undergo less stretching if the same force is applied.

Stellenbosch University http://scholar.sun.ac.za

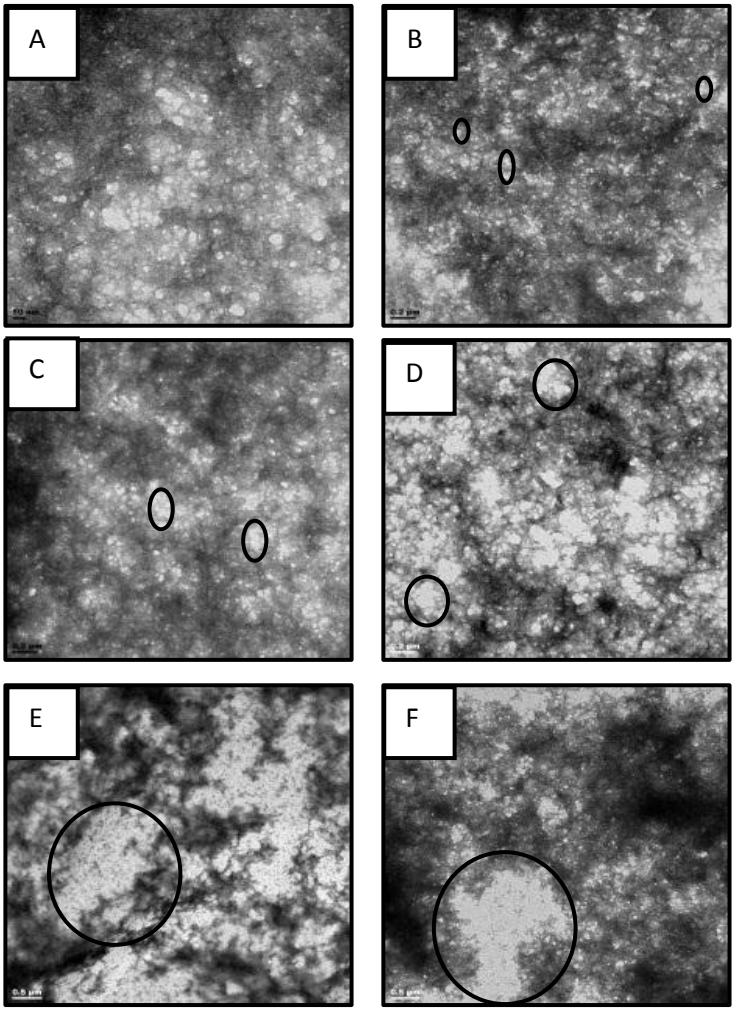

FIGURE 4-14: Typical images obtained by casting dilute solutions of polymers in DMF on copper grids. (A) PMAA homopolymer (B) 8.6 mol % PDMS (C) 12.2 mol % PDMS (D) 21.4 mol % PDMS (E) 30.6 mol % PDMS (F) 31.5 mol % PDMS

A further factor that can influence the fibre morphology and fibre diameter is the conductivity. It is known that with charged polymers, the inclusion of non-polar side chains reduces the conductivity. If the number of side chains increases, or if the length of the side chains increases, the conductivity is reduced. The reason for this is that the charge density of the polymer decreases[27]. In the system with PMAA and PDMS, as the PDMS content of the polymers increase, we could expect some decrease of the charge density, essentially leading to lower conductivity of the solution. Ultimately this could have led to lower stretching forces and overall increase in fibre diameter[28]. The complex relationship between the polymer composition and

Stellenbosch University http://scholar.sun.ac.za

fibre morphology was further investigated by the manipulation of the various electrospinning parameters.

4.2.2. Electrospinning parameters

4.2.2.1. Voltage

The effect that the electrospinning voltage has on the fibre morphology was investigated for the copolymers of different composition. All other variables such as concentration and ambient parameters were constant. The charge applied to the solution was kept at a constant value of 5 kV, with the charge applied to the collector being varied for every measurement. The potential difference between the solution and the collection plate was varied between 10, 14, 18, and 25 kV. Smooth fibres could not be obtained with higher voltages due to breakage of the jets and resulted in highly beaded fibres or simple electrospraying. See Figure 4-15. Also refer to start of Section 4.2 where the electrospinning was discussed. There mention was made as to why the collector voltage was varied instead of the charge on the polymer solution. The discussion here focuses only on studies where the polymer solution was kept at 5 kV.

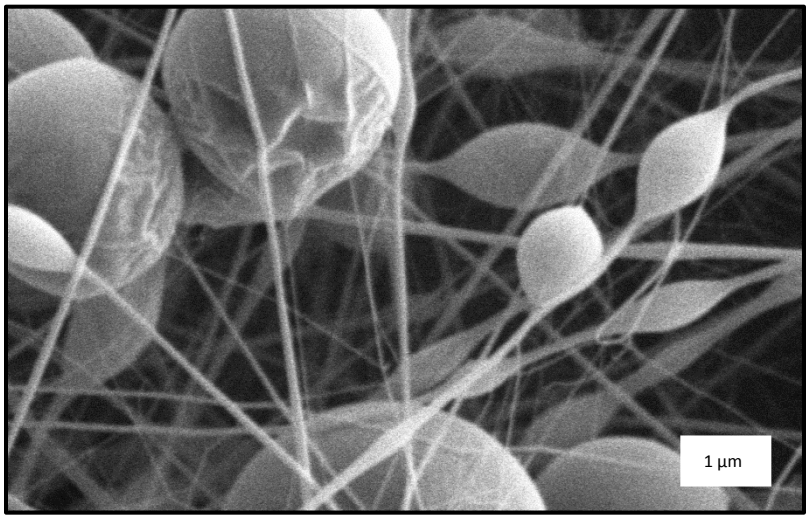

FIGURE 4-15: SEM image showing the example of the beading/spraying observed when fibres are electrospun at high voltages (8.6 mol % PDMS sample shown as example**)**

Stellenbosch University http://scholar.sun.ac.za

Figure 4-16 shows the relationship between the electrospinning voltage and the fibre diameter (with fibre diameter distribution) for copolymers of different composition. The general trend is an overall increase in fibre diameter as the potential difference was increased although it should be noted that there is not a clear trend and large deviation are observed. Several researchers have proposed that greater voltages will result in more solution being pulled out at the syringe tip to cause the formation of larger fibre diameters[23]. In addition, fibres are pulled towards the collector at a faster rate, which would reduce the stretch time and result in a larger diameter. As the PDMS content (or the graft content) of the fibres increased, the relationship between the voltage and fibre diameter changed to some extent. This is evident when the shape of the curves for graphs A-C is compared to graphs D-F in Figure 4-16. PDMS clearly had some influence on the behaviour of the polymer samples[24] with the higher content PDMS samples have consistently larger fibre diameters.

Stellenbosch University http://scholar.sun.ac.za

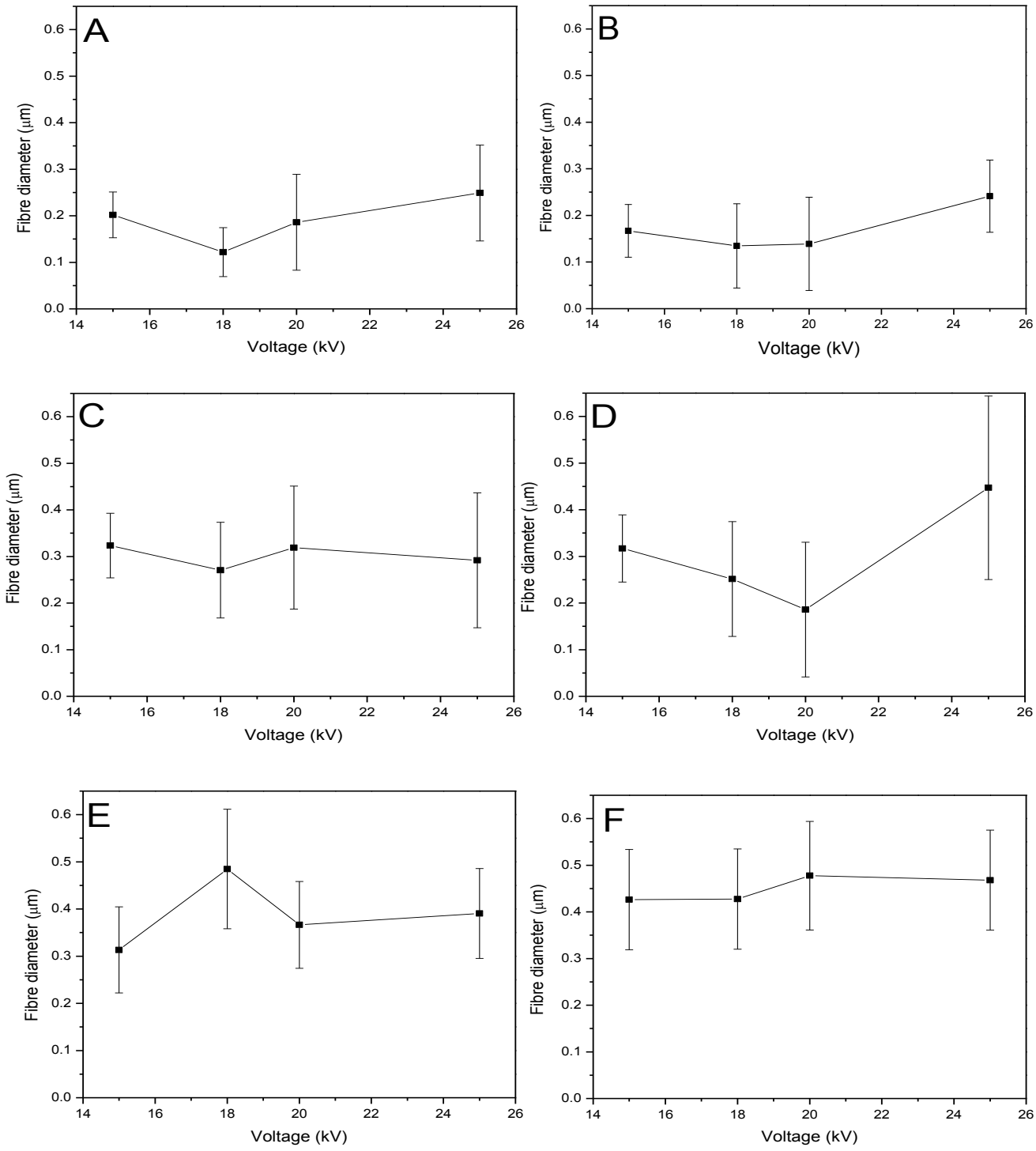

FIGURE 4-16: Graphs of fibre diameter and distribution as a function of voltage for samples with different PDMS contents (A) PMAA homopolymer (B) 8.6 mol % PDMS (C) 12.2 mol % PDMS (D) 21.4 mol % PDMS (E) 30.6 mol % PDMS (F) 31.5 mol % PDMS

Stellenbosch University http://scholar.sun.ac.za

4.2.2.2. Influence of solvent

The electrospinning solvent is one of the most important parameters affecting the electrospinning process and resultant fibre morphology. Solvent properties of importance are the dielectric constant, vapour pressure, solvent quality and surface tension. In the case of amphiphillic copolymers, the solvent quality will determine the solution conformation of the molecules and any self-assembled solution structures. In the case of this study, the solution behaviour was of great importance as the large incompatibility of the two polymers was expected to result in changes in the phase separation behaviour when the solvent quality is varied. In the current study, different combinations of DMF and $CHCl_3$ were used to study the solvent effect. In this case DMF is a good solvent for the PMAA, while $CHCl_3$ is a good solvent for the PDMS side chains. In effect, by increasing the $CHCl_3$ content, we have an increasingly good solvent for the side chains and an increasingly poorer solvent for the backbone. Figure 4-17 shows the effect of the solvent composition on the fibre diameter. In the case of the PMAA homopolymers, the solvent composition has little effect on the fibre morphology. However, in the case of the copolymers, a more dramatic effect is seen. For the series up to 21.4 mol % PDMS, a general increase was observed with the addition of chloroform to the solution. Addition of chloroform reduces the conductivity of the solution, as chloroform has a low dielectric constant. An increase in fibre diameter would then be the expected as a result of a smaller electrostatic force pulling on the polymer. In comparison, the polymers with more PDMS indicated a slight decrease. Anomalous results were also found for the 30.6 and 31.5 mol % PDMS-containing polymers with the rheology measurement. The decrease in fibre diameter for polymer with higher PDMS inclusion must then be explained by different solution conformations, but more details regarding the conformations are required in order to prove this statement.

Stellenbosch University http://scholar.sun.ac.za

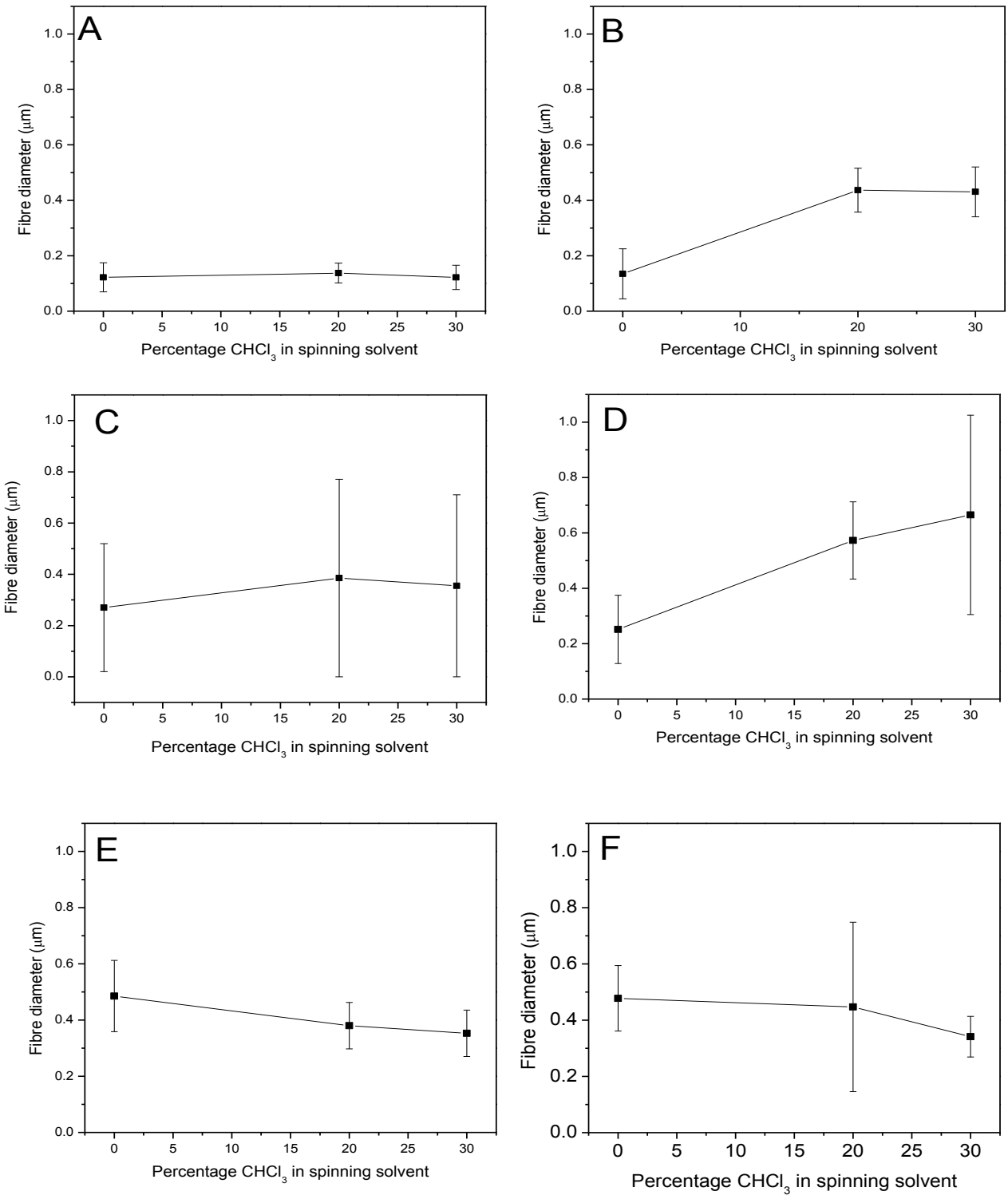

FIGURE 4-17: Graphs illustrating the influence of solvent on the fibre diameters for samples with different PDMS contents. (A) PMAA homopolymer (B) 8.6 mol % PDMS (C) 12.2 mol % PDMS (D) 21.4 mol % PDMS (E) 30.6 mol % PDMS (F) 31.5 mol % PDMS

Stellenbosch University http://scholar.sun.ac.za

The distribution in fibre diameters for the PMAA homopolymer and copolymers showed clear differences. In all the solvent combinations that were investigated the copolymers showed larger distributions. This is probably related to the distribution in composition of the polymers. The copolymer samples contain chains with different compositions; some chains will have more grafts than others. Some of the samples also contain PMAA homopolymers. The range of fibre diameters that is obtained will be influenced by these differences.

Although it was clear that copolymers showed broader size distribution, a clear correlation between solvent and fibre diameter distributions could not be made. The only observation that can be made is that all samples showed either a higher, or more or less the same, distribution when chloroform was added, but the distributions did not decrease with addition of chloroform.

4.2.3. Internal morphology of fibres

In the previous section, it was shown that the fibre diameters were influenced by the PDMS content. In this section, the focus shifts towards the fine structure of the fibres, that is, how PDMS will affect the surface and internal morphology of the fibres. Previous studies have shown that the PDMS content can result in differences in the internal and surface fibre morphology[2].

Figure 4-18 shows an example of the initial analyses performed with the figure on the left shown the FE-SEM analysis of as spun fibres and the figure on the right the resin prepared sample. The surface of all the as-spun fibres appeared smooth. This is in contrast to the results of Bayley and Mallon, where, in the case of PAN-g-PDMS copolymers, a porous type fibre structure was observed[2]. It should be noted that there were some difficulties in using this technique. The polymer nanofibres tended to swell/dissolve when placed in a resin for embedding. This was especially the case for PMAA homopolymer which disappeared completely in the resin. The copolymers in some cases could be imaged, but the quality of images obtained was poor. It is clear that this preparation method is not suitable for the samples in this study and alternative methods had to be used to obtain cross-sections of the fibres. Figure 4-18 represents an example of one of the few images that could be obtained using this

Stellenbosch University http://scholar.sun.ac.za

method. As mentioned this could only be seen for the high PDMS content nanofibres. It is clear from this result that the PDMS content does affect the solubility of the fibres, but this is not a suitable method.

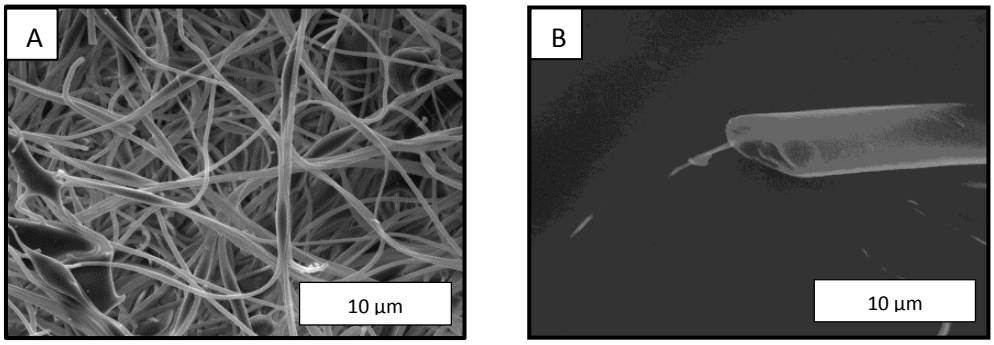

FIGURE 4-18: FE-SEM images for the sample containing 21.4 mol % PDMS (A) and surface (B) embedded in resin

An alternative method was explored to prepare the sample for the imaging of the internal nanofibres morphology. In this method the electrospun nanofibres were placed in liquid nitrogen and these frozen samples were “freeze fractured” by crushing the frozen samples. This method proved to be more effective and circumvented the problem of swelling and dissolution of the fibres with the resin embedding method. Figure 4-19 shows the 21.4 mol % PDMS copolymer nanofibres produced with different electrospinning solvent compositions. Similar images were produced for the other copolymer series. The surface as well as internal morphology appeared smooth in all solvents. The images are representative for all other samples. It is clear from the D, E and F images of that no internal structure can be seen in the fibres, and the nanofibres have a smooth surface morphology. This is in contrast to the results that have been reported for PAN-graft-PDMS copolymers where distinct internal fibre morphologies were observed[2].

Stellenbosch University http://scholar.sun.ac.za

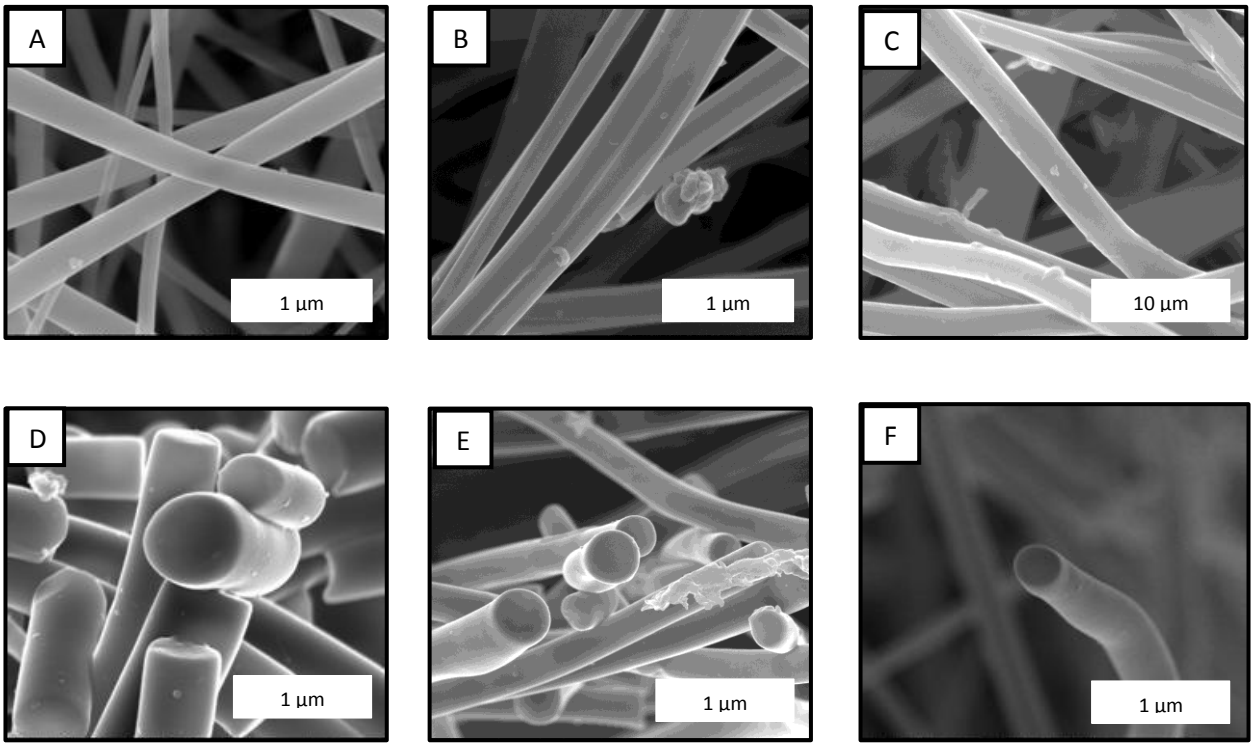

FIGURE 4-19: Typical FE-SEM images of the surface and internal morphology for copolymer containing 21.4 mol % PDMS as function of solvent composition: (A+D) DMF, (B+E) DMF/$CHCl_3$ (8:2), (C+F) DMF/$CHCl_3$ (7:2)

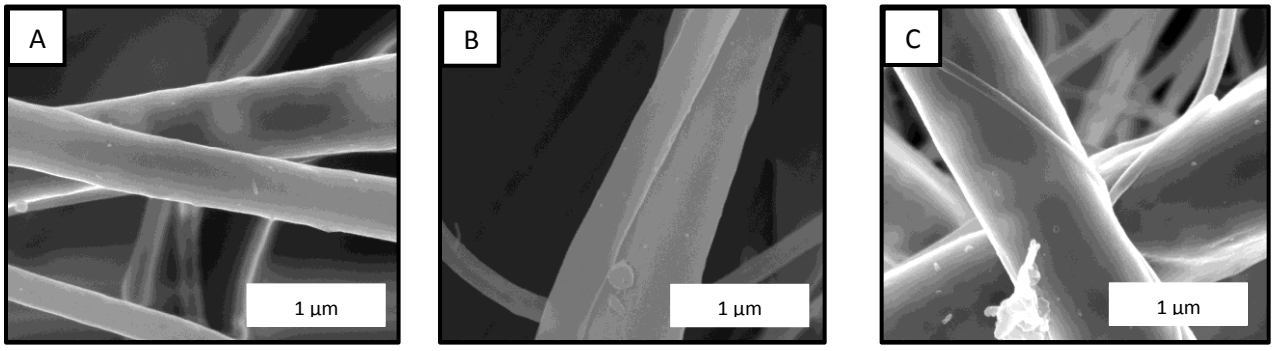

FIGURE 4-20: Surface morphology for fibres with different PDMS content: (A) PMAA homopolymer, (B) 12.2 mol % PDMS (C), 21.4 mol % PDMS

Stellenbosch University http://scholar.sun.ac.za

Figure 4-20 shows the fibre surfaces for samples with different PDMS content. Pictures are shown for 3 representative samples. Smooth fibres were observed for all. It appears as though the PDMS content did not have an influence on the fibre surface.

As mentioned above, it has been shown that the electrospinning of similar copolymer series resulted in a highly porous internal morphology. In this case, the observed morphology was explained by the "freezing-in" of the solution structure as a result of the rapid solvent evaporation during the electrospinning process[2]. It's unlikely that the smooth fibres observed in the current study are due to a lack of a similar self-assembly in solution. The high incompatibility of the two constituents of the copolymers will result in some self-assembly in the electrospinning solution and phase separation in the solid state. In the case of the PMAA-graft-PDMS copolymers the lack of any surface or internal features can be explained as being due to the following:

1. It is possible that the acid molecules present in the polymer form hydrogen bonds with the solvent (DMF). Strong interactions like this will prevent solvent molecules from rapidly evaporating, leaving the fibres to be elongated for longer and preventing phase separation during the short time it takes for the fibres to "fly" from the electrospinning needle to the collector plate. Solvent loss is one of the mechanisms by which phase separation occurs during electrospinning[29]. The rapid evaporation of the solvent during the electrospinning process is at least partially responsible for the "freezing in" of the structures. If solvent molecules were bound by hydrogen bonding, the evaporation rate would be slowed and the fibres will be in solution longer, allowing smooth fibres to be formed[30]. The DMF may also have a plasticisation effect on the PMAA segments, meaning the material will have a lower Tg allowing the annealing out of any structure initially formed in the fibre.

2. A second factor is that PMAA has a lower critical solution temperature (LCST) than PAN. The lower critical solution temperature refers to the temperature where a change from

Stellenbosch University http://scholar.sun.ac.za

soluble to phase separated will occur in solutions or blends. Polymers with a LCST will be soluble below a certain temperature; and above the LCST the polymer will become insoluble. No mention of this factor could, to the best of our knowledge, be found in any literature regarding the electrospinning process. It should, however, affect the fibre morphology if the mechanism of fibre formation during electrospinning is considered. Pore formation on fibres is a complex process which depends on a number of factors, of which phase separation is one. During electrospinning the flash vaporization of solvent from the jet leads to cooling. It is this cooling effect that is responsible for the formation of polymer rich and polymer poor domains due to the decreased solubility at lower temperatures[29;30]. The importance of the formation of polymer rich and polymer poor domains in the obtainment of structured fibres was covered in the literature section. For most polymers the lowering of the temperature will lead to phase separation as solubility goes down as temperature decreases. Important to note is that in the case of a polymer with a LCST, the polymer will be more soluble at a lower temperature. Instead of freezing in phase separated structures, the polymer is continually pulled and dries in a non-separated state. Normal polymers would become insoluble at the same reduced temperatures.

3. A third factor preventing the preservation of any phase separated domains in solution is the lack of any crystallization of polymer. Crystals formed during electrospinning would act as types of physical supports which should keep the solution structures intact. This was the case for PAN-graft-PDMS copolymers[2]. Crystallisation influences the rate of solvent evaporation. The use of volatile solvents often results in porous fibres[30; 31]. Crystallisable polymers will solidify faster than amorphous polymers when the polymer concentration becomes high during electrospinning[32]. This will result in pores; refer to Sections 2.1.4 and 2.3.3 for a discussion on the mechanism of pore formation during fast evaporation of the solvent. The onset of crystallisation will thus lead to solidification of the fibres. The method and time of solidification will influence the fibre morphology.

It is clear that a number of factors could have prevented the formation of surface or internal structures in the fibres. This again highlights how a process which seems so simple (obtaining nanofibres via electrospinning), is actually a combination of a number of complex

Stellenbosch University http://scholar.sun.ac.za

processes. Although no fancy fibre morphologies could be formed with the current system, other interesting properties were identified, as will be revealed in the following sections.

4.3. PROPERTIES OF THE FIBRES

In this section the moisture and water resistance of the copolymer fibres are discussed. As mentioned previously nanofibres hydrogels have many potential applications. Polymers of PMAA homopolymer are very moisture sensitive and will dissolve after a short period of time if kept under normal atmospheric conditions. Preservation of the fibrous structures for prolonged times required them to be stored in desiccators. We observed that the fibres formed from the copolymers did not show the same moisture sensitivity. The polymers themselves also didn't dissolve in water as did the PMAA homopolymer. Even after long stirring times the polymers only formed suspensions in water. This is a good indication that the nanofibres are in fact nanofibres hydrogels. This directed us to investigate the influence of PDMS on the moisture and water stability of the fibres. In addition, the chemical crosslinking of fibres was also investigated as a means to establish water stability.

4.3.1. Static water contact angle studies (SCA)

The inclusion of hydrophobic segments such as polystyrene and PDMS into polymers has been used as a means of modifying polymer hydrophobicity[22;31]. Water contact angle studies were performed to investigate whether this was the case for polymers consisting of very hydrophilic PMAA with PDMS side chains. No contact angle could be determined for the PMAA homopolymer as the fibres dissolved instantly when a water droplet was placed on the fibre mat. The polymers containing PDMS did, however, show increased hydrophobicity. Figure 4-20 shows the images of micro drops immediately after being placed on the surface of the electrospun nanofibres. It should be noted that these images changed over time and this is discussed in this section.

Stellenbosch University http://scholar.sun.ac.za

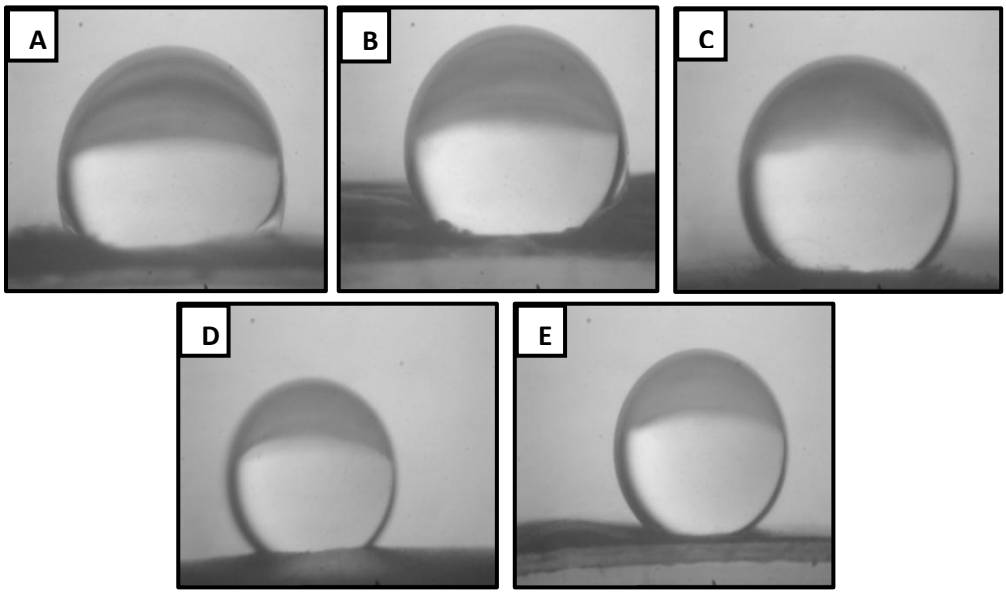

FIGURE 4-21: Images showing the change in static contact angle (SCA) with increasing PDMS content from A to E

Typical images obtained for samples containing varies amounts of PDMS are shown in Figure 4-21. The average contact angle as a function of PDMS content is shown in Figure 4-22. A clear increase in the contact angle was observed when the PDMS content increased from 8.6 mol % to 12.2 mol %. Further increases to 21.4 and 30.6 mol % did not result in drastic changes of the contact angle, although a clear increase was observed between 30.6 and 31.5 mol %. The preferential segregation of PDMS to the surface is mostly likely what causes the change in hydrophobic character[32]. Factors such as the fibre surface properties (surface structures or pores) and the roughness of the fibre mats have also been shown to affect contact angles of fibre mat[28]. Since in this case all fibres appeared smooth, the changes must be mainly due to the variation in PDMS content and the structure of the non-woven fibre mats. Previous studies involving the inclusion of PDMS in PMMA fibres indicated a continued increase in the contact angle when the PDMS content increased[32]. The results for the present study are possibly a combination of mat roughness and PDMS content, but the fibre mat roughness was not investigated[33].

Stellenbosch University http://scholar.sun.ac.za

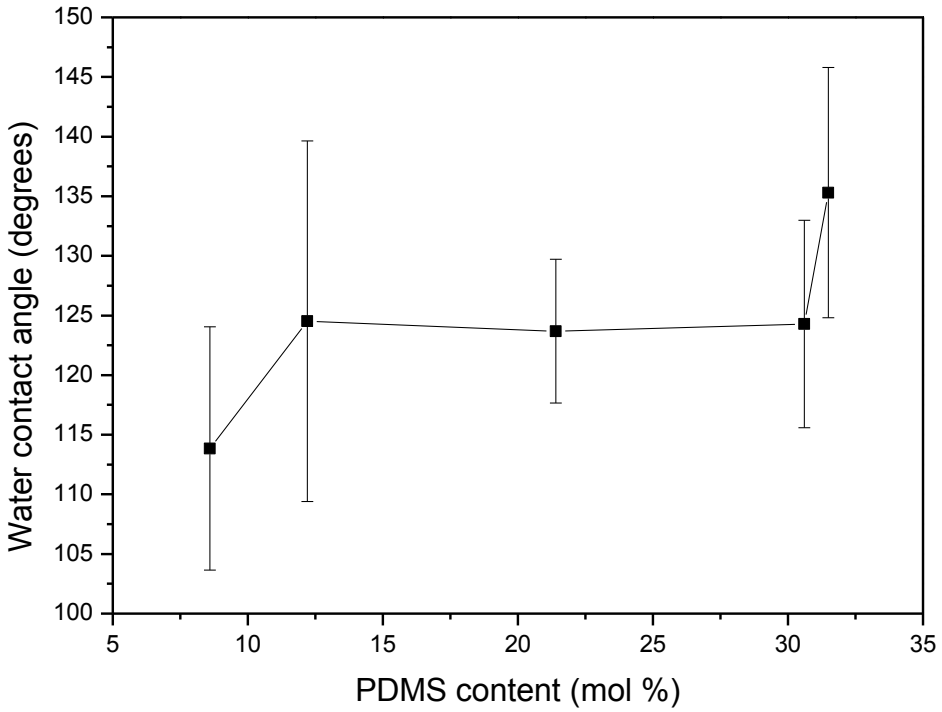

FIGURE 4-22: SCA as a function of PDMS content

The standard deviation of the values was quite large, which is due to the fact that the contact angles change with time. Images had to be acquired at a quick rate as the samples absorb water and the SCA changes over time. So even small variations in the time when the photos were taken would have resulted in different contact angles measured. The influence of PDMS on this time dependent behaviour of the SCA was investigated further. The results of this study are shown in Figure 4-23 where the change in the SCA as a function of time is shown for different PDMS content samples. The contact angle for samples with less hydrophobic character changed at a quicker rate; the droplet disappears earlier. Droplets disappeared after 0, 13, 16 and 22 min respectively as the content increased from 8.6 to 30.6 mol % PDMS. In Figure 4-24 a series of images is given showing the change in the droplet for the sample containing 8.6 mol % PDMS over time. This quick change of contact angle explains the relatively large distributions that were mentioned earlier. It is also clear from the result that the

Stellenbosch University http://scholar.sun.ac.za

PDMS content has a dramatic effect on the rate of the water absorption, the higher content PDMS fibres showing a slower water uptake rate. This is an interesting result since it suggests that the moisture absorption properties of the fibre hydrogels can be controlled by variation of the PDMS content of the nanofibres.

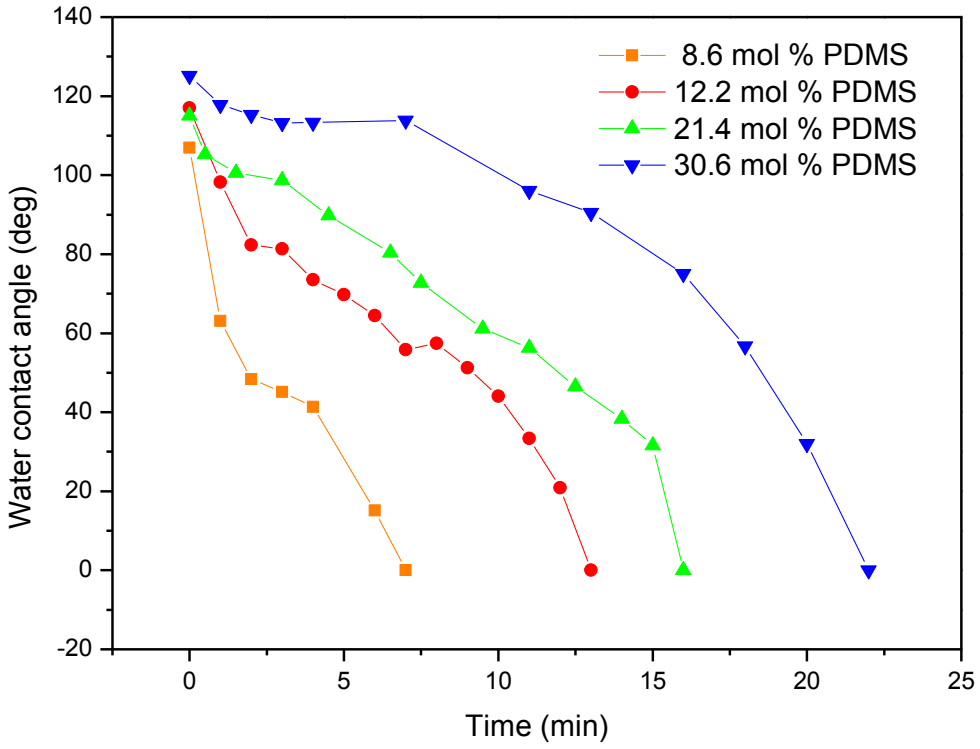

FIGURE 4-23: Change in SCA over time for polymers with different PDMS contents.

Stellenbosch University http://scholar.sun.ac.za

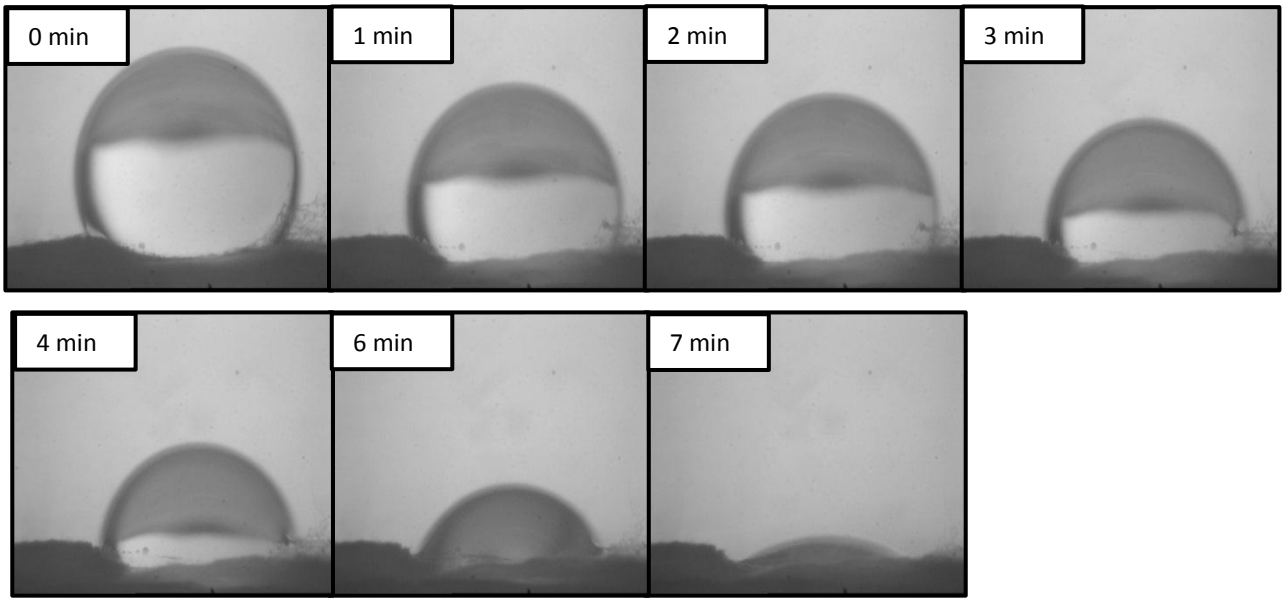

FIGURE 4-24: Series of images showing how the contact angle changed with time for a sample containing 8.6 mol % PDMS

4.3.2. Fibres in moisture

It was demonstrated in the previous section that the PDMS affects the hydrophobicity of the fibre mats. It was also mentioned that the PMAA homopolymer is not stable in high moisture or humidity environments. Stability in moisture and aqueous environments is a requirement if the fibres are to be used for applications such as copper removal from water or as nanofibre hydrogels[33;34;35].

In order to better understand the water absorption behaviour of the nanofibres, time dependence studies were done on the absorption of water from a high humidity atmosphere. This was done by measuring the mass as a function of the exposure time. Experiments were performed on an in-house built, modified TGA instrument. More details regarding the instrument was given in Section 3.5. There were some advantages in using this instrument as opposed to manual weighing in the lab. This included the fact that only small sample masses were required as the instrument is very sensitive to small changes in mass. In addition, the sample mass is

Stellenbosch University http://scholar.sun.ac.za

calculated every 2 seconds, which would not be possible by manual weight measurement studies. The only disadvantage of using this measurement technique was the fact that the moisture content in the chamber could not be too high, as this led to accumulation of water droplets on the pan. This obviously created erroneous weight values. The highest moisture content which allowed measurement without adding additional weight was chosen. This was around 75% humidity. Fibre weight was recorded as a function of time and the plots for the different PDMS content fibres are shown in Figure 4-25.

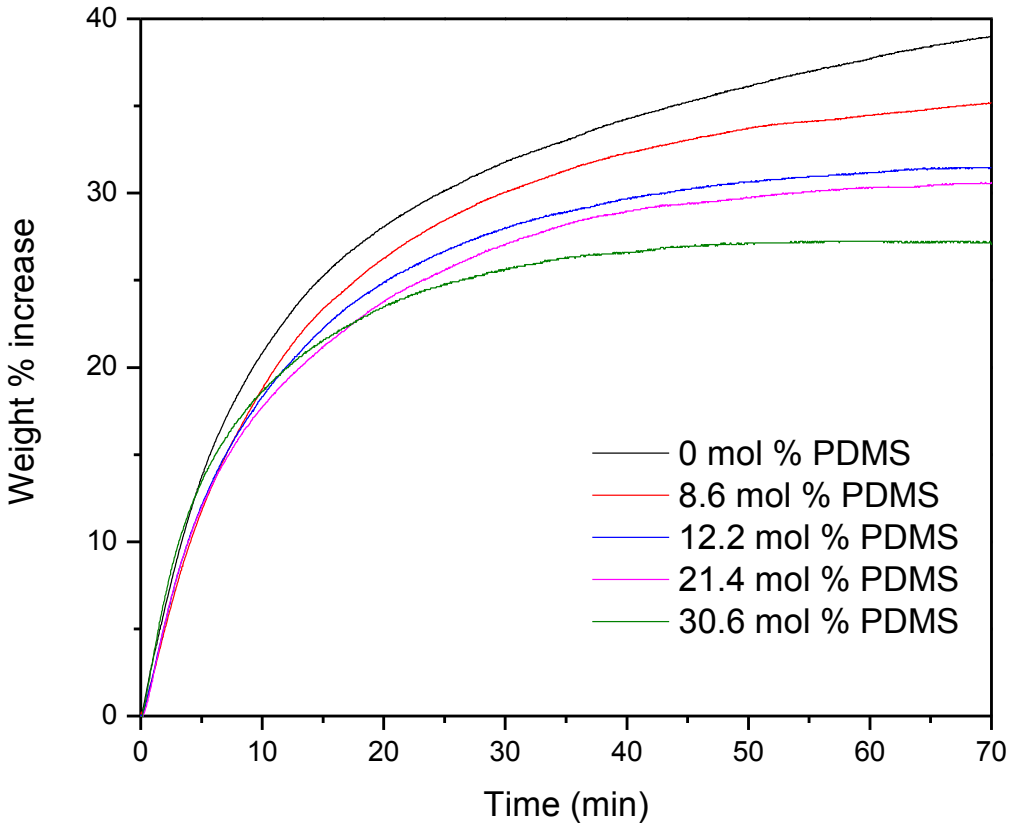

FIGURE 4-25: Fibre weight as a funtion of time until equilibrium is reached

The general trend observed from the graphs was that the amount of PDMS led to a reduction in the equilibrium moisture content of the fibres as indicated by the plateau in the weight gain curves. Curve fitting (using Origin) was performed to get a better understanding of the absorption processes and to quantify the behaviour of the polymers.

Stellenbosch University http://scholar.sun.ac.za

The Equation 4.1 was found to give the best fit. All the data were found to fit the above equation with R2 values of at least 0.999. The fitting with a single exponential equation do not provide a good fit. This gives some indication that the absorption is not a simple process. It was mentioned during an earlier discussion that a number of factors can influence the absorption by the fibres. This is now supported by the data fitting.

$$wt\ \% = A_1 e^{(-t/\tau_1)} + A_2 e^{(-t/\tau_2)} + \beta \qquad (4.1)$$

In the equation t is the time (min), τ_1 and τ_2 are time constants, β the equilibrium wt % and A_1 and A_2 are constants. The τ_1 and τ_2 values are plotted in Figure 4-26. A clear trend of the τ_1 parameter with an increasing PDMS content is noted. The τ_1 parameter is an indication of the rate of change of the initial part of the absorption curves. A bigger τ_1 value will indicate a slower initial absorption rate as we have $1/\tau_1$ in equation 4.1. It is clear that the initial rate of water absorption increases with an increase in the PDMS content. On the other hand the rate of the second term decreases with increase in the PDMS content. Various factors influence the rate of absorption by the fibres, including the hydrophobicity, fibre diameters, mat porosity, humidity, area exposed to moisture. Attempts were made to keep all variables except the hydrophobicity constant, yet it is difficult to explain the findings focusing on only one parameter.

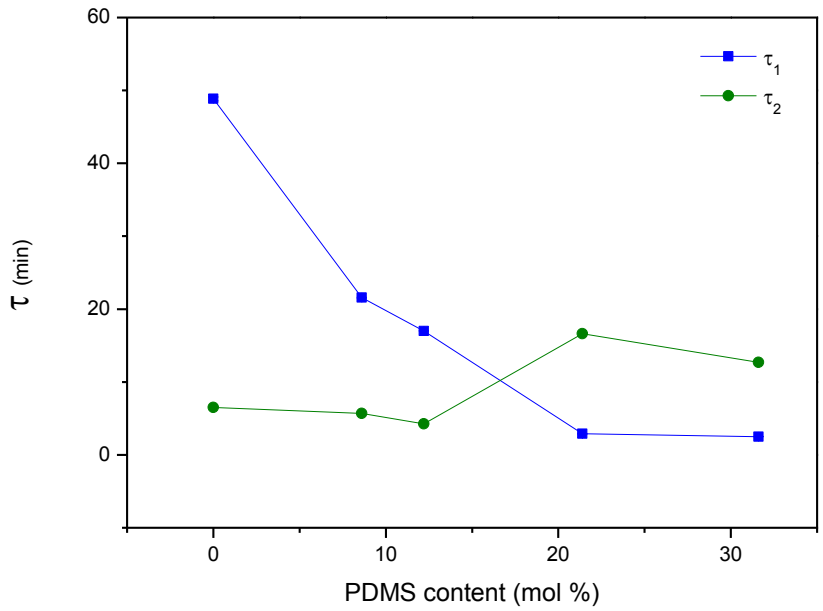

FIGURE 4-26: τ_1 and τ_2 values determined from equation 4.1 as a function of PDMS content

Stellenbosch University http://scholar.sun.ac.za

The equilibrium moisture content of the polymers were compared by plotting the β (equilibrium or maximum weight % increase) as a function of the PDMS content in Figure 4-27. The influence of the PDMS was clearly observed. Increased PDMS lowered the maximum moisture content of the fibres. This is not strange, PDMS is very hydrophobic so water will be less attracted and will be repelled by the siloxane groups present in the fibres. PMAA homopolymer increased around 40 percent its initial weight, this was 15 percent higher than that of the sample containing 30.6 mol % PDMS. Variable moisture absorption and release properties of polymers have been investigated for possible applications in soil humidity control. Polymers which can retain moisture and release it again at a certain rate are desired in such applications. As Teodora *et al.*[36] showed, copolymers with more hydrophobic character will release water at a faster rate. Nanofibres, with their greatly increased surface area, will be advantageous, especially if they can maintain their fibre integrity[36]. In this case, we observed that even the high PDMS content polymers absorb 25% of their weight. It is believed that the release properties will also be influenced by the PDMS content, although this was not studied.

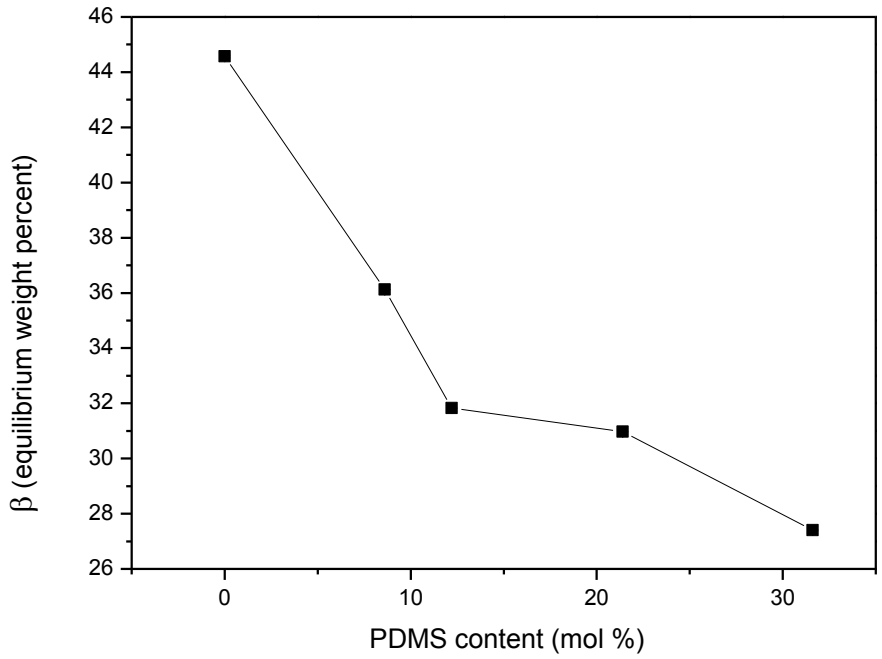

FIGURE 4-27: Equilibrium moisture values (β in equation 4.1) as a function of the PDMS content

Stellenbosch University http://scholar.sun.ac.za

Subsequent to the moisture absorption studies, SEM analyses were performed for representative samples to determine the influence of the moisture absorption on the fibre mat morphology. Images are shown in Figure 4-28. Increased fibre diameters were observed for PMAA homopolymer as well as the 8.6 mol % PDMS sample when compared to the fibres before exposure to moisture. Samples with 21.4 and 30.6 mol % PDMS were not affected to the same degree. It should be noted that the PMAA homopolymer appears to have dissolved, and there is significant film formation and merging of the fibres. It is clear that during absorption of the water, the fibres swelled to a significant degree resulting in the observed structure after exposure. Accurate quantification using SEM is not possible due to the fact that the high vacuum in the instrument leads to water loss. It does however allow us to compare how the fibre mats were changed by moisture. As the PDMS content increased, the fibre structures changed less. This can in part be explained by the fact that PDMS segregates to the surface. PDMS is a low surface tension polymer and will usually segregate to the surface[33;37]. In addition, PDMS is a very hydrophobic polymer, so moisture in the atmosphere would have less interaction with the fibre mat if PDMS was present on the surface. It would also be expected that the diffusion of the moisture into the fibres would have then been slowed due to the presence of the PDMS.

The other contribution to the stability of the fibres is that the PDMS segments can act as “physical” crosslinks that prevent the loss of fibre integrity during moisture exposure due to their hydrophobic nature[35]. This would explain the moisture absorption of the fibres without the loss of fibre integrity. In effect any PDMS domains in the fibres act as crosslinking points. The presence of hydrophobic interactions can prevent the expansion of polymer chains[24]. Interaction between PMAA and PDMS is possible through hydrophobic interactions as well as hydrogen bonding[38]. Hydrogen bonding between acid and siloxane groups can occur. Van der Waals forces also play a role when methyl groups are present on the polymer[39]. All these interactions contribute to the resistance of the fibres to expand/swell, but doesn’t prevent it completely. If the expansion forces increase, the interactions will be lost with time[25].

Stellenbosch University http://scholar.sun.ac.za

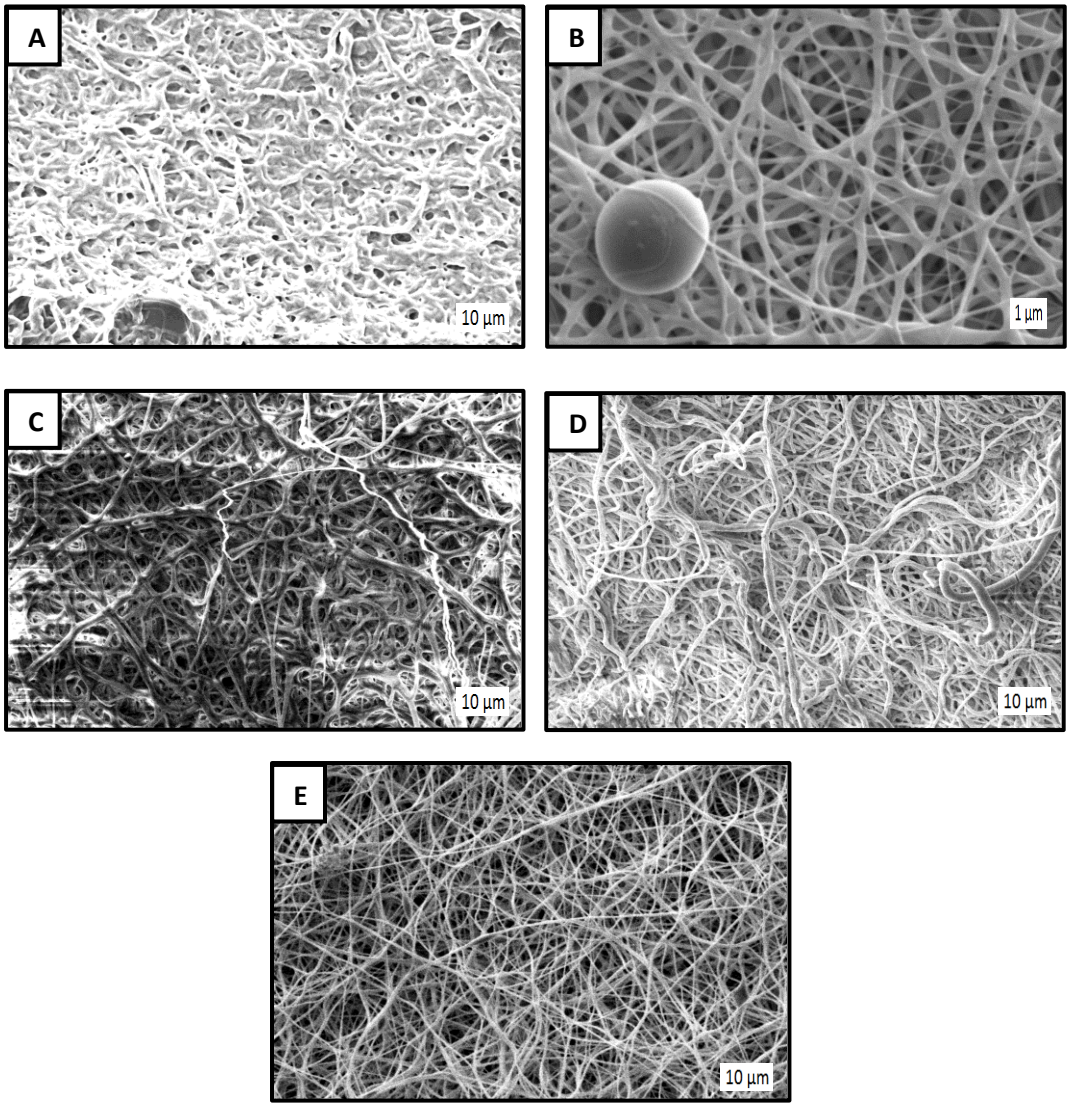

FIGURE 4-28: SEM images after equilibrium moisture content was reached for samples (A) PMAA homopolymer (B) 8.6 mol % PDMS (C) 12.2 mol % PDMS (D) 21.4 mol % PDMS (E) 30.6 mol % PDMS

4.3.3. Water stability

In the previous section, the creation of fibre mats which are stable in high moisture environments were realised by the inclusion of PDMS. This motivated us to investigate whether the fibres could also be made water stable and water swellable, with the aim of creating nanofibres hydrogels. Nanofibres hydrogels are being developed and applied in applications

Stellenbosch University http://scholar.sun.ac.za

such tissue engineering, drug delivery, optical lenses, cell and enzyme immobilization, sensors, and filters[40]. The increased surface to volume ratio leads to greater interaction with surrounding tissue and quick responses. Some examples of hydrogels formed from electrospun fibres include polyacrylic acid[41], poly(N-isopropylacrylamide-co-acrylic acid), poly(vinyl alcohol) (PVA)[42], PVA/PAAc[43], multiblock poly(ester urethanes)[44], and poly(2-hydroxyethyl methacrylate)[45]. Even more interesting is the stimuli-sensitive type hydrogels such as those produced by Nakagawa *et al.*[46] In their study they used a poly(AAc-co-nBMA) copolymer to create a nanofibre gel actuator, which showed pendulum like motion under the influence of an oscillating pH environment. In this example, the poly acrylic acid acted as hydrophilic and pH sensitive component, whereas the butyl methacrylate was added to create a physically crosslinked hydrogel, which unlike homo poly(acrylic acid), did not dissolve in water. The polymers in the present study resembles this last mentioned system, with the PMAA acting as the hydrophilic (and potentially stimuli responsive) component, and the PDMS acting as the crosslinker to prevent dissolution of PMAA.

4.3.3.1. Influence of PDMS on water swelling behaviour

Fibre mats were investigated with SEM to determine if the fibre integrities remained intact after immersing the fibres in water. As expected, the PMAA homopolymer nanofibres dissolved as soon as it was immersed in water. This behaviour is as a result of a lack of crosslinking between the chains that resulted in the polymer chains dissolving in the water.

The introduction of PDMS into the polymer fibres leads to a different behaviour of the fibre mats. The SEM images of the fibre mats obtained after the removal of the fibres for the water are shown in Figure 4-26. The top row of images are the images obtained after 5 min of water immersion and the bottom row are the images obtained after 3 hour of water immersion. The polymers containing 8.6 mol % PDMS and 11.4 mol % did not dissolve when placed in water, but instead, swelling was observed. This can be seen in the SEM images where it is clear that the fibres have “collapsed” after the removal of the water. This results in film formation after removal from the water although it is clear that some fibre structure has been maintained. This indicated that the PDMS content in the fibres was too low to provide enough physical crosslinks

Stellenbosch University http://scholar.sun.ac.za

for fibre preservation, although it was strong enough to prevent the polymers to completely dissolve. It is expected that in the water solution the fibres remained intact as very heavily swollen hydrogels.

The inclusion of more PDMS in the polymer resulted in the fibre mats showing nanofibre hydrogel behaviour. Figure 4-29 shows that the samples that formed interconnected webs after 5 min (A–C) and 3 hours (D-F) in water. From the images the interconnected web-like structures are clearly visible. What was interesting is that the morphology of the fibres mats did not change significantly between 5 min and 3 hours in water. This indicated that fast absorption occurred initially, and the equilibrium hydrogel forms very rapidly.

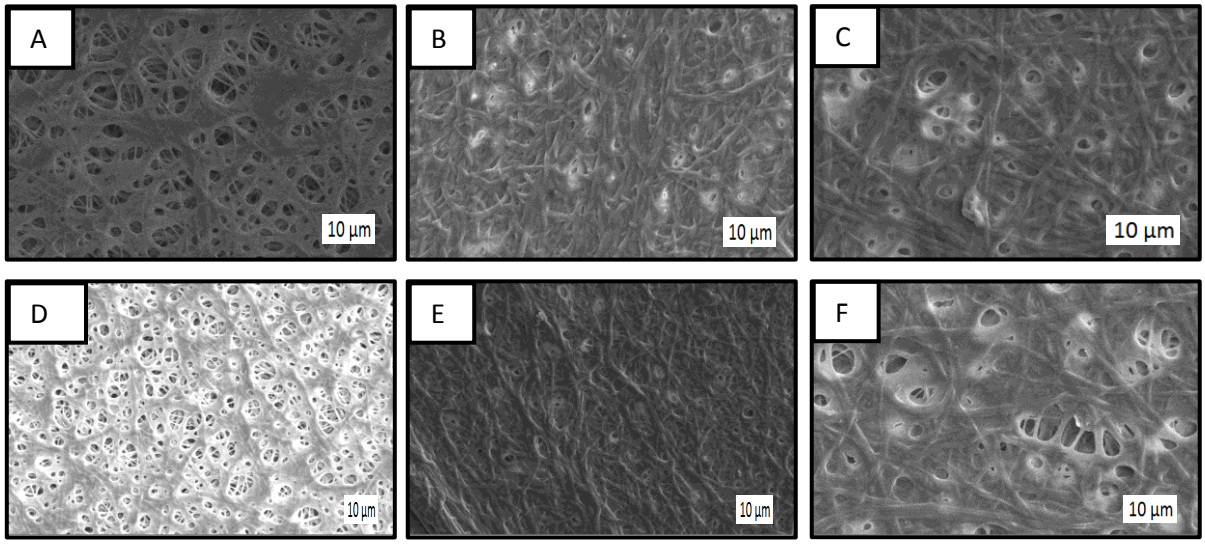

FIGURE 4-29: SEM images for samples (A+D) 21.4 mol % PDMS (B+E) 30.6 mol % PDMS (C+F) 31.5 mol % PDMS. The top row was taken after 5min of water exposure and compared to the bottom row which was after 3 hours. Other samples formed films when immersed for 3 hours so no images are included

4.3.4. Chemical crosslinking

In the previous section it was shown that the PDMS domain in the nanofibres can act as physical crosslinks resulting in hydrogel nanofibres. Physical crosslinking are, however, not always the strongest method of crosslinking relative to chemical crosslinking. Chemical

Stellenbosch University http://scholar.sun.ac.za

crosslinking, which involves the formation of bonds via chemical reactions between polymer chains, are known to produce stronger and stiffer bonds. Chemical crosslinking of nanofibre mats can be performed in a number of ways. In one method, known as reactive electrospinning, the crosslinking occurs as the polymer solution is electrospun. The electrospinning solution consists of polymer, crosslinker and photo-imitator. With the application of UV irradiation, crosslinking starts while the jet is in-flight. The drawback of this method is the viscosity problems that arise when the fibres are crosslinked[47].

Another method that has been reported to induce crosslinks in electrospun nanofibres is the post-electrospinning crosslinking which can be performed in one of two ways. The fibre mat, after spinning, can be placed in a solution containing crosslinker. This type of solution-based crosslinking works well for microfibres, but fails when fibres are in the range of 100 nm. The dissolution of the smaller fibres occurs so quickly that the crosslinks needed to form the gel simply does not form in time[41].

The other option is that the crosslinker is electrospun with the polymer solution, but crosslinking is only performed later. Crosslinking can be initiated by UV or heating[41]. One such example is the crosslinking of fibres electrospun from PVA/PAA blend solution, which after spinning were placed in an oven at 145 °C for a few minutes to induce an esterification reaction between the acid and hydroxyl groups[43]. In the current study we investigated the use of a similar method to crosslink the PAA fibres by including a crosslink agent, cyclodextrin, in the spin solution. This crosslinker consists of a number of hydroxyl groups which can form ester bonds with the acid on the polymer chains. The acid groups on the PMAA molecules were reacted with hydroxyl groups of the crosslinker in a post electrospinning process by heating the samples.

4.3.4.1. The influence of crosslinker on the electrospinning

The addition of molecules to the electrospinning solution can affect the viscosity and dielectric properties of the solution[48]. Small molecules have been shown to act as plasticizers to enhance the movement of polymer chains in solution[20]. In addition, the low molar mass molecules may

Stellenbosch University http://scholar.sun.ac.za

affect the conductivity of the solution. In some cases, salts are added to enhance the conductivity in order to make otherwise unspinnable polymers spinnable. In this study, changes in how the spinning solution behaved with the addition of the cyclodextrin were observed. Table 4-3 shows a summary of the effect on the fibre morphology that is observed as a result of the presence of the cyclodextrin. Also included in the table is a summary of the effect of the crosslinking of the fibres and the analysis of the fibre diameters after the fibres were immersed in water.

Fibres were successfully obtained for PMAA homopolymers, however, it should be noted that some "spitting" was observed during the process. This was already discussed under section 4.2. As was mentioned, conditions were chosen to minimize spitting, but it could not be completely eliminated. The flow and electrospinning behaviours were however changed by the addition of cyclodextrin molecules, resulting in better flow properties. The overall spinning was better with very little spitting that was observed.

The influence of crosslinking on fibre diameters for the fibres with different PDMS contents were investigated and the results shown in Table 4-3. Generally the fibre diameters increased with the addition of crosslinker. Further increases were observed after the fibres were crosslinked. This is possibly due to contraction and consequent thickening of the fibres. Shrinking of the fibre mats were observed after removal from the oven. Similar results were found for PAA fibre mats[34;49].

Table 4-3**:** Summary of the electrospun fibre diameters with and without crosslinker, as well as after crosslinking and moisture exposure

PDMS content (mol %)	**0**		**8.6**		**12.2**		**21.4**		**30.6**		**31.5**	
	Fibre diameter (µm)	Std dev	Fibre diameter (µm)	Std dev	Fibre diameter (µm)	Std dev	Fibre diameter (µm)	Std dev	Fibre diameter (µm)	Std dev	Fibre diameter (µm)	Std dev
No crosslinker[a]	0.12	0.05	0.14	0.10	0.27	0.10	0.25	0.12	0.48	0.13	0.48	0.12
With crosslinker[b]	0.16	0.04	0.32	0.10	0.41	0.18	0.35	0.11	0.46	0.14	0.46	0.24
After crosslinked 60 min	0.14	0.03	0.43	0.09	0.45	0.09	0.53	0.57	0.45	0.14	0.43	0.23
After moisture and drying	1.07	0.17	0.54	0.11	0.45	0.06	0.54	0.25	0.54	0.12	0.53	0.22

[a] Electrospinning conditions: 22°C, 50 % RH, no airflow [b] Electrospinning conditions: 22°C, 50 % RH, with fumehood airflow on

Stellenbosch University http://scholar.sun.ac.za

Fibre diameters were also determined for the samples after moisture absorption and drying. Fibre mats were kept in a desiccator overnight before SEM analysis. We observed that the samples containing up to 21.4 mol % PDMS showed increased fibre diameters after being exposed to moisture. PMAA homopolymer showed the biggest increase. The polymers with higher PDMS contents slightly decreased or remained the same. This must be related to the moisture absorption and release properties.

Figure 4-30 shows the influence of cyclodextrin concentration on the fibre diameters for PMAA homopolymer and a selected high PDMS containing copolymer. With the increase of cyclodextrin from 4 to 10% the average fibre diameters for the copolymer decreased slightly. It is possible that the addition of cyclodextrin up to 10 wt % increased the conductivity to an extent where it resulted in smaller fibre diameters. PMAA homopolymer however showed increased diameters as the cyclodextrin was increased. An increase was also observed for the copolymer sample when 20% cyclodextrin was added to the solution. This is in contrast to what would be expected if conductivity was considered. Usually, the addition of polar molecules increases the charges which will results in smaller fibre diameters. The increase must be related to entanglement properties of the polymers which changes with the addition of cyclodextrin. Enhanced movement can result in better entanglement, which in turn will result in larger fibre diameters[50].

In the case of the copolymer, a slight reduction of the average fibre diameters was observed with the addition of cyclodextrin. Conductivity was probably the controlling factor in this case. As noted earlier, the introduction of hydrophobic molecules can result in reduced conductivity. It is possible that the addition of cyclodextrin up to 10 wt % increased the conductivity of the PDMS containing polymers to an extent where it resulted in smaller fibre diameters. We observe that at a concentration of 10 wt % the PMAA homopolymer and copolymer had almost the same fibre diameter. With a further increase in the cyclodextrin content, both polymers showed a significant increase in average fibre diameters.

Stellenbosch University http://scholar.sun.ac.za

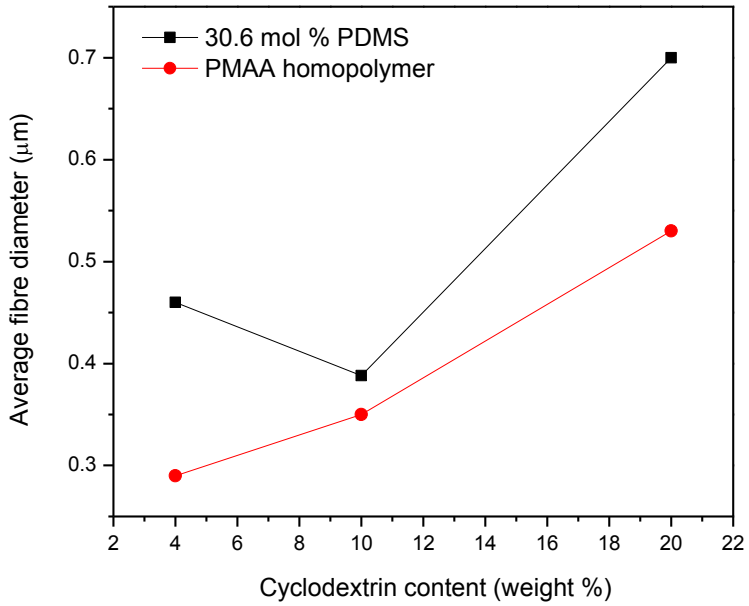

FIGURE 4-30: Influence of cyclodextrin concentration on the fibre diameters for PMAA homopolymer and a high PDMS content copolymer

4.3.4.2. Influence of chemical crosslinking on water swelling behaviour

The control of fibre behaviour when exposed to water is very important. The swelling and mechanical properties of the fibres are strongly influenced by the crosslink density. Hydrogels are usually characterized by low stress strain hysteresis, low strain to break, and low toughness[51]. In the past, crosslinking and the control of crosslink density were challenges that were faced with polyelectrolytes[41]. Simple methods have been developed to obtain crosslinked fibres, although not all those, such as the use of ester linkages as crosslinks, allow for a wide range of crosslink densities. It is however possible to control it to some extent by varying crosslinker concentration and crosslink times.

Stellenbosch University http://scholar.sun.ac.za

4.3.4.3. Effect of crosslinking time on water solubility

Time can be used to control the degree of crosslinking. Longer crosslinking times are usually associated with a lower degree of swelling due to the higher crosslink density. Figure 4-31 shows the SEM image of the sample containing 21.4 mol % PDMS after 3 hour immersion in water for the same amount of the cyclodextrin crosslinker, but crosslinked for different times. It was clear that mats crosslinked for shorter times show a more collapsed structure after the deswelling, indicating that they were more highly swollen in the gel state. As expected, an inverse relationship existed between crosslinking time and swelling when cyclodextrin was used as crosslinking agent.

A difference between PMAA homopolymer and copolymer behaviour was observed when crosslinking time was investigated. PMAA homopolymer required a crosslinking time of 120 minutes in order to maintain the fibres structure after immersion in water for 3 hours. The copolymer nanofibres, showed the same behaviour after only 60 minutes. It is not necessarily that the PMAA homopolymers dissolve with crosslinking less than 120 minutes, most likely the swelling is of such extent that the fibres disappear from the foil. Fibres were kept on foil when placed in water. This made the handling easier. If the fibres were to form a completely swollen gel it could swell to the extent that it is removed from the foil and floats in the water.

Stellenbosch University http://scholar.sun.ac.za

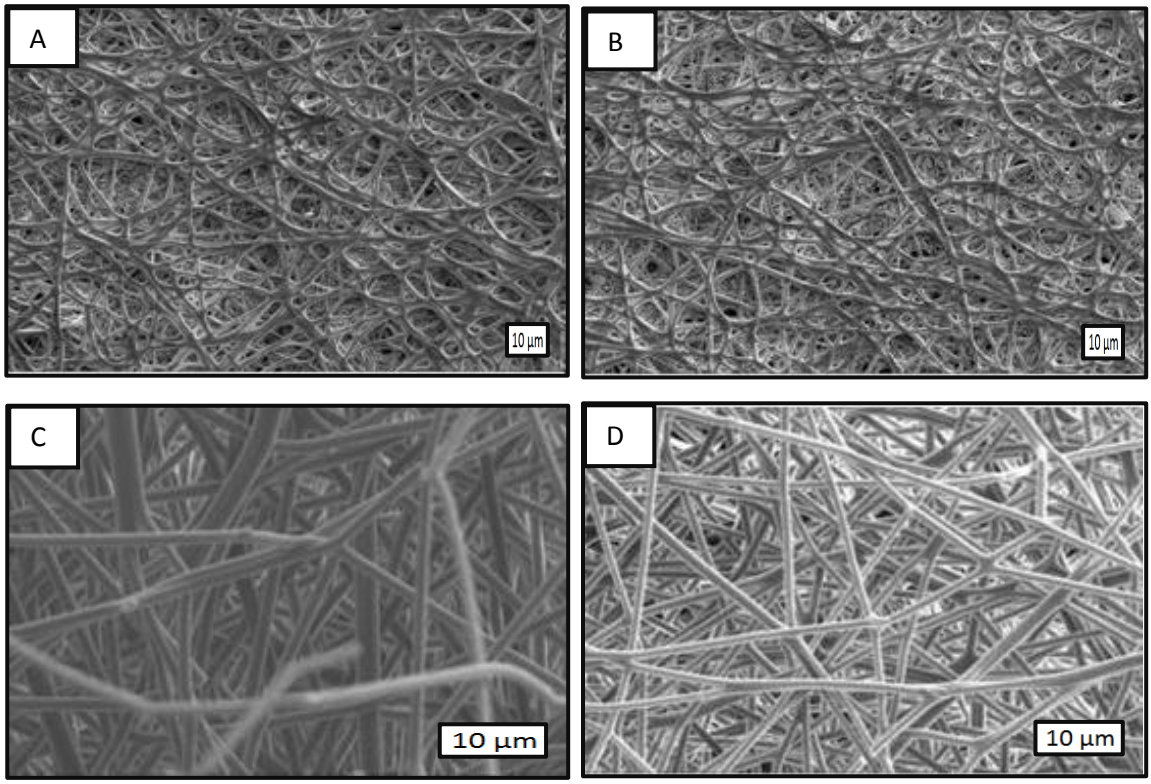

FIGURE 4-31: Images showing the swell differences with crosslinking time for a representative sample (containing 21.4 mol % PDMS with 10 % cyclodextrin) (A) 20 minutes (B) 30 minutes (C)60 minutes (D) 120 minutes

4.3.4.4. Effect of crosslinking concentration on water solubility of PMAA

Figure 4-32 shows the effect of the crosslinking concentration for PMAA homopolymers where image A represents a concentration of 5 weight % and B represents 10 wt % cyclodextrin content. These samples were crosslinked at 145° for 60 minutes. Although no quantitative results were obtained, it is clear that the fibre mat properties were different due to different swelling behaviour. The fibre mat with less cyclodextrin is more swollen and in the deswollen state there are a large number of merged, interconnected fibres. The higher concentration sample showed that the fibres intact after deswelling. This was as expected. It is a common phenomenon to observe less swelling with higher crosslink density. In fact, superabsorbent materials are usually only lightly crosslinked to induce higher swelling[52].

Stellenbosch University http://scholar.sun.ac.za

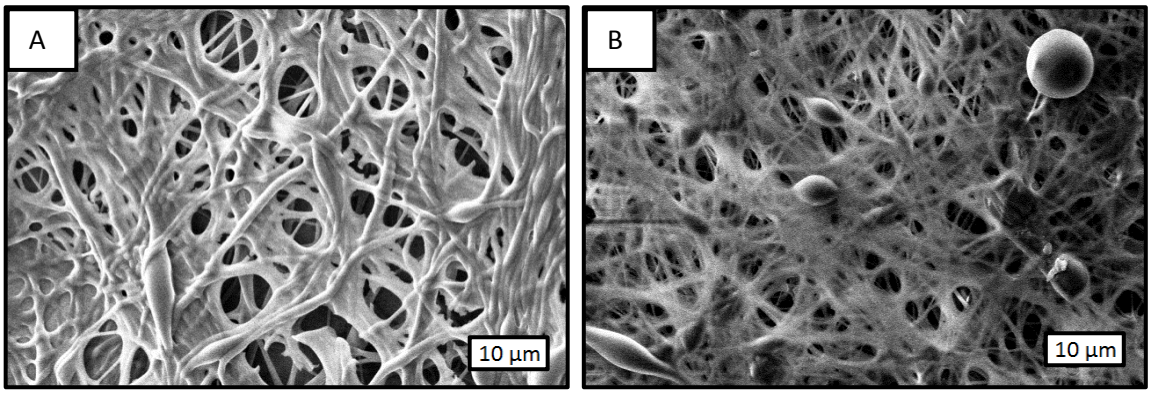

Figure 4-32: Influence of crosslinker concentration on fibre swelling. PMAA homopolymer containing (A) 0.8 wt % (B) 2 wt % (C) 4 wt % (D) 5 wt % nanocellulose crosslinked for 60min and submerges for 5min

4.3.4.5. Physical vs chemical crosslinking

The same moisture and water absorption studies were performed for the chemically crosslinked samples as was done for the uncrosslinked samples. The results for the moisture studies are shown in Figure 4-33 and the fitting parameters given in Table 4-4. Samples in general reached equilibrium quicker than the samples with no cyclodextrin. With cyclodextrin the longest time to reach the equilibrium was 40-45 minutes. Without cyclodextrin, up to 70 minutes were needed to reach equilibrium (see Figure 4-25). No clear trend could, however, be identified with regards to the PDMS content. Even with the presence of crosslinks, we would still expect polymers with PDMS to absorb less than PMAA homopolymers. In this case, however, homo PMAA had a value of around 25% whereas that of a 21.4 mol % PDMS sample had a value of 34%.

Stellenbosch University http://scholar.sun.ac.za

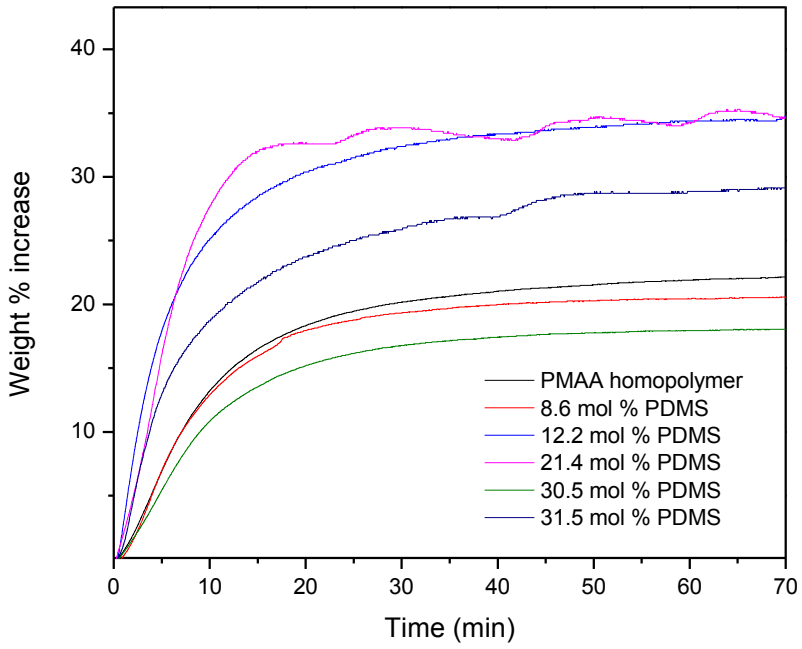

FIGURE 4-33: Weight percent increase with time in a high humidity atmosphere for polymers containing 4% cyclodextrin and crosslinked for 60 min

TABLE 4-4: Parameters for polymer moisture absorption curves as fitted to equation 4.1 for polymers crosslinked with cyclodextrin

PDMS mol%	τ_1 (min)	±	τ_2 (min)	±	β (weight %)	±	R^2
0	92.26	7.93	8.18	0.03	24.82	0.27	0.99963
8.6	7.87	0.03	48.53	4.22	21.11	0.07	0.99962
12.2	23	0.29	4.3	0.02	34.5	0.02	0.99837
21.4	5.35	17.10	5.36	17.09	34.10	0.01	0.98900
30.5	8.94	0.04	119.09	37.16	19.64	0.55	0.99939
31.6	3.33	0.03	20.50	0.12	29.76	0.02	0.99861

It is difficult to find an exact explanation for the results that were obtained. One possibility could be moisture absorption during handling of the materials. The surrounding atmosphere during these studies was high (above 70%) due to weather conditions. During the studies performed on the uncrosslinked polymers, the conditions were dry. It is therefore possible that the materials could've absorbed moisture during spinning, as well as afterwards when samples

Stellenbosch University http://scholar.sun.ac.za

were removed for various analyses purposes. Also, the duration that samples were exposed to the atmosphere (removed from the desiccators) was not necessarily the same for all. In an attempt to identify whether absorption of water during handling could explain the findings, TGA experiments were performed to determine the water loss from the samples prior to the moisture absorption studies. The idea was to identify a possible link between initial water content and the absorption that is observed. The TGA analysis of the sample prior to the measurements is shown in Figure 4-34. For clarity, the water absorption and initial water loss was also compared in Table 4-5.

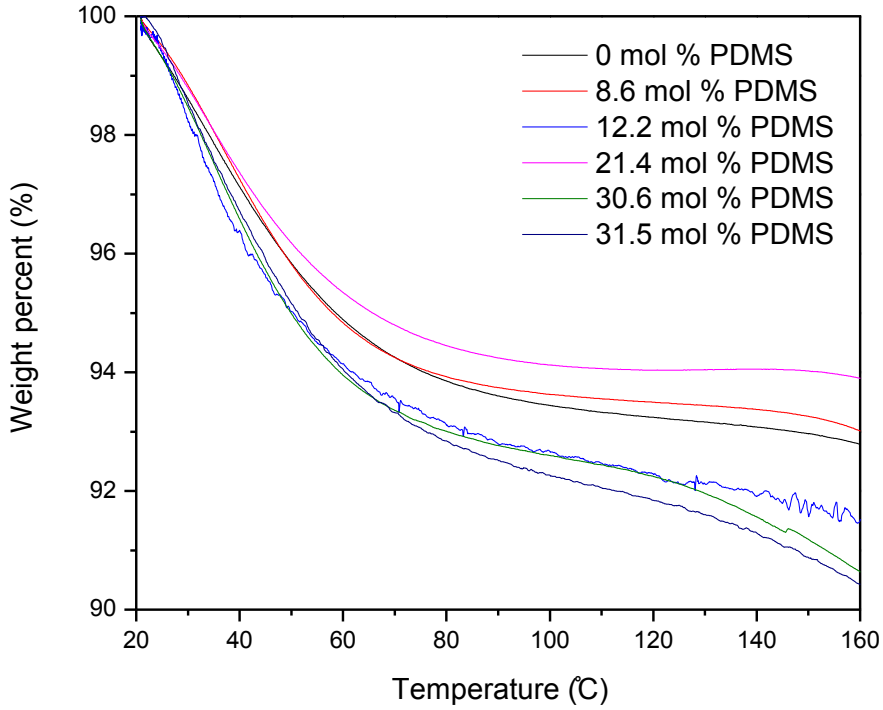

FIGURE 4-34: TGA curves show the water loss between 20 and 160°C for samples containing cyclodextrin before moisture absorption measurements

As seen in Table 4-5, a clear correlation between initial moisture content and absorption was not obtained. However, we do observe that the sample with 21.4 mol % PDMS showed the highest moisture absorption and the lowest initial water content. With the results available it is not possible to conclude what the effect of cyclodextrin on the moisture absorption properties were. This is in contrast to the case where no crosslinker was present and a clear trend with

Stellenbosch University http://scholar.sun.ac.za

PDMS content could be seen. It appears as though the sample's sensitivity to moisture affected the quality and repeatability of the results. The absorption process is influenced by a number of factors which could all contribute (and complicate) the results obtained. Absorption will be influenced by factors such as humidity of the surrounding atmosphere and the chamber, sample surface area, fibre sizes, fibre mat porosity, actual amount of sample, and the hydrophobicity. The humidity in the chamber, actual amount of sample and surface area of the fibre mat was held more or less constant. However, different fibre sizes and mat porosity will result in different surface area of the fibres that are able to absorb moisture. Nanofibres pose a particular difficulty on the process due to the "fluffy" nature of the samples. The samples are sensitive to handling and the shape changes easily, which could result in dimension changes after being measured and weighed. It was also not always possible to control the humidity in the surrounding atmosphere. All of these factors can have some influence on the actual absorption. It is not just simply a function of the hydrophobicity.

TABLE 4-5: Table relating the initial moisture content to the moisture absorption

Sample	Water loss before moisture absorption (%)	Water absorption (weight % increase)
0 mol % PDMS	6.9	22
8.6 mol % PDMS	6.7	20.4
12.2 mol % PDMS	7.7	34
21.4 mol % PDMS	6	34
30.6 mol % PDMS	7.7	18
31.5 mol % PDMS	8.1	28.9

Despite the difficulty in getting good result for the moisture absorption studies, the stability of the fibres are submersion in water was investigated. The samples containing crosslinker was submerged in water and the morphology of the fibre mats investigated after 5 min and 3 hours. The images are shown in Figure 4-35.

Stellenbosch University http://scholar.sun.ac.za

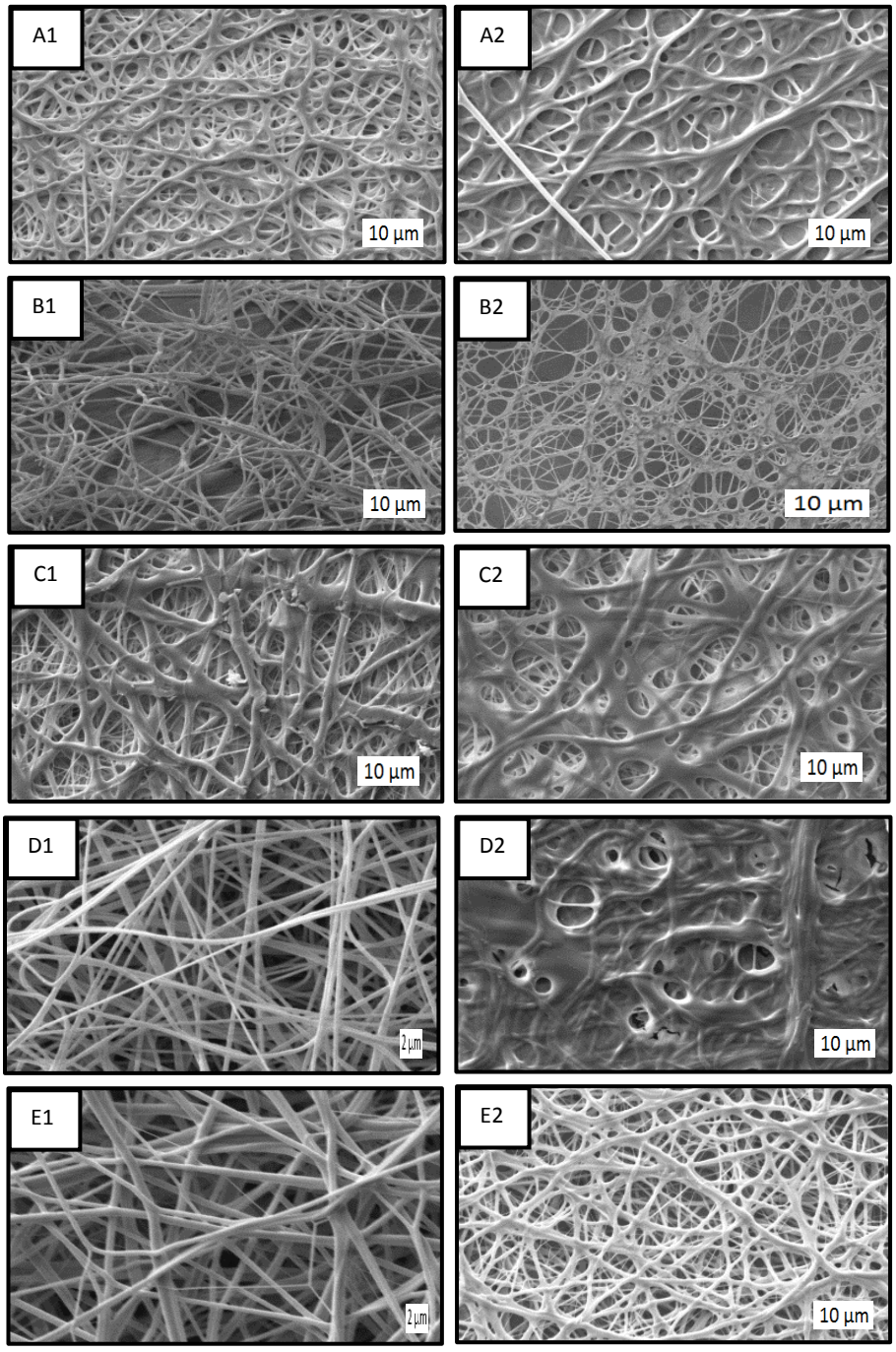

FIGURE 4-35: SEM images showing the morphology of fibres after 5 min (left) and 3 hours (right) for samples containing 4 % cyclodextrin and crosslinking time of 60 min (A) 8.6 mol % PDMS (B) 12.2 mol % PDMS (C) 21.4 mol % PDMS (D) 30.5 mol % PDMS (E) 31.6 mol % PDMS

Stellenbosch University http://scholar.sun.ac.za

All the samples retained fibres structures, or at least formed swollen interconnected webs. This is in contrast to the uncrosslinked samples where stability after 3 hours was only observed for samples containing more than 20 mol % PDMS. It was mentioned already that physical crosslinks are not always the strongest mode of bonding. The addition crosslinking will reduce the swelling and change in fibre morphologies. Here we observe that crosslinking induced water stability even as low as 4%. In fact, the polymers with above 30 mol % did not show much change in the fibre morphology after 5 minutes. In the uncrosslinked state these fibres were highly interconnected and merged due to excessively swelling after only 5 minutes (compare with Figure 4-29) The results for samples without crosslinking did not indicate big difference for samples between 5 minutes and 3 hours. In contrast here, all of the samples showed some changes of the fibre morphology with longer water exposure time.

It is clear that the moisture absorption properties and water swelling behaviour is highly affected by the number and type of crosslinks present. The advantage of this is that it will allow for a wide range of possible ways to vary the properties of the fibre mats to suit specific end-uses. A lot of focus these days tends to focus on the inclusion of nanomaterials due to the numerous advantages that they offer. In light of this a nanomaterial resembling cyclodextrin was studied as an attempt to identify if it is plausible and worthwhile to look into in future studies. This was only a general study; more detailed investigations were not within the scope of this project.

4.3.5. Investigating the possibility of crosslinking with nanomaterials

Nanomaterials are gaining tremendous attention due to the enhanced properties which can be obtained by the high surface to volume ratio. The inclusion of nanomaterials into nano fibres for various application and properties is one research area which is receiving more attention. One such example is the inclusion of nanocellulose in fibres and other materials. Nanocrystalline cellulose is the chemically inert and physiologically stable, rod-like shaped crystals obtained when the amorphous parts of cellulose is removed by acid hydrolysis[53]. Even more desirable is the fact that it is a renewable form of nanomaterials, being obtained from the most abundant

Stellenbosch University http://scholar.sun.ac.za

polymer on earth, cellulose. Other advantages include high specific strength and modulus, high surface area, and unique optical properties[54].

Nanocellulose molecules contain a number of hydroxyl groups. Hydroxyl groups provide various routes to modification, eg. via esterification, etherification, oxidation, silylation, and polymer grafting[53]. In this study we were interested to see whether we could use these nanomaterials to crosslink nanofibres using the same esterification chemistry as was used for cyclodextrin.

4.3.5.1. Nanocrystalline cellulose (NCC) in the spinning solution

The major challenge with nanomaterials is dispersion. Nanomaterials tend to agglomerate, reducing their efficacy in most applications, since it is their high surface to volume ratio which is required for the enhanced properties. Nanocellulose, with the large number of hydroxyl groups are polar, and are usually better dispersed in more polar solvents such as water and DMF. Incorporation into hydrophobic materials usually requires some degree of modification. Incorporation of nanocellulose in this study was achieved by first dispersing the nanocellulose in DMF, then adding the polymer solution, stirring overnight and sonicating the solution for 3 hours.

4.3.5.2. Effect of NCC on electrospinning

The addition of NCC did not result in the same spinning behaviour as cyclodextrin. The electrospinning conditions had to be adjusted somewhat since the addition of NCC resulted in increased spitting, much worse than without any crosslinker. In fact, spitting was so severe that the fibre mats were “dissolved” by the spitting. This is possibly related to agglomeration of the nanocellulose. The areas of agglomeration could have acted as unentangled areas, which could be the cause of more spitting and instability of the jet. So, although fibre formation was observed, no fibre mats were actually obtained. In order to obtain fibres the spinning conditions had to be adjusted. Instead of spinning with a (+) 5 kV to (-)13 kV (collector) the spinning was

Stellenbosch University http://scholar.sun.ac.za

(+) 10 kV to (-) 5 kV. The influence of NCC on fibre diameter was investigated at these conditions. The results are shown in Figure 4-36.

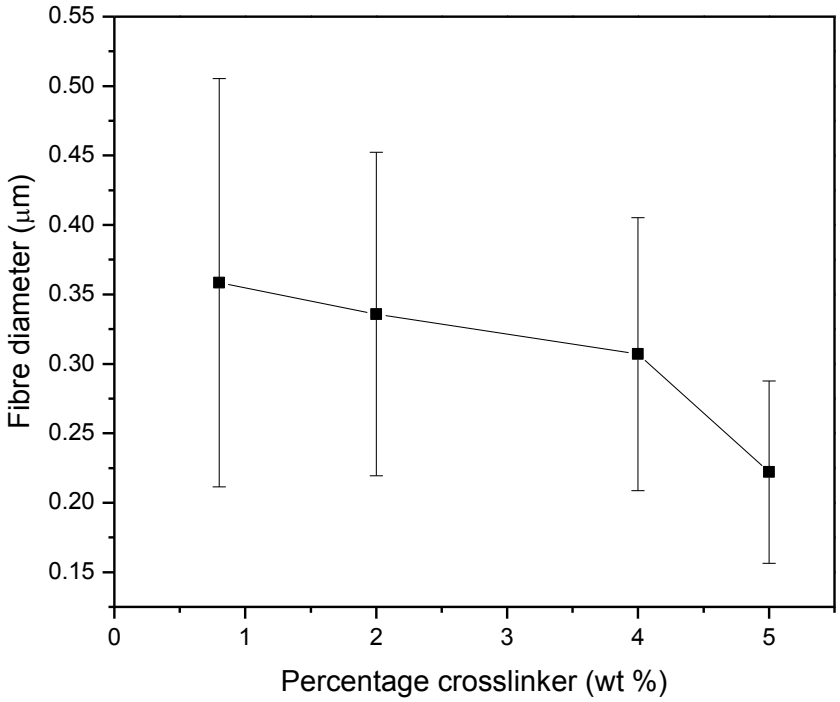

FIGURE 4-36: Influence of nanocellulose on the fibre diameters

Fibre diameters decreased with increased NCC content. The reduction of fibre diameter with the addition of nanocellulose has been shown for a few polymers[55]. The smaller fibre diameters most probably as a result of increased conductivity due to the high number of hydroxyl groups present in nanocellulose. The distribution in fibre diameters got smaller as the nanocellulose content increased.

Stellenbosch University http://scholar.sun.ac.za

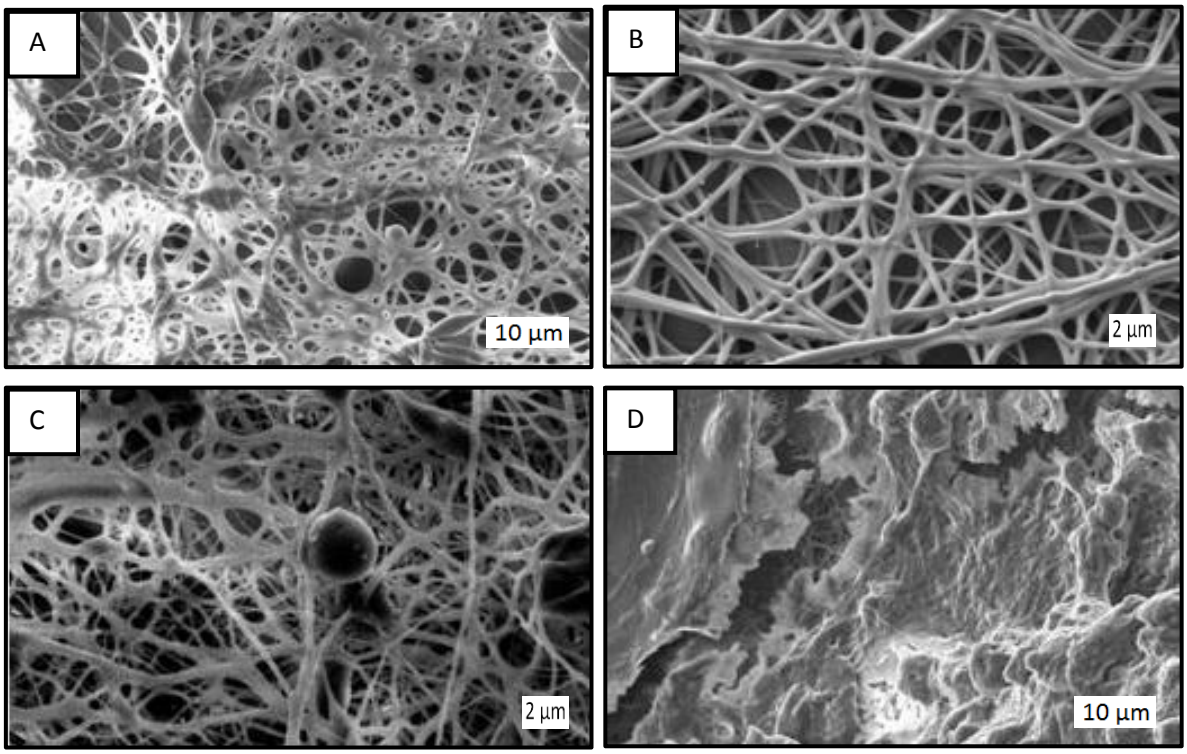

Figure 4-37: Influence of concentration on fibre swelling for PMAA homopolymer containing (A) 0.8 wt% (B) 2 wt % (C) 4 wt % (D) 5 wt % nanocellulose crosslinked for 60min and submerges for 5 minutes

In Figure 4-37 images are shown for samples containing various amounts of nanocellulose after being crosslinked for 60 minutes, submerged in water for 5 minutes, and kept in a desiccator overnight before imaging. Some differences were observed between the fibre morphologies of the samples. Both the 0.8 and 2 wt % containing samples showed merging of the fibres. Connections formed where fibres crossed each other. The fibres for the 2 wt % samples showed an almost flattened structure. The samples with 4 wt % also showed some interconnections at fibre crossings, but not as severe as the other samples.

The biggest differences were observed for the sample containing 5 wt % nanocellulose. The fibre mat after drying was brittle. As observed in the image it was as though a brittle film layer formed at the top of the fibres. Two possible reasons can be mentioned here. Firstly, agglomeration was observed when the sample was prepared. It was clear that we could not get efficient dispersion. Poor dispersion, and thus poor crosslinking throughout the fibres, could be

Stellenbosch University http://scholar.sun.ac.za

the reason for the lack of fibre integrity and brittleness observed. Another factor for observing such a different result could be the average fibre diameter of the sample. The average fibre diameter was smaller than that of all the other samples. This would lead to a much greater surface area, which in turn will result in faster and more absorption. Since fibres were obtained and did not dissolve in water, it was clear that even though agglomeration was observed, we could still form fibres with crosslinks. It is most likely a result of both factors– faster absorption due to smaller fibres and some possible contribution by poor dispersion of crosslinks.

4.3.5.3. Electrospinning of copolymers with nanocellulose

Nanocellulose was also electrospun with copolymers. The absorption of PDMS containing polymers with 4 wt % nanocellulose, the maximum which could be added to PMAA homopolymers, was investigated. The hydrophobic character of PDMS should be expected to affect the dispersion. Highly polar environments favour dispersion of this type of nanocullose[54]. No dispersion studies were performed to investigate how the presence of PDMS influenced the dispersion; however, it was clear that it was indeed possible to electrospun the nano crosslinker with the copolymers. The fibre diameters were in general higher in this case, but as mentioned the spinning conditions were different, so it cannot be compared to the uncrosslinked samples.

TABLE 4-6: Fibre diameters for some copolymers containing 4 wt % NCC

PDMS content (mol %)	Fibre diameter (µm)
8.6	0.37
12.2	0.63
21.4	0.58

Stellenbosch University http://scholar.sun.ac.za

The absorption results are shown in Figure 4-38. The same curve fitting procedure was followed as for the polymers without any NCC. Figure 4-39 shows the fitting data determined by fitting the absorption data to Equation 4.1 for the NCC crosslinked nanofibres and the no NCC containing fibres.

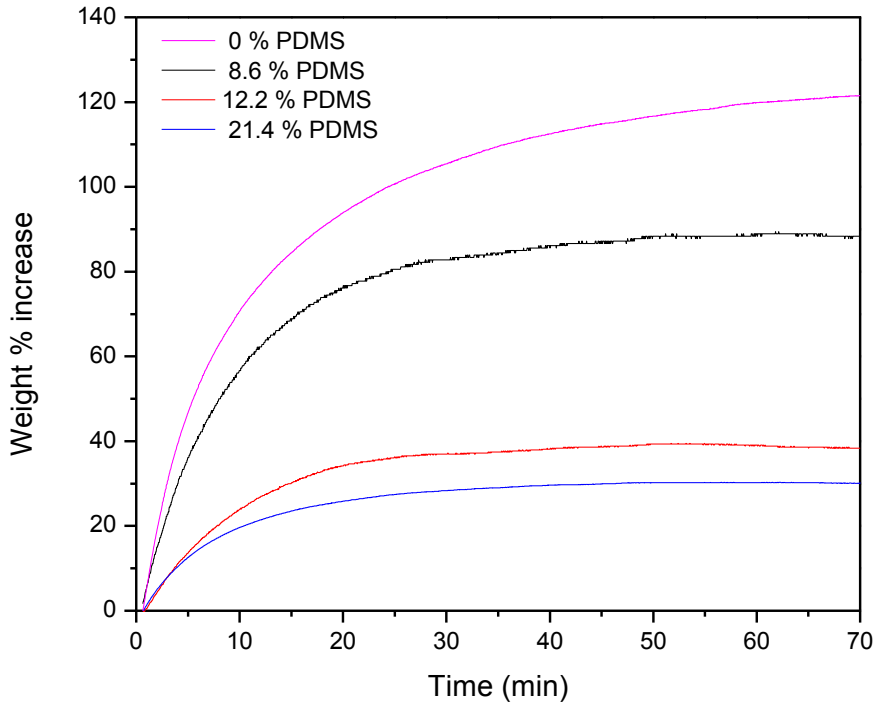

FIGURE 4-38: Moisture absorption graphs for polymers containing 4 wt % NCC

The time constant values are generally lower for the NCC containing fibres, indicating a faster rate of absorption. Interestingly, in this series the τ_2 parameter shows the greatest dependence on the PDMS content. This is dramatically different from the results observed without NCC. This suggests that NCC has a major influence on the absorption properties of the fibres. The generally larger fibre diameters could possibly play an important role here as well.

Stellenbosch University http://scholar.sun.ac.za

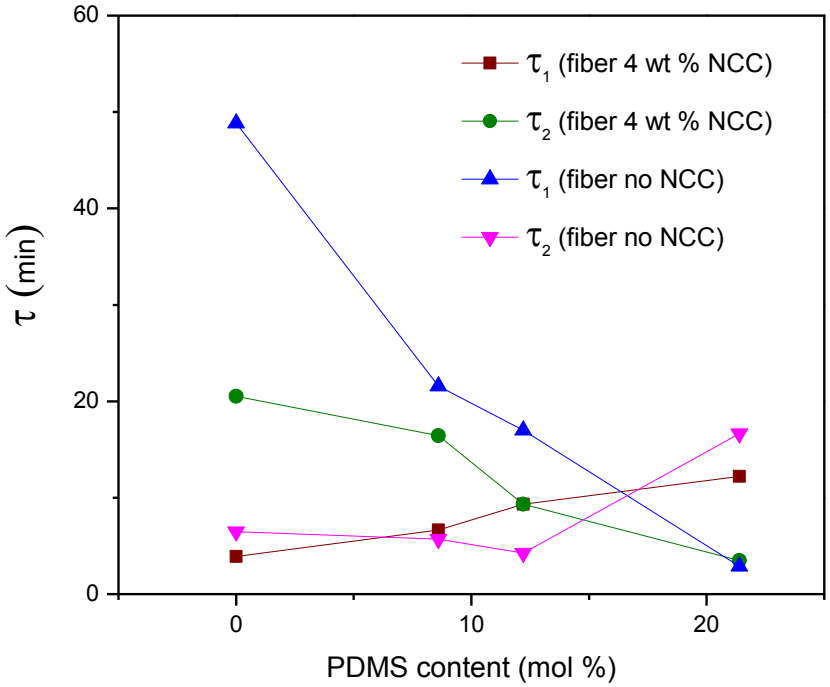

FIGURE 4-39: Comparison of τ_1 and τ_2 values as a function of PDMS content for fibres with and without NCC

When the maximum moisture content is compared in Figure 4-40, the NCC containing fibres showed higher values in most cases. The difference between the maximum absorption of fibres with and without NCC got smaller as the PDMS content increased. A general downward trend of maximum moisture content was observed as the PDMS content increased. This agrees with the results obtained for the fibres without NCC.

Stellenbosch University http://scholar.sun.ac.za

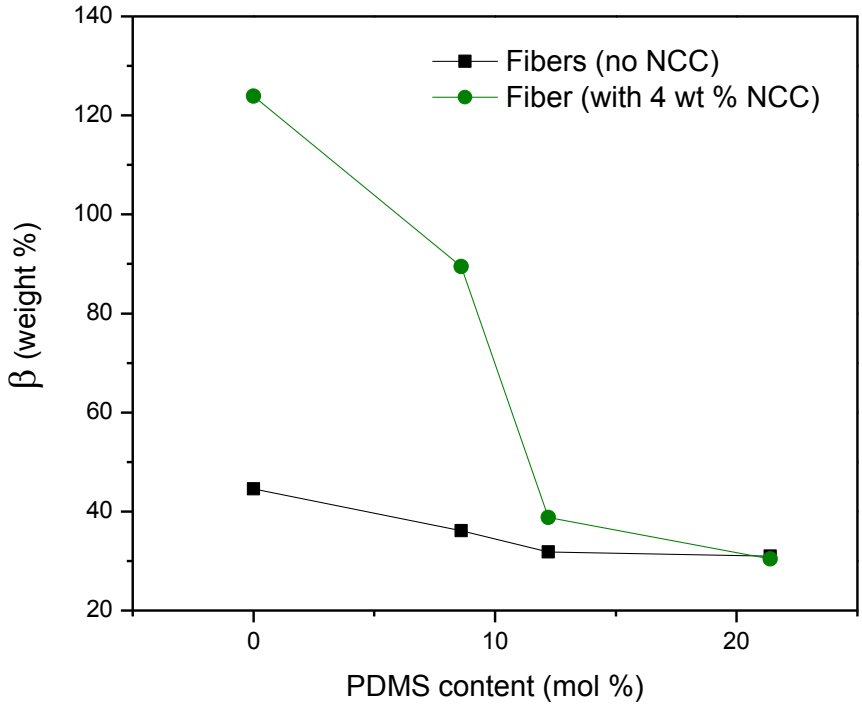

FIGURE 4-40: Comparison of β values for samples with and without any NCC

The above results suggest that the inclusion of NCC can actually increase the absorption capacity of the fibres. More in depth studies in a more controlled environment should be performed to get a thorough understanding of what variables play the major role in absorption by the fibres. As mentioned at an earlier stage, the absorption is influenced by a number of factors. It was clear though that inclusion of NCC affected the absorption process of the fibres.

Stellenbosch University http://scholar.sun.ac.za

4.4. REFERENCES

1. Li, J., Yi, L., Lin, H. & Hou, R. *Journal of Polymer Science Part A: Polymer Chemistry,* **2011,** 49, (6), 1483-1493

2. Bayley, G. M. & Mallon, P. E. *Polymer,* **2012,** 53, (24), 5523–5539

3. Pichot, C., Hamoudi, A., Pham, Q. T. & Guyot, A. *European Polymer Journal,* **1978,** 14, (2), 109-116

4. Pinteala, M., Budtova, T., Epure, V., Belnikevich, N., Harabagiu, V. & Simionescu, B.C. *Polymer,* **2005,** 46, (18), 7047-7054

5. Kühnel, E., Laffan, D., Lloyd-Jones, G., Martínez del Campo, T., Shepperson, I. & Slaughter, J. L. *Angewandte Chemie International Edition,* **2007,** 46, (37), 7075-7078

6. Hou, Y., Schoener, C. A., Regan, K. R., Munoz-Pinto, D., Hahn, M. S. & Grunlan, M. A. *Biomacromolecules,* **2010,** 11, 648-656

7. Ito, K. & Kawaguchi, S. *Advances in Polymer Science*, **1999**, 142, 129-178

8. Haris, M., Rosemal M. H., Kathiresan, S. & Mohan, S. *Der Pharma Chemica*, **2010,** 2, (4), 316

9. Teramachi, S., Sato, S., Shimura, H., Watanabe, S. & Tsukahara, Y. *Macromolecules,* **1995,** 28, (18), 6183-6187

10. Zetterlund, P.B., Yamazoe, H., Yamada, B., Hill, D.J.T. & Pomery, P.J. *Macromolecules,* **2001,** 34, (22), 7686-7691

11. Podzimek, S. *Light scattering, size exclusion chromatography and asymmetric flow field flow fractionatio,.* New Jersey: John Wiley and Sons. Inc. **2011**

12. Siewing, A., Lahn, B., Braun, D. & Pasch, H. *Journal of Polymer Science Part A: Polymer Chemistry,* **2003,** 41, (20), 3143-3148

13. Pasch, H., Adler, M., Rittig, F. & Becker, S. *Macromolecular Rapid Communications,* **2005,** 26, (6), 438-444

14. Glockner, G. *Polymer characterization by liquid chromatography.* Berlin: Elsevier, **1987**

15. Schunk, T. C. & Long, T. E. *Journal of Chromatography A,* **1995,** 692, (1–2), 221-232

16. Teramachi, S., Sato, S., Shimura, H., Watanabe, S. & Tsukahara, Y. *Macromolecules,* **1995,** 28, (18), 6183-6187

Stellenbosch University http://scholar.sun.ac.za

17. Ma, M., Hill, R. M., Lowery, J. L., Fridrikh, S. V. & Rutledge, G. C. *Langmuir,* **2005,** 21, (12), 5549-5554

18. Kalra, V., Mendez, S., Lee, J., Nguyen, H., Marquez, M. & Joo, Y. *Advanced Materials,* **2006,** 18, (24), 3299-3303

19. Kalra, V., Kakad, P. A., Mendez, S., Ivannikov, T., Kamperman, M. & Joo, Y. L. *Macromolecules,* **2006,** 39, (16), 5453-5457

20. Ruotsalainen, T. *Soft Matter,* **2007**, 8, (3), 978

21. Sharma, Y. *International journal of biological macromolecules,* **2012,** 51, (4), 627-631

22. Bai, S., Quan, J., Nie, H. & Zhu, L. *New Chemical Materials,* **2013,** (41), 4, 62-64

23. Swart, M., Olsson, R. T., Hedenqvist, M. S. & Mallon, P. E. *Polymer Engineering & Science,* **2010,** 50, (11), 2143-2152

24. Bhardwaj, N. & Kundu, S. C. *Biotechnology Advances,* **2010,** 28, (3), 325-347

25. Haglund, B. O., Joshi, R. & Himmelstein, K. J. *Journal of Controlled Release,* **1996,** 41, (3), 229-235

26. Kikuchi, A. & Nose, T. *Society,* **1997,** 9297, (96), 896-902

27. Bio-Imaging SWDSOP. **2013**. *Negative staining.* http://web.path.ox.ac.uk/~bioimaging/bitm/instructions_and_information/EM/neg_stain.pdf

28. Winnefeld, F., Becker, S., Pakusch, J. & Götz, T. *Cement and Concrete Composites,* **2007,** 29, (4), 251-262

29. Casper, C. L., Stephens, J. S., Tassi, N. G., Chase, D. B. & Rabolt, J. F. *Macromolecules,* **2004,** 37, (2), 573-578

30. Lin, J., Ding, B., Yu, J. & Hsieh, Y. *ACS Applied Materials & Interfaces,* **2010,** 2, (2), 521-528

31. Megelski, S., Stephens, J. S., Chase, D. B. & Rabolt, J. F. *Macromolecules,* **2002,** 35, (22), 8456-8466

32. Peng, P., Chen, Y., Gao, Y., Yu, J. & Guo, Z. *Journal of Polymer Science Part B: Polymer Physics,* **2009,** 47, (19), 1853-1859

33. Swart, M. & Mallon, P. E. *Pure Applied Chemistry,* **2009,** 81, (3), 495-511

34. Xiao, S. *Journal of Applied Polymer Science,* **2010,** 116, (4), 2409-2417

35. Hennink, W. E. & Van Nostrum, C. F. *Advanced Drug Delivery Reviews,* **2002,** 54, 223-236,

Stellenbosch University http://scholar.sun.ac.za

36. Rusu, T., Loan, S. & Buraga, S. C. *European Polymer Journal,* **2001,** 37, (10), 2005-2009

37. Pike, J. K., Ho, T. & Wynne, K. J. *Chemistry of Materials,* **1996,** 8, (4), 856-860

38. Boscaini, E., Alexander, M. L., Prazeller, P. & Märk, T. D. *International Journal of Mass Spectrometry,* **2004,** 239, (2–3), 179-186

39. Eagland, D., Crowther, N. J. & Butler, C. J. *European Polymer Journal,* **1994,** 30, (7), 767-773

40. Zhu, M. F. Liu,Y., Sun,B., Zhang,W., Liu, X. L., Yu, H., Zhang, Y., Kuckling,D. & Adler, H. J. P. *Macromolecular Rapid Communications,* **2006,** 27, 1023

41. Gestos, A., Whitten, P., Spinks, G. & Wallace, G. *Soft Matter,* **2010,** (6), 1045

42. Shin, M. K., Kim, S. I., Kim,S. J., Kim, B. J., So, I., Kozlov, M. E., Oh, J., Baughman, R. H. *Applied Physics Letters,* **2008**, 93, (16)

43. Li, L. & Hsieh, Y.L. *Nanotechnology,* **2005,** 16, (12), 2852

44. Loh, X. J., Peh, P., Liao, S., Sng, C. & Li, J. *Journal of Controlled Release,* **2010,** 143, (2), 175-182

45. Kim, S. H., Kim, S., Nair, S. & Moore, E. *Macromolecules,* **2005,** 38, (9), 3719-3723

46. Nakagawa, H., Hara, Y., Maeda, S. & Hasimoto, S. *Polymers,* **2011,** 3, (1), 405-412

47. Ji, Y., Ghosh, K., Li, B., Sokolov, J. C., Clark, R. A. F. & Rafailovich, M. H. *Macromolecular Bioscience,* **2006,** 6, (10), 811-817

48. Ramakrishna, S., Fujihara, K., Teo, W. E., Lim, T. C., Ma, Z. *An introduction to electrospinning and nanofibers.* Singapore: World Scientific, **2005**

49. McKee, M. G., Hunley, M. T., Layman, J. M. & Long, T. E. *Macromolecules,* **2006,** 39, 575

50. Cui, J. *Biomacromolecules,* **2012,** 13, (3), 584-588

51. Philippova, O. E., Hourdet, D., Audebert, R. & Khokhlov, A. R. *Macromolecules,* **1997,** 30, 8278

52. Habibi, Y., Lucia, L. A. & Rojas, O. J. *Chemical reviews,* **2010,** 110, (6), 3479-3500

53. Peng, B. L., Dhar, N., Liu, H. L. & Tam, K. C. *The Canadian Journal of Chemical Engineering,* **2011,** 89, (5), 1191-1206

54. Martínez-Sanz, M., Olsson, R. T., Lopez-Rubio, A. & Lagaron, J. M. *Journal of Applied Polymer Science,* **2012,** 124, (2), 1398-1408

Stellenbosch University http://scholar.sun.ac.za

A. APPENDIX A

A.1. ^{1}H-NMR SPECTRA FOR PMAA-GRAFT-PDMS COPOLYMERS

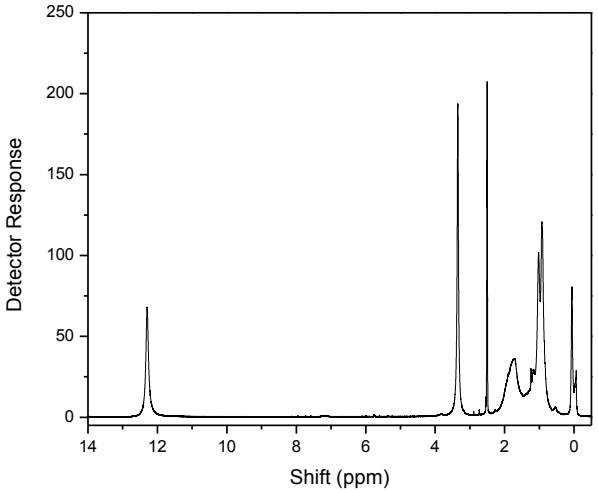

FIGURE A-1: ^{1}H-NMR spectra of a copolymer with 8.6 mol % PDMS

Stellenbosch University http://scholar.sun.ac.za

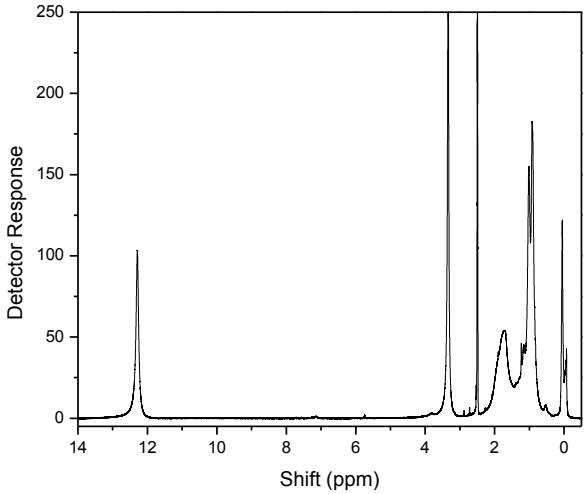

FIGURE A-2: ^{1}H-NMR spectra of a copolymer with 12.2 mol % PDMS

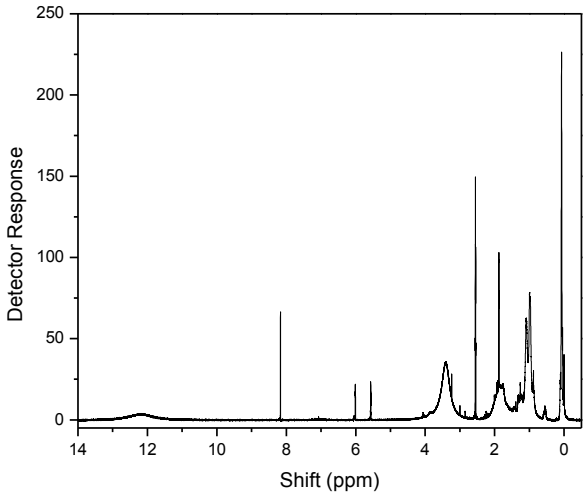

FIGURE A-3: ^{1}H-NMR spectra of a copolymer with 30.5 mol % PDMS

Stellenbosch University http://scholar.sun.ac.za

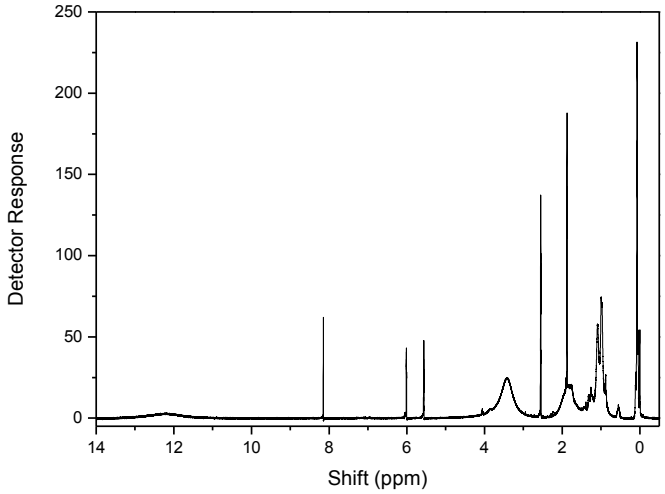

FIGURE A-4: ^{1}H-NMR spectra of a copolymer with 31.5 mol % PDMS

A.2. ^{1}H-NMR SPECTRA FOR PMMA-GRAFT-PDMS COPOLYMERS

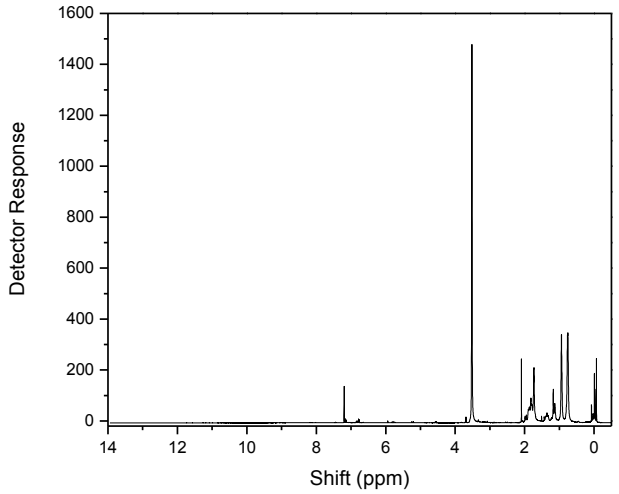

FIGURE A-5: ^{1}H-NMR spectra of a copolymer of PMMA-g-PDMS with 8.6 mol % PDMS

Stellenbosch University http://scholar.sun.ac.za

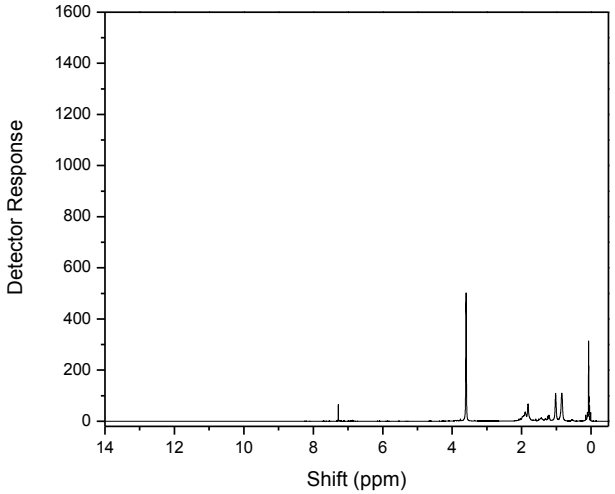

FIGURE A-6: ^{1}H-NMR spectra of a copolymer of PMMA-g-PDMS with 12.2 mol % PDMS

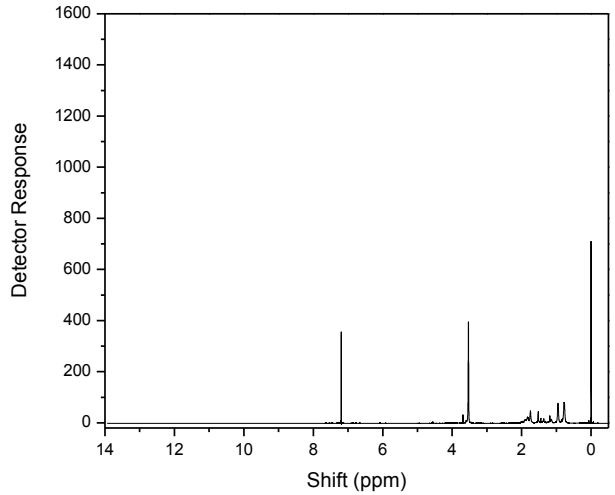

FIGURE A-7: ^{1}H-NMR spectra of a copolymer of PMMA-g-PDMS with 30.6 mol % PDMS

Stellenbosch University http://scholar.sun.ac.za

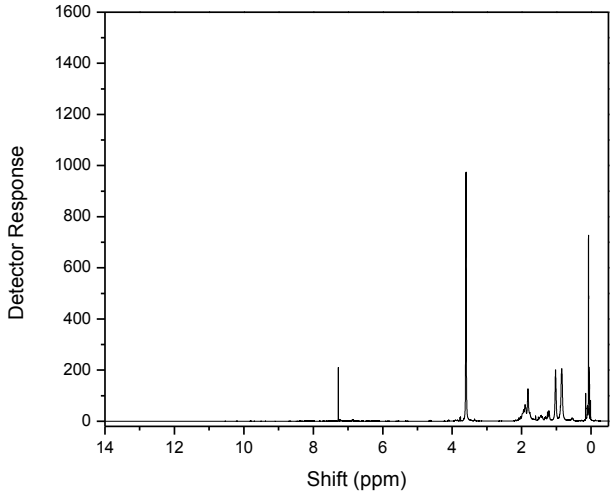

FIGURE A-8: ^{1}H-NMR spectra of a copolymer of PMMA-g-PDMS with 31.5 mol % PDMS

A.3. MOISTURE ABSORPTION FITTING PARAMETER TABLES

TABLE A-1: Parameters for polymer moisture absorption curves as fitted to equation 4.1

PDMS mol%	τ_1	±	τ_2	±	β	±	R^2
0	48.843	0.251	6.492	0.013	44.569	0.046	0.99996
8.6	21.559	0.080	5.689	0.060	36.123	0.005	0.99928
12.2	17.010	0.032	4.270	0.023	31.829	0.004	0.99992
21.4	2.896	0.026	16.642	0.039	30.968	0.007	0.99977
31.6	2.499	0.017	12.672	0.028	27.405	0.004	0.99979

TABLE A-2: Parameters for polymer moisture absorption curves as fitted to equation 4.1 for polymers crosslinked with NCC

PDMS mol%	τ_1	±	τ_2	±	β	±	R^2
0	3.904	0.014	20.502	0.043	123.871	0.026	0.9999
8.6	6.639	0.086	16.430	0.324	89.440	0.043	0.9997
12.2	9.311	61.465	9.312	61.488	38.815	0.009	0.9984
21.4	12.228	0.039	3.468	0.039	30.424	0.005	0.9998